TRANSACTIVE ENERGY CONTROL OF ELECTRIC ENERGY STORAGE TO MITIGATE THE IMPACT OF TRANSPORTATION ELECTRIFICATION IN DISTRIBUTION SYSTEMS

by

Sherif Abdelsamad Madkour

A Thesis Submitted in Partial Fulfillment

of the Requirements for the Degree of

Doctor of Philosophy

in

The Faculty of Engineering and Applied Science

in the Department of Electrical, Computer and Software Engineering

University of Ontario Institute of Technology

November 2016

Abstract

The adoption of Plug-in electric vehicles (PEVs) as a substitute to gasoline-based internal combustion engine vehicles represent a major change in the transportation sector. Typically, PEVs uses electricity to charge the on-board batteries instead of gasoline which is used in internal combustion engines. The main advantage of electrifying the transportation sector is to help lower fuel costs and reduce GreenHouse Gases (GHGs). Despite being an environmentally friendly means of transportation, the increased penetration of these electric vehicles may have negative impacts on the electrical power distribution system components (e.g. distribution primary feeders, transformers and secondary distribution lines), and as a result of these impacts, modification and upgrading of the distribution system components may be required. This can be achieved by increasing the distribution transformer sizes and adding new lines to the existing system, which may be considered an expensive solution. Several studies have been conducted to reduce the distribution system modification and upgrading costs, by coordinating the charging behavior of these vehicles either using centralized or decentralized control schemes. However, these methods limit the authority of vehicles' owners regarding when to charge their vehicles which might be inconvenient for some. On the other hand, electric utilities offer different incentive programs for their customers to control their energy usage in order to reduce the probability of system failures and to increase the system reliability while decreasing the costs of infrastructure upgrade. However, most of these programs have not met the expected response from customers.

In this dissertation, a new strategy is proposed to accomplish self-healing for the electric grid in order to reduce the negative impacts of PEVs charging demand. This novel

technique is based on applying the Transactive Energy (TE) control concept. The proposed implementation of the TE concept in this work is based on the adoption of a multi-agent system at different levels of the electric power distribution system (e.g., residential homes, neighborhood areas, and the Distribution System Operator (DSO)). These agents work in a cooperative manner in order to reach a state of consensus between the electric power distribution system resources owned by the electric utility (e.g., distributed generation, community energy storage) and the resources owned by the homeowners (e.g., rooftop solar photovoltaic, home battery energy storage). Moreover, the multi-agent system will allow the customers to use their own resources in an optimal way that can gain the maximum benefits offered through different incentive programs.

The results have shown that the negative impacts on the electric power distribution system due to the plug-in electric vehicles charging demand can be mitigated by applying the proposed TE control which requires at least 30% of customers to own controllable battery energy storage unit.

Keywords: Plug-in electric vehicles, energy storage, transactive energy, multi-agent system, cooperative control, distributed generation.

Acknowledgment

I would like to express my deepest appreciation and sincerest gratitude to my supervisors, Dr. Walid Morsi Ibrahim and Dr. Tarlochan Sidhu, for their continuous support and patient guidance throughout my research work. They provided me with the motivation and supervision that helped me to overcome all the challenges I faced during my Ph.D. research.

My appreciation and deep thanks to all my friends and colleagues in Dr. Walid's Smart Grid research group at UOIT.

Special thanks and love go to my Father and my wife, Reham, and my daughter, Judy, for their continuous encouragement and for joining my academic journey. This work wouldn't have been accomplished without their efforts and unwavering support.

Table of Contents

List of Tables

List of Figures

Nomenclature

C_t	Price of unit energy ($/kWh)
E_b	Battery specific capacity in kWh
E_{con}	Consumed energy
$IR_{s\beta}$	Solar irradiance
I_{mpp}	Current at maximum power point
I_{sc}	Short circuit current
N_{houses}	Number of residential house
N_{veh}	Number of vehicle
P_{D_t}	Consumer power demand at hour t
P_{G_t}	Grid imported power,
P_{LL_t}	Line power losses
P_{TL_t}	Transformer power loss,
P_{PV}	PV power generation
P_{Rated}	Energy storage rated power
P_{sto}	Storage power (kW)
R_{st}	Global irradiance on a horizontal surface (kW/m^2)
SOC_{max}	Maximum energy storage state of charge
SOC_{min}	Minimum energy storage state of charge
T_{OT}	Nominal operating temperature of cell
T_a	Ambient temperature
T_c	Cell temperature

$\bar{V}$	Mean of wind speed
V_{max}	Maximum allowable voltage
V_{min}	Minimum allowable voltage
V_{mpp}	Voltage at maximum power point
V_{oc}	Open circuit voltage
V_t	Voltage at the distribution transformer bus
k_i	Current coefficient
k_v	Voltage coefficient
ρ_0	Reference air density
τ_{TO}	Oil thermal time constant of transformer
τ_w	Winding time constant at the hot-spot location
Δt	Time period duration
$\propto$	Average vehicle per house
A	Swept area of the wind turbine rotor
A_C	PV array surface area
ACL	Agent Communication language
AEVs	Battery Plug-in Electric Vehicles
ANN	Artificial neural network
ANSI	American National Standards Institute
BES	Battery Energy Storage
CDF	Cumulative Distribution Function
CDV	Cluster Distribution Validity
CP	Power coefficient

DERS	Distributed Energy Resources
DG	Distributed Generation
DOD	Depth of Discharge
DST	Distribution Substation Transformers
DT	Distribution System
ESS	Energy Storage System
EWAPG	Excess of Wind Active Power Generation
F_{AA}	Aging acceleration factor
FCVs	Fuel Cell Electric Vehicles
F_{EQAA}	Equivalent aging acceleration factor
FF	Fill factor
FIPA	Foundation for Intelligent Physical Agents
FIT	Feed in Tariff
GHGs	GreenHouse Gases
G_{sb}	Geometric factor
HEMS	Home Energy Management Systems
HoCom	Home Owner Comfortable
IESO	Independent Electricity System Operator
LOL	Loss of Life
MAS	Multi-agent System
MCS	Monte Carlo Simulation
MDP	Markov Decision Process
MG	Micro-Grid

MILP	Mixed Integer Linear Problem
NAEMS	Neighbourhood Area Energy Management System
NB	Nash Bargaining
NCDC	National Climatic Data Center
NHTS	National Household Travel Survey
N_{PV}	Rooftop solar photovoltaic capacity
OPF	Optimal Power Flow
P	PEV penetration
PAPR	Peak over Average Power Reduction
PDAL	Previous Day Average load
PDLL	Previous Day Lagged Load
PDS	Primary Distribution System
PEV	Plug-in Electric Vehicle
PHAL	Previous Hour Average Load
PHEVs	Plug-in Hybrid Electric Vehicles
P-OPF	Probabilistic Power Flow
PV	Photovoltaic
PWLL	Previous Week Lagged Load
R	Ratio of load loss at rated load to no-load loss
RPF	Reverse Power Flow
RPFR	Reverse reactive power flow
SDG	Smart Distribution Grid
SDS	Secondary Distribution System

SG	Smart Grid
SOC	The State of Charge
SOLR	System over Load Reduction
SSE	Sum of the Squares Errors
SWLL	Similar Weather Lagged Load
TOU	Time of Use
v	Actual wind speed
WAEMS	Wide-Area Energy Management System
X_s	Hourly diffuse fraction
K	Weibull shape parameters
c	Weibull scale parameters
d	Daily mileage driven in miles
Γ	Gamma function
$\Delta\theta_{H,R}$	Winding hot-spot rise over ambient temperature
$\Delta\theta_H$	Winding hottest spot rise over top-oil temperature in ˚C
$\Delta\theta_{TO,R}$	Top-oil rise over ambient temperature at rated condition
$\Delta\theta_{TO}$	Top-oil rise over ambient temperature
ε	Specific energy consumption in kWh/mile
η	Charger efficiency
ρ	Reflectance of the ground
σ	Standard deviation of wind speed

Chapter 1: Introduction

1.1 Background

The use of plug-in electric vehicles (PEVs) instead of gasoline-based vehicles is expected to bring several socio-economic and environmental benefits such as reducing Carbon Dioxide (CO_2) emissions. Also, since PEVs uses electricity from the power grid to charge an on-board battery instead of using gasoline, the operating costs of PEVs are significantly less compared to the gasoline-based vehicles, and it is estimated to be one-third according to [1]. Such benefits have motivated governments to offer incentives which take the form of rebates and/or tax credits to increase the adoption of PEVs. In 2010, the Ontario government started offering incentives ranging from $5,000 to $8,500 to consumers when they purchased PEV [2]. Other similar programs also exist in Quebec (Drive Electric Program), and British Columbia (Clean Energy Vehicle Program) [3].

Fig. 1.1 shows the projected annual market share of PEVs based on forecasted annual sales up to 2050[4], similar study done by Plug'N Drive organization [5] to forecast the PEVs sales in the next 5 years, the study show that the PEVs sales expect to increase by 100% in 2020. Given that the power drawn by PEV is comparable to that of a typical house [6], these PEVs will impose additional demands on the power grid, which will cause severe problems for several distribution system components.

On the other hand, distributed energy resources (DERs) (e.g. wind, solar photovoltaic) have gained consideration due to the reduction in initial costs and due to being environmentally friendly [7]. In Ontario, two renewable energy programs exist, which include the Feed-in Tariff (FIT) program for large applications, and the second is the

micro Feed in Tariff (microFIT) for small applications [8]. In the FIT program, the target capacity ranges from 10 kW up to 500 kW. Due to this large capacity, the installation of DERS is limited to the primary electrical distribution system (PDS) which starts from the distribution substation and ends at the primary of the distribution transformers feeding homes [9]. However, solar PVs and in particular, rooftop PVs installed in residential areas (i.e. secondary distribution systems, which starts from the secondary of the distribution transformer and ends at a customer's smart meter) are part of the microFIT program, which targets applications with less than 10 kW power.

The increased penetration of renewable energy sources, and the increased demand due to PEV charging, will certainly have significant impact on the aging infrastructure of the electric power distribution grid. At present, there are no integrated tools to help the electric utilities to manage the increase in the power generation from the integration of renewable energy sources and the increase in demand due to the integration of PEVs. Previous researcher [10-11] has proposed the use of DERs to supply PEVs charging locally. Similarly, a group of PEVs charging in the same neighborhood at the same time will also overburden the grid even with the presence of DERs.

Distribution transformers are one of the most affected components in the power distribution system when PEVs are introduced [12]. This causes a problem since the distribution transformers represent the most expensive asset to electric utilities, both as an initial and operating cost. Distribution transformers represent about 9 to 20% of electric utility expenses in a year [13].

The focus of this dissertation is to calculate the combined impact of PEVs, and DERs on distribution transformers and propose a suitable strategy to mitigate the impact on their loss of life.

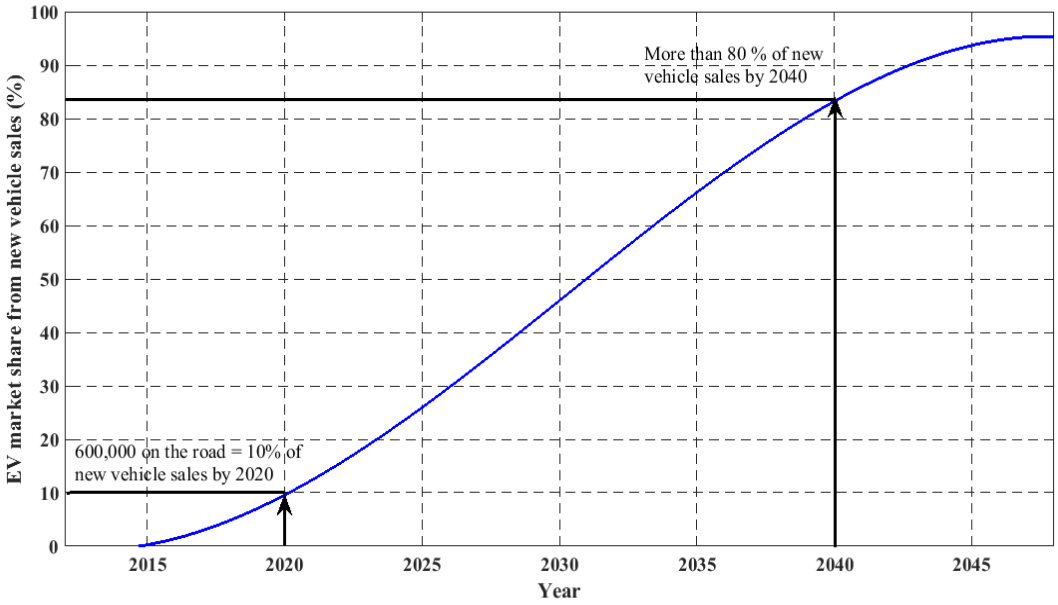

Figure 1.1 PEV Annual Market Share Future Forecast up to 2050 [4].

1.2 Overview of the Electrical Power System

The electric power system can be divided into three main subsystems; 1) the generation system typically has capacity in the range of 5 MW to 1000 MW [14]. 2) The transmission system contains the transmission substation and the transmission lines. The transmission substation is used to increase the voltage to a range of 35 kV to 230 kV and is usually located at the power generation station [14]. The transmission lines supply distribution substations with transmission voltages where the high voltages step down to lower levels using the distribution substation transformers (DST). 3) The electric power system ends by the distribution system which makes up the last link of supplying electric power to the customers. The distribution system is commonly broken down into three sections: the distribution substation, the primary distribution system (PDS), and

the secondary distribution system (SDS). More details about these three sections will be provided below.

Fig. 1.2 shows the details of the electric power system starting from the generation to the customer and indicates the operating voltage of each subsystem.

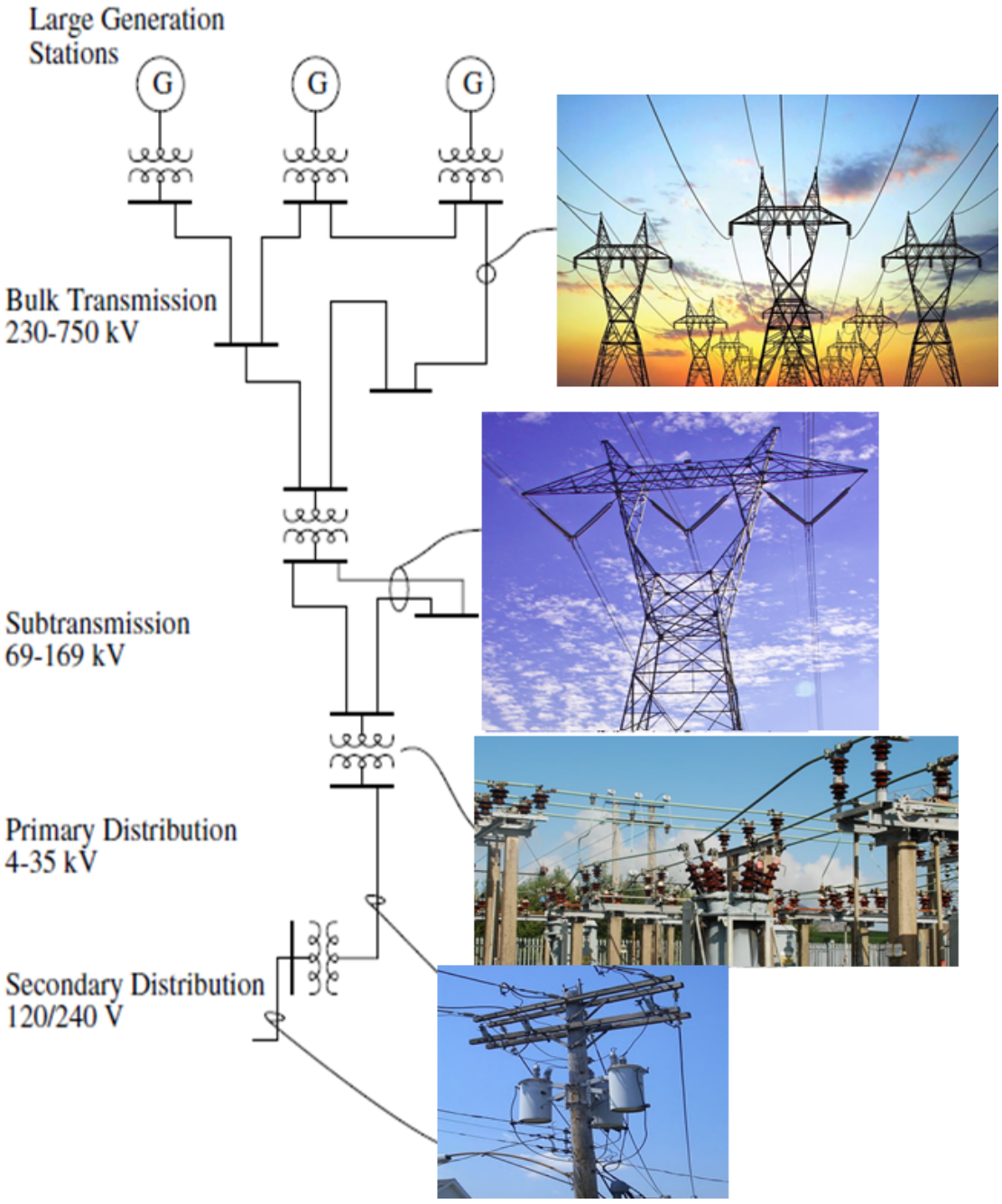

Figure 1.2 Overview of the Electric Power System Infrastructure [14]

1.2.1 Distribution Substation

The voltage in the transmission system is stepped-down by the DST. A distribution substation consists of one or more power transformer banks, voltage regulating devices, buses, and switchgear. The substation bus arrangement can have different topologies which can be classified as:

a) Single Bus.

b) Single Bus with Bus Sectionalizers.

c) Double-bus.

d) Double Breaker.

e) One and A Half Breaker Bus

f) Main and Transfer Bus System

g) Ring Bus System

The distribution substation voltage is usually in the range of 12 kV to 14.4 kV. Fig. 1.3 shows the typical distribution substation with several feeders.

1.2.2 Primary Distribution System

The PDS represents the part of the distribution system between the distribution substation and the distribution transformers feeding the residential homes [8]. The PDS consists of several different circuits called distribution feeders, which start on the secondary side of the distribution substation.

Two different types of PDS are commonly used called radial and network systems. Radial systems use a single path to deliver power to loads. A network system has many different paths which together deliver power to the loads.

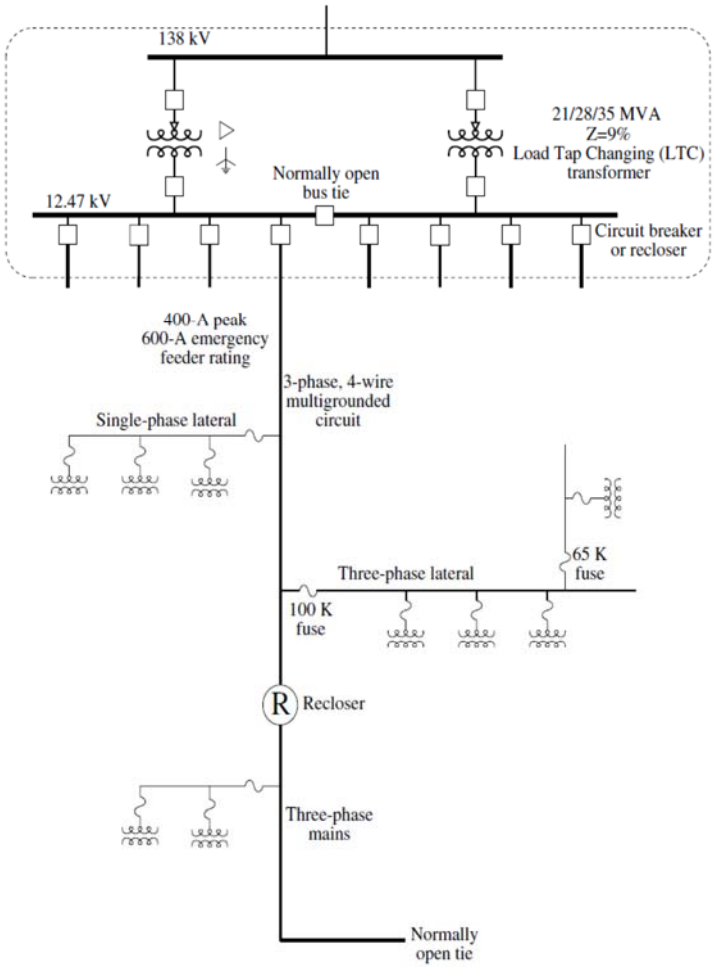

Figure 1.3 Distribution Substation with Several Feeders [14]

1.2.3 Secondary Distribution System

The SDS is the part of the system which starts at the distribution transformer and ends at the customer's meter [15]. The SDS consists of a step-down transformer and secondary circuit with the final usable voltage. In North America, residential neighborhoods are usually single-phase, while commercial and industrial applications use three-phase.

Various circuit arrangements exist in the SDS, the most basic circuits are radial. Common voltages used in the SDS are given in Table 1.1.

Table 1.1 Utilization Voltage in Secondary Distribution System [15]

Voltage level	Number of phases	Number of conductors
120	Single	2
120/240	Single	3
208Y /120	Three	4
240	Three	3
480Y/ 277	Three	4
480	Three	3
600	Three	3

1.2.4 Distributed Energy Resources

There is a growing awareness that increasing the number of distributed energy resources (DERs) and energy efficiency devices is crucial to help reduce climate change and our dependence on fossil fuels. The Canadian government is planning to spend $5.9 to $8.3 billion on climate change initiatives over the next five years [16]. Fig. 1.4 shows the outcome of a study performed by the Ontario's government to track the greenhouse gas (GHG) reduction and determine the required reduction in GHG by 2050 in Ontario. As depicted in Fig. 1.4, the study showed that the Canadian government was able to reduce the GHG in Ontario by 6% in 2014 and target to 80% reduction by 2050. By increasing the deployment of DERs (e.g., renewable-based distributed generation and energy storage) it will not only help reducing the GHG but will also create new economic opportunities, and provide energy to billions of people.

Environmental and security concerns have shown great interest in homeowners to having small scale renewable sources for power generation. Many countries around the world have started a different set of incentive programs to encourage homeowners to deploy distributed resources. In Ontario, the microFIT program [7] is meant to target homeowners looking to add renewable sources to their homes.

The term "Distributed Energy Resources" (DERs) can be defined as smaller power sources that generate electric power on the same site where that power is consumed. DERs may take many forms, including geothermal, micro-hydroelectric, solar, wind and battery storage systems.

Figure 1.4 Ontario GHG Emission Reduction Target [16]

Energy storage systems can operate as either an electric load or an electric source. One of the great advantages of energy storage is the fast and accurate response to the changes in the system operation. This also allows for smooth integration of renewable energy sources that are intermittent in nature. The problem of energy storage is the missing tools to evaluate and understand the economics of energy storage.

Energy storage can provide different functions based on where the storage is installed and these functions help utilities face the uncertain of peak load growth occur in the distribution systems and the high variability of the power generated from renewable energy sources. The different energy storage functions [17] can be seen in the list below:

A. Peak load management

B. Frequency regulation

C. Capacity market

D. Voltage regulation/reactive power support

E. Backup power/islanded grid operation

F. Accommodate rapid power swings

G. Provide low-voltage ride through for wind farm

H. Provide ancillary services

I. Demand clipping

J. Time of use (TOU) period time shifting

K. Response to real-time pricing signals

L. Utility control in emergencies or as needed

M. Load shifting and output smoothing

N. DC fast charging and vehicle energy storage

O. Demand response support

1.2.5 Plug-in Electric Vehicles

The large adoption of PEVs brings potential, social and economic benefits to the society. The focus of promoting the use of PEVs for transportation is crucial to address the climate change problem and reduce the fast depletion of fossil fuels. However, there are lots of doubts in the market about how far the customers will accept moving from gasoline-based vehicles to PEVs. These doubts present in the high initial and operation costs and the insufficient number of charging stations. Table 1.2 shows the top six countries adopting PEV in 2015 [18].

There are several types of PEVs, each with different features and battery sizes. Some of the new types of vehicles include Battery All Plug-in Electric Vehicles (AEVs), Plug-in Hybrid Electric Vehicles (PHEVs), and Fuel cell electric vehicles (FCVs). Fig. 1.5 shows the different electric vehicles technology.

Table 1.2 Number of New PEVs Sales in the Top Six Selling Countries

Country	PEV adoption
China	176,627
United States	115,262
Netherlands	43,971
Norway	34,455
United Kingdom	28,188
France	27,701

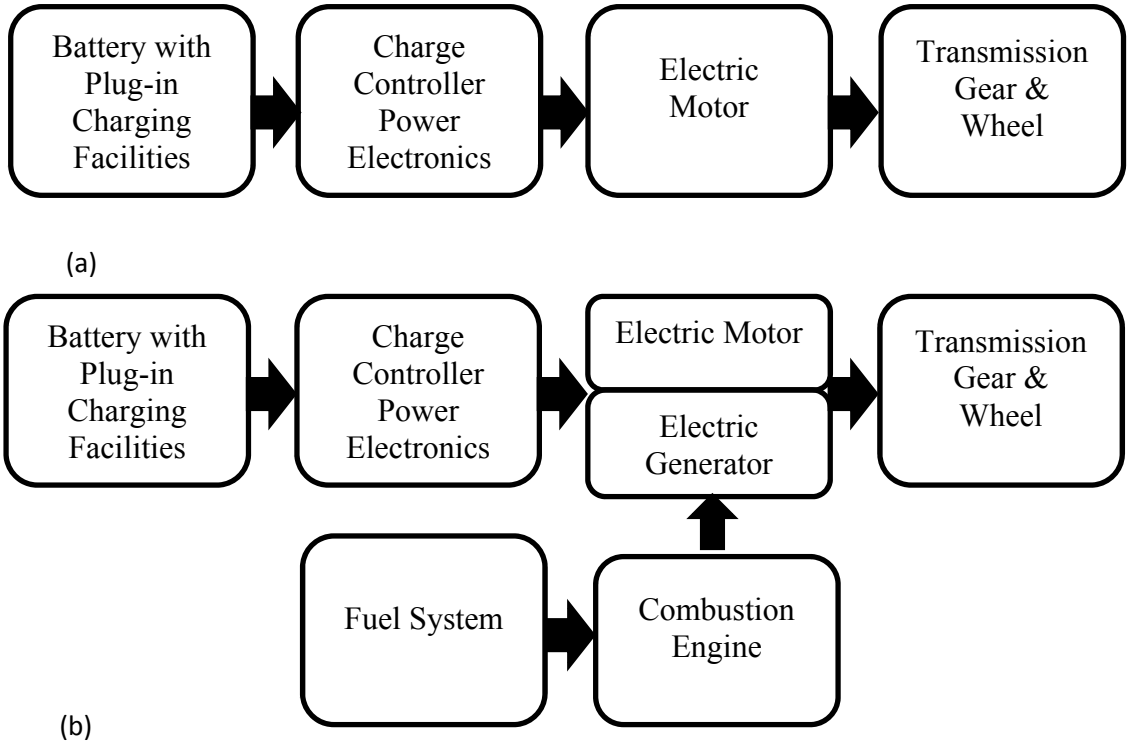

Figure 1.5 Plug-in Electric Vehicles Configuration, (a) All Electric Vehicles, (b) Plug-in Hybrid Vehicles

Using PEVs will allow for lowering fuel costs, reducing greenhouse gases (GHGs) emissions, and performing ancillary services to utilities like facilitating demand-side management if the PEVs are equipped with the communication technology.

Despite the advantages of PEVs, the charging demand required by these vehicles is seen as an additional demand from the system point of view. This additional demand must be supplied by any available generation, which will increase the power flow in the distribution system. The impacts vary based on PEVs penetration level and charging pattern. This can be seen as an increase in the case of uncontrolled charging PEVs, at which the car owners driving pattern and charging timings are unpredictable. On the other hand, the impact may be mitigated in the case of off-peak charging of PEVs, which will improve the demand curve seen by electric utilities.

The negative impact of PEV adoption on the power grid can be listed as follow:

A. Power supply shortage

B. Phase imbalance

C. Power Quality issues

D. Transformer degradation and failures

E. Circuit Breakers and Fuse Blow-outs

More discussion and explanation will be in chapter two.

1.3 Smart Distribution Management System

The smart distribution grid (SDG) will open an avenue for the end user (homeowner) to participate in power generation and/or energy saving programs. The SDG can define as the portion of the Smart Grid (SG) intelligent functions that deployed in the utility DS, on the higher level, it allows the electric utilities to operate their grid infrastructure and

resources in a more efficient, economic, and reliable manner. In order to operate the electric grid in an optimal way sometimes it will come with a sacrifice on the part of homeowners. These sacrifices include moving their load operation to off-peak periods which will be inconvenient for most people.

Homeowners have a set of questions which need to be satisfied in order to encourage consumers into these smart grid operations. These questions look like “What's in it for me?" or “Does that need a lot of effort and time?”.

The best way to address these question is to make sure the entire level of the power grid is managed in an optimal way. Fig. 1.6 shows the different management system that should exists within any smart distribution system from the author’s perspective, more details will be given in the following subsection.

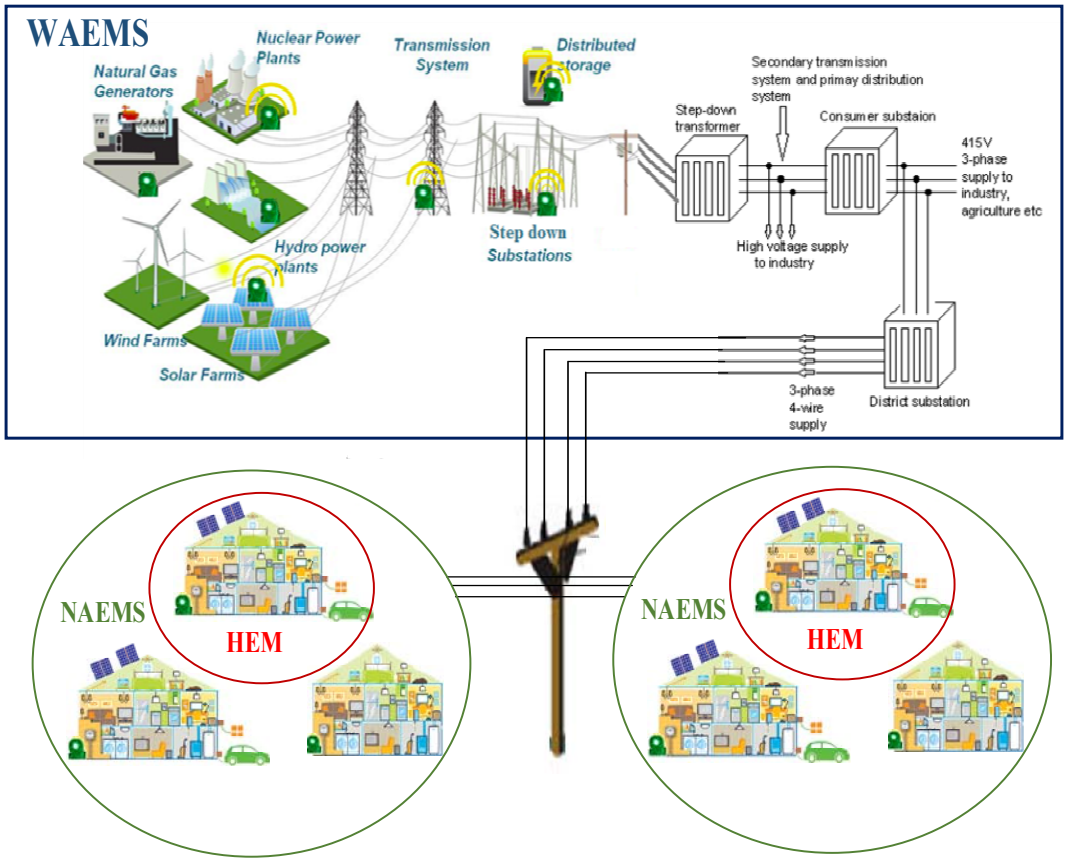

Figure 1.6 Different Levels of Energy Management Used in Power Distribution System

1.3.1 Home Energy Management System

Home energy management systems (HEMS) include any product or service that is capable of monitoring, controlling, and/or performs analyses on the measured data within the residential customers' premises (i.e., home). Also, some of these products are able to automatically respond to the residential utility demand response incentive programs, execute automation services, energy management, data analysis and visualization of the homeowners' energy profile, and finally, they can perform security services.

Home energy management systems can connect to utility's revenue smart meters that are currently used for billing the residential customers and are considered networked home energy management systems. These systems can communicate with the smart meter to get energy data for billing, temperature information and time of use pricing as well as to perform control actions within the home. These controlling functions are usually called home automation and have shown to provide significant energy savings of up to 20% [19].

Since HEMs first hit the market in 2008, many new companies have begun producing products that fall under this umbrella. Fig. 1.7 shows the different HEMS products that are being developed and the market for HEMS is split into different categories. The defining split between the products is whether they are utility or consumer focused solutions.

Utility-focused solutions are aimed at electric utilities and the households which are enrolled in HEMS programs. These solutions are highly customized for a specific utility and typically aim to control and monitor only one load in the home. This monitoring

provides the utility with real-time information regarding the loads operation and the control allows the utility to toggle the state of the load in order to satisfy demand response or energy efficiency programs. One of the most popular utility solutions is the demand response in which the utility can actively control loads inside the home with additional hardware. These solutions usually range from free to several hundred dollars and if consumers allow them to work properly, can reduce energy usage by 2 to 20% [19]. However, utility benefits are much greater than just the energy reduction as it allows them to perform additional functions for outage management or critical peak periods.

Most HEMS operate independently without utility intervention and are easily integrated with utility communication systems.

Some functions do not involve the utility at all and allow the homeowner to set up their own smart home. These HEMs functions are usually focused on economic savings and can be sometimes in conflict with one or more of the utility's objectives (e.g. customers can charge their vehicles and energy storage system when the cost of electricity is low which will significantly degrade the DS infrastructure, which against the utilities objective to maximize the life time of DS equipment's and minimize the required upgrade cost). The HEMS providers most of the time targeting consumers directly and ignoring the utility's objectives.

For any HEMS to achieve market success, the industry must overcome challenges to enable homeowners to easily sell, install and manage their solutions. Fig. 1.8 show samples of HEMS.

Figure 1.7 Products Used for Home Energy Management (source Iris company products)

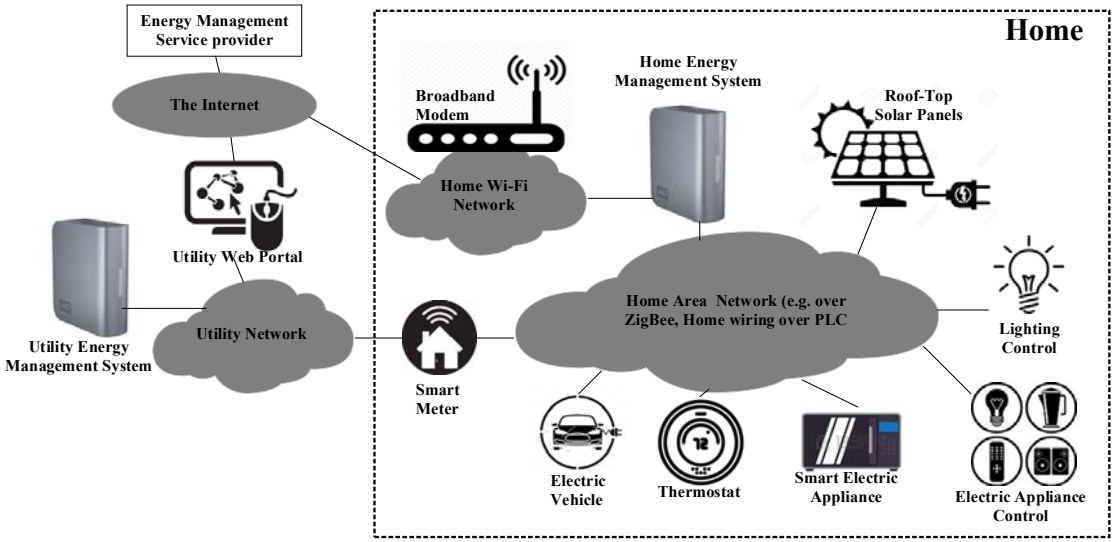

Figure 1.8 HEM Systems Connected to Utility Network [20]

1.3.2 Neighbourhood Area Energy Management System

The role of this level is to perform energy management and control in a neighborhood through a cooperative way by communicating with the Home Area Energy Management Systems within neighborhoods (HEMS), as well as controlling the DERs, and other

loads which exist at the neighborhood level (e.g. street lighting). Fig 1.9 show the layout of the NAEMS.

In order to implement this system, it should be able to send and/or receive information from various neighbourhood HEMS installed in customers' homes and DERs owned by electric utilities, then be able to analyze these data to determine the energy consumption pattern, the peak and off-peak periods, and provide advice and control actions to both consumers (home owner) and utilities in order to improve energy usage.

Different communication protocols are used to ensure reliable data transfer between the HEMS and the NAEMS. Advanced Metering Infrastructure (AMI) [21] is one of the new features that add to the smart meter to enable the HEMS to connect with utilities or NAMES. AMI uses two way communications to be able to send/receive data and commands between the HEM and NAEM. Another scheme is using the home Wi-Fi network to deliver the information through the internet.

This level will convert the homeowners to have and active role in the smart grid operation, the required control actions will help to meet the daily load requirements with suggested actions that can be taken to reduce energy usage. It will also help the DSO to operate the distribution system in the most economical way, improve energy efficiency and lower carbon emission in neighborhoods. Moreover, it will define and validate their business strategies and pricing schemes, ensure maximum utilization of DERs in neighborhoods, and enable load shifting and peak clipping services.

In order to ensure the success of the neighborhood management system, it should also provide the right information at the right time to take the most suitable control action, it

needs to encourage the end user's engagement through social networks and increase energy consumption awareness.

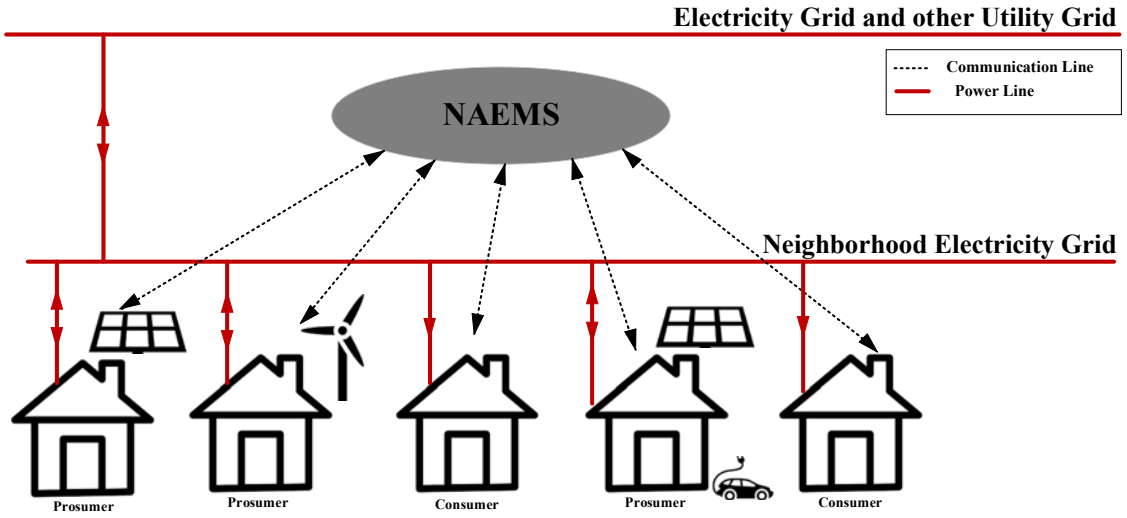

Figure 1.9 Neighborhood Energy Management System

1.3.3 Wide Area Management System

Wide area management systems enable advanced analysis of energy data received from the neighborhood management system (NAEMS). Early detection of power quality problems can also be performed with tracking and determining energy usage in NAEMS. This will enable facility capacity planning and maintenance. The data provide trending information which can be used to troubleshoot potential issues and enable the utility to change their pricing schemes from the time of use pricing to dynamic real-time pricing. This will improve energy usage, and decrease the stress over the power system infrastructure as shown in Fig. 1.10. The WAEMS will also ensure the optimal power generation allocation from different stockholders. The following functions can perform through WAEMS:

A. Grid optimization

B. Outage time reduction

C. Situational awareness

D. Asset utilization and optimization

E. Crew management and safety

F. Distributed resources integration

G. Demand response integration

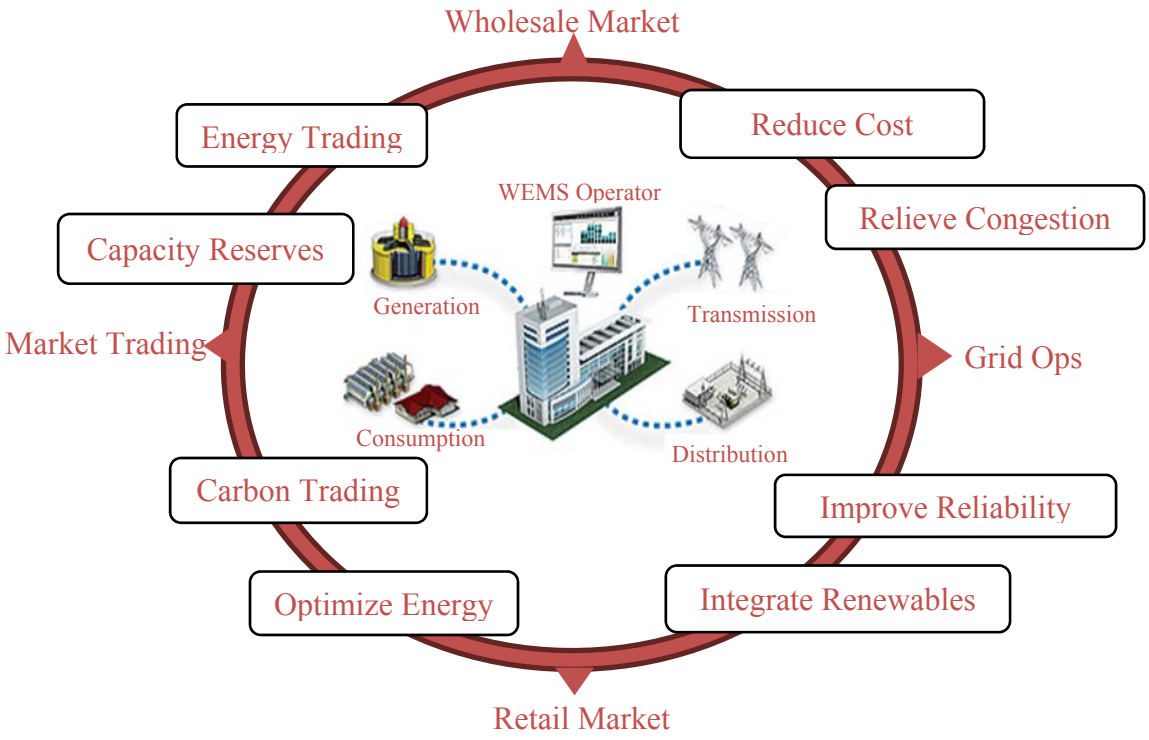

Figure 1.10 Wide Area Management System [21]

1.3.4 Transactive Energy Market

With the previous explanation of the smart distribution energy management system, it is required to define the best control scheme that will be able to achieve the maximum benefits of the intelligent components installed on distribution system either in the utilities or homeowners' level.

Different schemes are used to establish the communication between the electric utilities and their customers in order to involve them in the smart grid operation.

These schemes [22] can be summarized as follow:

The first scheme, is the active market at which the customers respond to price signal sent from the central controller, then the HEM can react to the price signal, the drawback of this scheme it doesn't provide feedback to central controller if it will accept or reject the respond to the price signal.

The second scheme, is the interactive market which is similar to the active market scheme. However, the customer can feedback their decision to the central controller to dynamically adjust the pricing signal.

The last scheme, is the Transactive market which is defined as "A set of economic and control mechanisms that allows the dynamic balance of supply and demand across the entire electrical infrastructure using value as a key operational parameter" [23]. This scheme will allow active engagement of end user by applying negotiation and different bidding strategy to the available capacity and resources owned by customers until they reach an agreement with the electric utilities. Up to now, most of utilities applied the active energy market. However, the interactive and Transactive energy market are not deployed in the distribution system.

1.4 Problem Statement and Motivation

In Canada, electricity is at an inflection point where many changes are starting to take place in many different areas of the electric grid. Most of Canada's electricity infrastructure is nearing the end of its lifespan and this has forced electric utilities for massive investment in grid modernization. This investing is essential for a reliable, cost-

effective and sustainable power grid for years to come. However, the cost associated with this infrastructure upgrade will be at least $350 billion in capital investments over the next 20 years [24].

This is an unprecedented infrastructure investment and as such is driving up electricity prices. The average electricity price is expected to be approximately 20 percent higher by 2035 compared to prices in 2013 [25]. Fig. 1.11 shows the expected rapid increase in electricity rates. A systematic approach to innovation is needed for it to be possible to both create new technologies and to meet rapidly change in customers demand while finding new efficiencies to mitigate the impact of rising prices.

Some of the current drivers of this work are to reduce GHG emissions; increasing system reliability and to come back climate change. This will empower customers and help them play more of a role in shaping the future electricity system while lowering costs.

One of the promising solution that will help utilities to maximize their profit and reduced the upgrade cost is using Transactive Energy control, which will enable the active involvement of customers without interrupting them.

Electrical utilities reports [24], shown that the distribution network is suffering and requires an upgrade. Electric utilities aim to add a set of energy services through a data exchange between utility and the customer management system that include responsive loads, PEVs, and DERs. However, the integration of PEVs or DERS can negatively affect the distribution system due to the uncertainties associated with the process of PEVs charging such as time of charge, battery state of charge, number and location of PEVs, and the power generated from the DERs.

All of these problems and motivations have stimulated researchers to think about the best strategy that can be used to solve these issues. This work aims to introduce a new energy management platform based on applying the Transactive Energy control concept, to help eliminating the negative impacts of charging PEVs in the distribution system. The proposed Transactive Energy based platform aims to help resolving the conflicting objectives between the customers and the utility while ensuring minimum cost of power delivery for electrical utilities at improved reliability and efficiency. One of the key players in this proposed Transactive Energy-based platform is the energy storage. However, the economic justification of using energy storage still requires the user to take full advantage of the energy storage benefits.

The widespread deployment of energy storage systems requires a coordinated effort on the part of technology developers and electric utilities to ensure that systems are designed to adequately address the consumers and the utility needs.

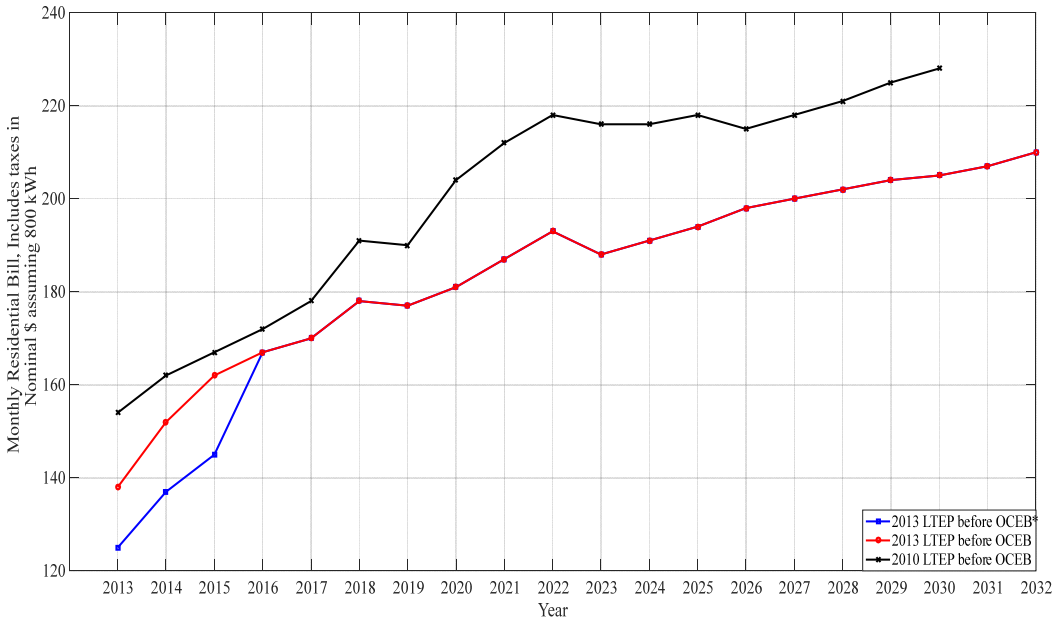

Figure 1.11 Ontario Energy Price Forecast [25]

1.5 Contribution

The contributions of this dissertation are summarized as follows:

The first contribution is to apply the Transactive Energy (TE) control to mitigate the impact of Plug-in Electric Vehicles (PEVs) on the distribution system. The new TE control platform will solve the conflicts between electric utility objectives and customer objectives. These conflicts are the major reason why the conservation programs offered by electric utilities are unsuccessful. The TE control platform is a novel concept which introduced in this work by the adoption of multi-agent systems in the power grid. By allowing the agents to work in a cooperative manner, the TE control platform will help electric utilities reach an agreement with customers (i.e., homeowners) on how to use their energy resources (solar PV and/or energy storage). A negotiation process between multi-agents systems is used to reach the agreement. The operation of the multi-agent system is mathematically formulated to ensure all agents achieve their maximum profit. By applying this new technique, the final TE control solution can improve the existing energy conservation programs offered by the Canadian Independent Electricity System Operator (IESO). The application of the TE cooperative control concept is what distinguishes this work from the existing literature.

The second contribution of this work is in improving distribution system component modeling. This can be done by improving the modeling of wind-based DGs, PEVs, and solar PVs. In wind DGs and solar PVs, the unsupervised clustering techniques is used to address the variability in weather data. This will overcome the issue of under/overestimating the power output from the DGs. The Cluster Distribution Validity (CDV) index is a new index introduced in this dissertation to assess the goodness of

clustering representative wind speed profiles produced using unsupervised clustering techniques needed to model the power output from wind-based DGs. On the other hand, a realistic estimation of the impact of PEVs on the primary distribution system is implemented by providing service nodes (i.e. homes), after modeling the secondary distribution system components to connect electric vehicles.

The results of this dissertation have been published in several peer-reviewed journals and conferences [27- 30].

1.6 Thesis Organization

The work of this thesis is organized as follows:

Chapter 2 surveys the previous work investigating the impact of plug-in electric vehicles on the Electric distribution system embedded with or without distributed energy resources. The aim is to provide the necessary background on how previous work has addressed the problem from a system impact analysis perspective and the different proposed solutions to mitigate the PEV impact including the potential of using battery energy storage and cooperative control. This chapter concludes by identifying the previous studies research gaps and the notable areas which can be improved.

Chapter 3 provides information on the research methodology used in this work. The survey summarizes the research methodologies that have been proposed to determine the best approach to optimally managing the distribution system resources so to satisfy all electric power distribution system participants. This chapter also presents the implementation of the control rules and the communication between different distribution system levels.

Chapter 4 describes the modeling and implementation of the electric power distribution system infrastructure used to evaluate the proposed research work. The system modeling includes the representation of both distribution system primary and secondary systems, plug-in electric vehicles, distributed energy resources. This chapter also presents the implementation of the multi-agent cooperative control used for optimal distribution system asset management based on day-ahead load forecasting.

Chapter 5 presents the results of implementing the proposed approach to managing the distribution system resources and mitigate the electric vehicle charging load to the IEEE 123-bus and IEEE 34-bus standard test systems after modifying the test systems to incorporate the secondary system.

Chapter 6 present the conclusions, recommendations and future work.

Chapter 2: Literature Review

2.1 Introduction

This chapter surveys previous work studying the impact of PEVs charging on the electric power distribution system. The solution methodologies developed in the literature will be carefully reviewed considering the integration of the distributed energy resources. Also, this chapter summarizes the previous studies which investigated the potential of energy storage and multi-agent cooperative control to address the problem in the electric power distribution systems.

2.2 Impacts of Plug-in Electrical Vehicles

Most of the work in literature tries to estimates the PEV charging demand on the PDS assuming that the PEV demand follows certain probability distribution [31-34]. A large part of this assumption is due to the deficiency of modelling the SDS components which is essential for modeling of the secondary points at which PEVs are connected and charged. Due to this assumption, most of the studies [35-39] have focused only on primary distribution assessments, and even fewer studies take into account the SDS [40-42].

In [43], the authors quantify the impact of PEVs on the electric power grid by using a set of different power quality indices. However, the study did not investigate the effect of PEVs on transformer loss of life.

In [44] the impact of PHEV's on the distribution system voltage, energy losses, load factor and maximum load were investigated. The technical and regulatory market prospective to adopt PEVs in Ontario was discussed in [45]. Sortomme et al. [46] show

the distribution system can have unacceptable voltage violations in the case of 10% PEV penetration.

Impacts of PEV charging on a low voltage power grid at different PEV penetrations is discussed in [47], the study conclude that increased peak load, increasing power losses, overload of transformers and lines, increased voltage drop and increased voltage asymmetry can affect the power grid due to PEV charging.

Assolami et al. [48] investigated the impact of extended battery PEV charging demand on the distribution system in terms of overload and transformer loss of life.

Paterakis et al. [49] investigated the optimal operation of DERs to prevent transformer overloading in the presence of PEVs.

In [50], the impact of PEV charging demand on the distribution network in British Columbia (BC) is investigated in terms of transformer overload using Monte Carlo simulation. The impact of PEVs on distribution transformer LOL was investigated by Rutherford and Yousefzadeh in [51]. In [52-55], transformer aging was estimated due to increasing PEV charging demand, it was reported that the transformer LOL may increase by up to 10000 times in the case of high PEV penetration. [56–58] assessed the impact of PEV charging on the distribution transformer for both hot-spot temperature and LOL. In [19] feasibility of charging PEVs using renewables sources (solar PVs), the authors estimate the probability of distribution transformers experiencing overload, without estimating the effect on the transformer's LOL, same approach can be seen in [59]. Geiles and Islam [60] investigated the impact of PEVs and solar PVs on a 200-kVA distribution transformer in Australia.

In [61] the impact of PEV charging demand on the distribution system was seen to increase the transformer failure ratio by 0.02 % per year and reduced the life of the transformer by 69 %, when PEVs used level 2 charging. The harmonic and load distortion, due to this higher penetration rate of PEVs was then seen to degrade the transformer life span by 40 % per year.

2.3 Mitigating PEV Impact on Distribution System

Most of the proposed solutions in the literature that aim to mitigate the impact of PEV charging demand on the electric power distribution system can be grouped into two categories: 1) using control and coordination of electric vehicle charging times; 2) using distributed energy resources.

The PEVs charging coordination techniques may include either centralized or decentralized strategies. In centralized strategies [62-64], a central operator dictates precisely when and at what rate every individual PEV should charge. The main drawback of this method is that it requires significant communication and computational capabilities and in the case of communication failure the whole control strategy collapses. Studies in [65-67], proposed decentralized or distributed strategies, in which individual PEV could determine their own charging pattern to within certain limits. Both strategies share the same drawback with limited authority of vehicles' owners regarding when to charge their vehicles which might be inconvenient for many.

In [68], a decentralized multi-agent system is developed to manage a power distribution system with PHEVs in order to perform different ancillary services such as Spinning, Regulation, and Peak shaving. In [69], a distributed, multi-agent PEV charging control strategy based on the Nash Certainty Equivalence Principle is introduced to remove the

impacts of PEV. In [70], an agent-based control system that coordinates the battery charging of PEVs in distribution networks is proposed. The solution to charge PEVs at times of low electricity prices within the distribution network is proposed in [70] with technical constraints. Neural networks are used in the decision making of agents. In [71], an optimal charging rate control of PEVs based on consensus algorithm is proposed, which aligns each PEV's interest with the system operating conditions. In [72], a decentralized pricing strategy is used to determine charging service reservations for PEVs.

In [73], the concept of introducing the vehicle to building (V2B) is presented. The controlled charging schemes of PEVs include a benefit to adding to a building energy system and the distribution grid.

In [74], market-based multi-agent systems that incorporate the distribution transformer and voltage constraints for the charging of a fleet PEVs are presented; the agents are assigned based on the charging power of PEVs with the highest need for energy.

In [75], supervisory control algorithm was proposed to reduce the PEV impact on the power system. In [76], a new algorithm for PEV charging based on scheduling and considering a probabilistic charging time was introduced. In [77], an optimization algorithm was used to coordinate PEV charging in order to minimize power losses in the distribution system. In [78], a comparison between dynamic programming and quadratic functions was done in order to reduce PEV charging impact. This study used deterministic and stochastic PEV charging demand models.

In [79], a simulation environment consisting of several different tools for simulating vehicle traffic, charging activities, power generation, and the electrical network, was

used to develop a simulation environment and charging strategy for optimizing the charging demand from PEVs.

The use of a surplus of power from wind DGs to charge PEVs was introduced in [10]. However, the proposed methodology was only limited to mitigate the impact of PEVs in the PDS and hence did not include transformer overload for the remaining secondary system components.

In [80], the mixed integer linear programming method was used to schedule the charging of PEVs in the presence of energy storage system (ESS) from the electricity market perspective. The use of ESS and an on-line management system to charge PEVs in islanding conditions is discussed in [81].

The author's previous work in [27] extensively studied the synergy between wind DG and PEV charging. The author introduced a new set of indices to measure the impact of PEV charging on the electric power distribution system. The author used Monte Carlo simulations to address the uncertainties associated with the changing wind speed and the stochastic nature of PEVs charging.

Melo et al. In [82] discussed the possibility of using solar PV's to reduce transformer overload, however, the proposed technique only partially mitigated the impact of PEVs on the primary system components only.

The author's previous work in [28] investigated the possibility of using rooftop solar PV's as a solution for the PEV charging problem and the authors reported that the PV can partially reduce the transformer overload problem. However, at high PV penetrations it was reported that many transformers have experienced overload which

was due to the reverse power flow and hence may lead to transformer premature replacement.

More of the authors' previous work can be seen in [29], in which an optimal distribution system retrofitting scheme is proposed to mitigate the PEV load on the distribution system. The author presented the optimal design for the new distribution system to include the effect of PEV charging demand at minimum cost.

2.4 Distributed Energy Resources for Reliable Distribution System

Most of the work done to date representing the DREs in the distribution system does not properly address the uncertainty of the DERs. For example, fluctuations in wind speed profiles need to be estimated in order to determine the power generation from wind-based DGs. This has been dealt with in the literature, either by assuming that it follows a certain probability distribution [83-84] or by using different clustering-based approaches [85-86]. The resultant wind speed profiles from both approaches are not accurate enough to represent the wind speed data. The developed profiles may over or underestimate the output power generated from wind DGs.

Battery energy storage as a DERs can be located at the supply side under utility control or at the demand side under the homeowner's control with or without utility recommended actions. From the application perspective, the battery energy storage can support the bulk integration of renewable energy generation, to get rid of the uncertainty and the intermittent behavior.

In [87-90], the authors investigated the use of BES to mitigate the negative impact of large wind power and PV installations. In [91], a linear-quadratic optimization algorithm is used to determine the optimal use of energy storage to improve the system reliability.

In [92], a convex optimization method was used for optimal DERs to perform a power system peak shaving function. In [93], a Markov Decision Process (MDP), and an on-line learning technique was used for real-time BES management for homeowner benefit maximization.

The second application is to use storage to reduce a homeowner's energy bill. Studies [94, 95] proposed energy management system for battery energy storage to perform demand response for electricity cost minimization.

2.5 Multi-Agent Cooperative Control in Power Distribution System

Multi-agent cooperative control has been used in many different applications in order to obtain a flexible control system that has the advantage of a centralized and decentralized control strategy. In this section, the basic application using multi-agent control in a distribution system will be highlighted. These application are categorized into three basic applications:

First, using the multi-agent control in a Smart grid application. In [96], the authors used three advantages of multi-agent control (autonomy, local view, and decentralization) to develop a distributed algorithm for grid service restoration after detecting and isolating a fault. In [97], the study proposed a demand response scheme based on smart utilization of building resources and allowing the building management system to participate in the electricity market. In [98], the study proposed a smart HEMS that allowed homeowners to have more flexibility in their consumption. In [99-101], the study proposed a smart grid self-healing service using a MAS to select the optimal switching operation for service restoration after locating and isolating faults. In [102], a MAS is used to control the operation of distributed energy resources to perform ancillary services.

The second category uses the multi-agent control in micro-grid (MG) applications. In [103], cooperation between micro-sources and the BES is used for frequency and voltage control during islanding operation. In [104], voltage regulation and reactive power control using distributed cooperative control in micro-grid operations are used. Xu et al. [105] proposed a supply–demand balance in an isolated distribution grid using cooperative control and coordination of energy storage. Hernandez et al. [106] proposed an active power management system in multiple MGs consisting of battery storage, solar PVs, and diesel micro-sources for both operating modes; grid-connected mode and islanded mode. Fazal et al. [107], proposed a real-time demand response model for a micro-grid in the presence of PEVs and energy storage.

The third category used the multi-agent control in distributed generation applications. In [108], the study proposed a control strategy of DGs to balance the power supply and demand, maximize power usage from DGs, and minimize cost. In [109], multi-agent cooperative control was proposed to adjust the distribution system voltage level by controlling the reactive power of multiple feeders having wind DG units. In [110], a cooperative control strategy used to regulate the power generated from multiple PV generators. In [111], the study proposed a control strategy in the distribution system in order to achieve optimal operating conditions, and maximizing the power point tracking of wind turbines and PVs.

2.6 Transactive Energy Control

There are very few studies in the literature regarding the implementation of the Transactive Energy market. In [112], game theory used to simulate the dynamic behaviour of the consumers who were able to actively participate in smart grid operation.

The authors used the Shapley Value method and Nikaido-Isoda function to get the best payoff for each energy cell (customer), with the use of the power loss minimization as the objective function. In [113] three different tariff scheme, TOU, flat rate, and feed-in-tariff were used to find the most cost-effective solutions to integrate solar PV and battery energy storage systems. The author found that the use of transactive energy management can help consumers making the proper decision whether to invest or not in solar PV systems and BESS. In [114] the author used the transactive control to find the best operation in vehicles to grid mode and grid to vehicles mode using double auction price market. In [22] transactive control was applied to decrease the distribution system congestion using demand response programs.

2.7 Research Gaps

The major gaps seen in the previous studies can be summarized as follow:

Until now applying the Transactive Energy (TE) control to extract the maximum benefits from the resources in the distribution system while encouraging customers to be more actively involved in the smart grid operations is not fully investigated. Specifically, using the TE control to solve the conflict between homeowners' objectives (e.g. reducing energy bills, continuity of supply, and comfortability by convince charging of their PEV at any time) and the electric utilities' objectives (e.g. minimize the operating cost, maximize profits, mitigate the PEVs charging demand impact on the distribution system without infrastructure upgrade), solving the previous conflicts were not presented in any of the previous studies.

The lack of accurate modeling of distribution system components result in inaccurate estimation of the impact of new loads such as the future impact of included PEV in the

distribution system at any penetration level. Moreover, since the renewable energy resources are weather conditions dependent, the variations in the power generation from these sources need to be properly represented otherwise the inaccurate representation of these resources may also generate a large error in the predicated generated power which may propagate into the analysis. On the other hand, energy storage, up to now most of the previous studies could not justify the cost and get the maximum benefits of including energy storage in the distribution system.

2.8 Research Objectives

The aim of this work is to apply and demonstrate the use of the Transactive Energy (TE) control platform to solve the conflicts between customers' objectives and electric utilities' objectives. Moreover, the TE control will enable the cooperative operation of the distribution system energy resources to mitigate the Plug-in Electric Vehicles (PEVs) impact on the distribution system. Also, this work introduces novel and accurate models that can quantify and assist the impact of integrating distributed energy resources and PEVs on the electric distribution system components.

The second objective is to quantify the transformer (which is the most expensive asset in DS) loss of life in the presence of PEVs, DERs connected to the electric distribution system.

The finial objective is to introduce the energy storage system into a different level in the DS (utility, distribution substation, and home level) with a new functions that will be able to alleviate the transformer overload and hence reduce the distribution transformers loss of life.

2.9 Summary

This chapter presents a comprehensive survey of the impact of charging plug-in electric vehicles (PEVs) on distribution system. Also, the proposed solutions of previous studies to mitigate the PEVs impact in order to operate the distribution system in optimal way are discussed in detail.

The author discusses a different way to mitigate the PEVs impact either using distributed energy resources to charge the PEV locally or using vehicles charging coordination techniques. Moreover, using the energy storage system in the distribution system to charge the PEVs or perform ancillary service is discussed.

The chapter also summarizes the previous work regarding using the Transactive Energy (TE) control to encourage customers to be actively involved in the smart grid operation.

The chapter also summarizes the previous work regarding using the transactive energy control to encourage customers to be actively involved in the smart grid operation.

The chapter concludes by identifying the research gaps (e.g. inaccurate modelling for either the DERS or PEV, and the absence of reliable tools to satisfy electric utilities objectives and the customers' objectives) and proposes a set of objectives to fill these gaps.

The next chapter explains the details of the methodology required to achieve the proposed objectives.

Chapter 3: Methodology

3.1 Introduction

With the introduction of the smart grid, consumer demand can be controlled by electric utilities (e.g. controlling the operation of air conditions), which will help utilities perform different self-healing functions (e.g. change the power generation, change customers' consumption (load shifting, load shedding)) to increase the system reliability. However, deciding whether and when to control a load is currently based on customers' preferences.

Most consumers want their preferences to remain private and utilities are faced with a hard time trying to convince homeowners to participate in any conservation program. There is a dire need to identify new incentives, new methodologies, and new technologies to encourage homeowners to actively participate in smart grid operation.

Two different approaches are currently used by utilities to manage and control energy resources. The first is centralized control, in which the utility offers rebate incentives for consumers to allow the utility to have control over their appliances in order to perform direct load control [115]. The drawback of this approach is that it does not address customer comfort and other desires.

The second approach is distributed control through the existing home management system. Homeowners are able to monitor and control the operation of their home appliances based on real-time pricing sent by the electric utility. The main drawback of this approach is that it suffers from customers' reluctance to participate and a lack of clear benefits [116].

Recently, the Transactive Energy (TE) market is introduced as potential solutions to get the benefits of centralized and distributed control, by increasing the consumers' role in

the smart grid operation. In this work the cooperative control of multi-agents system is used to implement the TE control paradigm.

In this chapter, the concept of applying cooperative control using the multi-agent system is introduced to create the TE control platform that will be able to solve all the problems in the power distribution system.

3.2 Cooperative Control Concept

When a group of independent agents works together using local interaction through a certain communication protocol to perform efficient collective group behavior, this is called cooperative control.

With the technology revolution and advanced communication tools such as sensors and actuators, it is possible to design a group of independent agents to cooperatively accomplish predetermined functions in order to improve system operating conditions, reduce costs, and improve the control system reliability when compared to using a single complex control entity. The consensus is one of the most common problems that can be solved using cooperative control.

Many researchers have been stimulated to use cooperative control of multi-agents. Especially, when the application needs monitoring and descriptions of collective behavior. For example, with the increasing penetration of using PEVs and their high charging power (e.g. level 2 charging can reach up to 20 kW) [117], this is equivalent to three or four houses running all their appliances at once. Typically, most PEV owners charge their vehicles in the secondary distribution system in their home garages [118]. Although, electric utilities oversize their distribution transformers by nearly 20%, homeowners in the neighborhood could charge their vehicles at the same time, leading

to potential transformer overload which will reduce its lifetime and hence service interruptions.

In order to mitigate this problem, electric utilities need to quadruple the capacity of their lines and transformers. In order to avoid the economic costs associated with the early upgrades, electric utilities must apply controlling techniques to manage these loads. A collective behavior can be formed between the homeowners to cooperate with each other by staggering their PEV charging times. This can be done if the control is done with local consumers within a global framework including electric utilities.

Cooperative control can take advantage of centralized and distributed control approaches. For example, researchers can design the system to have at least a central agent that can communicate with other local agents to collect data and initiate control action. This allows the local agents to interact together and exchange information with their neighbors.

Due to the limited capability of sensors, communication range, and the system overall cost, it is difficult to rely on one central agent, especially when the system has a large number of agents.

In this work, due to the complexity and the large number of agents, it is crucial to only depend on local information exchange between agents and their neighbors, which report all the information to one neighborhood agent, and then the central agent will only communicate with each of the neighborhood agents.

3.2.1 Multi-agent System

Systems that make many different autonomous decisions at the same time can be considered as a multi-agent system. These systems communicate with each other hence

they will able to negotiate back and forth allowing collaboration. Each agent cooperates with other agents to solve the problem so everyone wins. In a multi-agent environment, coalition formation is used in which agents can form coalitions in order to work together to solve the problem. Game theory can be combined with the multi-agent approach to resolving coalition conflicts as seen in [119] and [120]. By using game theory, it helps distribute the coalition value calculations among agents. This saves each single agent from performing all possible calculations which improves the execution time and the system reliability. Multi-agents prefer to form an optimal coalition which means maximizing the joint utility of the entire system rather than just focusing on its own utilities. The next section specifies more information on achieving optimal multi-agent solutions.

3.2.1.1 Intelligent Agent Architectures

Intelligent agents can be defined as "a software (or hardware) entity that is situated in some environment and is able to autonomously react to changes in that environment" [121]. Intelligent agents should have three properties:

- Reactivity which is the ability to react to changes in the environment and produce suitable actions to change the system in a timely fashion in order to perform predefined task as shown in Fig. 3.1.
- Pro-activeness, where the agent should exhibit goal-directed behavior.
- Social, agent should be able to interact with other agents in a social way.

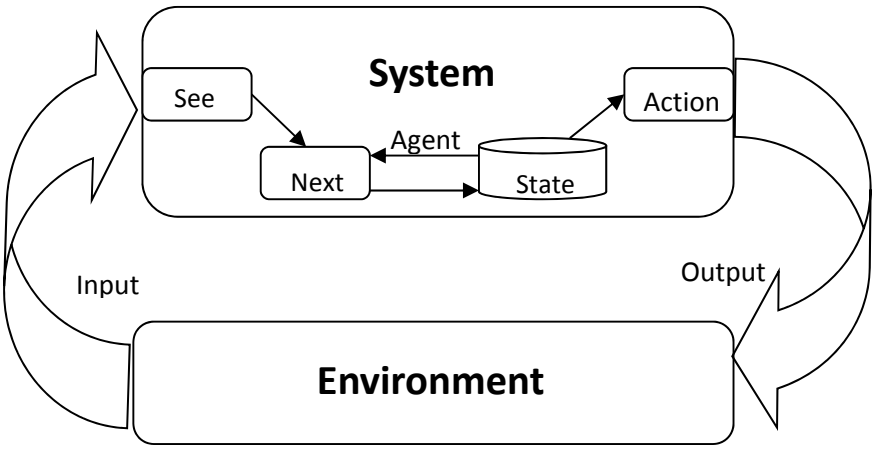

Figure 3.1 Sample Architectures for Intelligent Agents [121]

The mathematical model of MAS needs an accurate representation of the environment, the agent, and the system.

Assume the environment have a finite set E of discrete instantaneous states, the agent will have a set of action (SAC), for each state in the environment, and based on agent observations of the environment, the agent will make a decision and propose a SAC that will change the environment. The run R, of an agent in an environment, is a sequence of interleaved environment states and actions as given in (3.1).

$E = \{ e_1, e_2, \dots\dots\dots\dots, e_u, \dots\dots, e_n \}$, $SAC = \{ \mathrm{C}_1, \mathrm{C}_2, \dots\dots\dots\dots, \mathrm{C}_u, \dots\dots, \mathrm{C}_n \}$

$$R\colon e_1 \xrightarrow{\mathrm{C}_1} e_2 \xrightarrow{\mathrm{C}_2} e_3 \xrightarrow{\mathrm{C}_3} \dots\dots\dots\dots . e_u \xrightarrow{\mathrm{C}_u} \qquad (3.1)$$

Each agent builds a state transformer (τ) function based on system historical operations, the state transform then represents the set of environment-behavior (φ(E)), when the agent performs a certain possible run.

$$\tau\colon \mathrm{R}_{SAC} \rightarrow \varphi(E) \qquad (3.2)$$

With R_{SAC} represent all possible run that can be performed by an agent and end by action, the Environment can be finally represented as, $Env = \langle E, e_1, \tau \rangle$, where, $e_1 \in E$ is the initial state.

The agent (Ag) represents all of the sets of actions that map all the possible runs in the environment.

$$Ag: \mathrm{R}_E \rightarrow SAC \tag{3.3}$$

With R_E represents all of the possible runs that can be performed by an agent and end by an environment state. An agent then makes a decision for what action should be performed based on the history of the system.

Finally, the system can be represented by two attributes; the agent and an environment, which both of them will accompanying with the set of possible runs.

The agent (Ag) set of runs in the environment (Env) is denoted by $R(Ag, Env)$.

In any run $R \in (\ \mathrm{R}_{SAC} \cup \mathrm{R}_E\ )$ as described in (3.4), the environment state and the state action can be determined as follow:

$$C_1 = Ag(e_1),$$

$$\forall u > 0 : e_u \in \tau((e_0, C_0, ..., C_{u-1})) \wedge C_u = Ag((e_0, C_0, ..., e_u)) \tag{3.4}$$

3.2.1.2 Agent Utilities

In the multi-agent approach, there is no central authority responsible for assigning tasks among agents. Each agent has a set of predefined tasks and agents negotiate back and forth with each other until a consensus or coalition is formed to execute a predefined task.

The utility of an agent U is used to describe how an agent can delegate a predefined task without being given the steps to perform the required task. This mainly depends on the agent's capability to achieve the task, and can be mathematically defined as:

$$U: R \rightarrow IR \tag{3.5}$$

For each environment state, the agent performs a certain run (R); the agent utility can then be calculated for all the different possible runs. The best action associated with certain environment states will be based on the average utility over all of the runs. For example, in a HEMs, the agent is required to perform the maximum saving for the homeowner, based on agent observation in the environment (the house load conditions). The agent will then propose a set of actions based on the house resources for each suggested run, followed by the agent utility being calculated, and finally an action will be decided based on the average utility over all possible runs.

3.2.1.3 Agent Consensus

In a system with a set of agents, each agent will have a different utility and the consensus algorithm will try to establish an agreement between agents. This depends on their shared state information and the final goal is to form a consensus to equalize the utility of all agents as shown in Fig. 3.2

Consensus control is an algorithm that includes system control and graph theory, more details on graph theory can be seen in [122].

In this application, the distribution system can be represented by the graph:

G = (E, P), and $P=Pg \cup Pd$ (3.6)

Where P are the power elements (load (Pd) and generators (Pg)) that represent the vertices of the graph and E is the edge of the graph.

A set of agents can then be defined as a_1, a_2, a_3, …….$a_n \in A$, with agent objective functions $Ob_1, Ob_2, \ldots\ldots, Ob_n$ based on the agent equipped component. The agent then communicates and update their states to reach consensus using (3.7).

$$a_i(t+1) = a_i(t) - \varepsilon \sum l_{ij} (a_i(t) - a_j(t)) \quad (3.7)$$

where, $a_i(t)$ is the state of agent i at time step t, l_{ij} refers to the communication link between agent i, and agent j, ε is the sampling period.

Fig 3.3 represents a direct graph which consists of 10 agents. Fig. 3.3 shows the agent dynamics until they reach consensus.

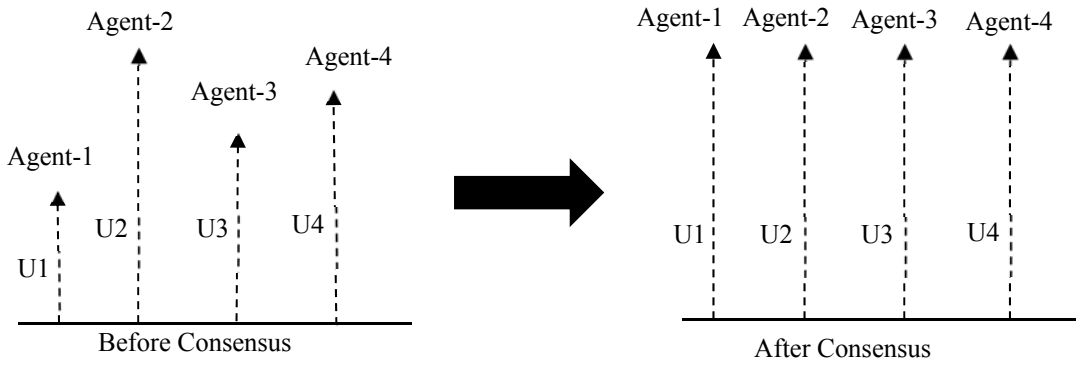

Figure 3.2 Agent Consensus Concept

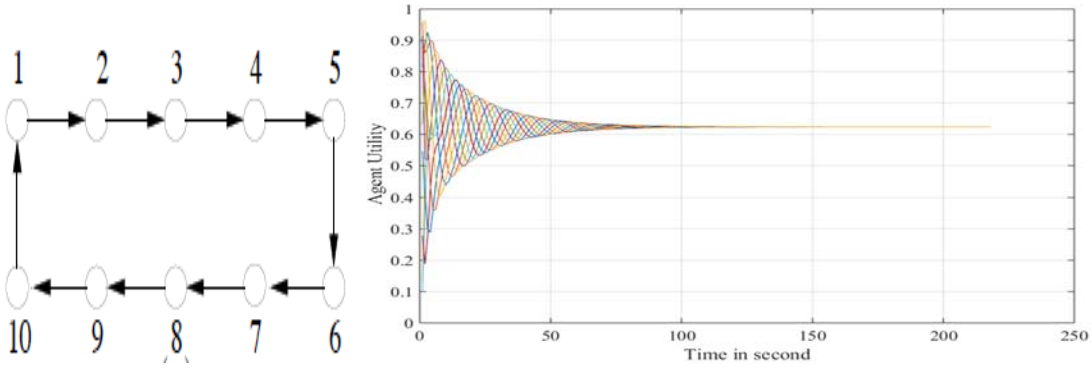

Figure 3.3 Consensus Protocols for Balanced Graphs

3.2.1.4 Agent Communication

The Foundation for Intelligent Physical Agents (FIPA) was founded in 1996 to help standardize software used in multi-agent based systems [123]. FIPA invented an agent communication language called ACL [124], which consists of twenty different ACL message types. Some examples are informing, requesting and composite speech acts. Fig. 3.4 shows the FIPA protocol to initiate interaction between multi-agents.

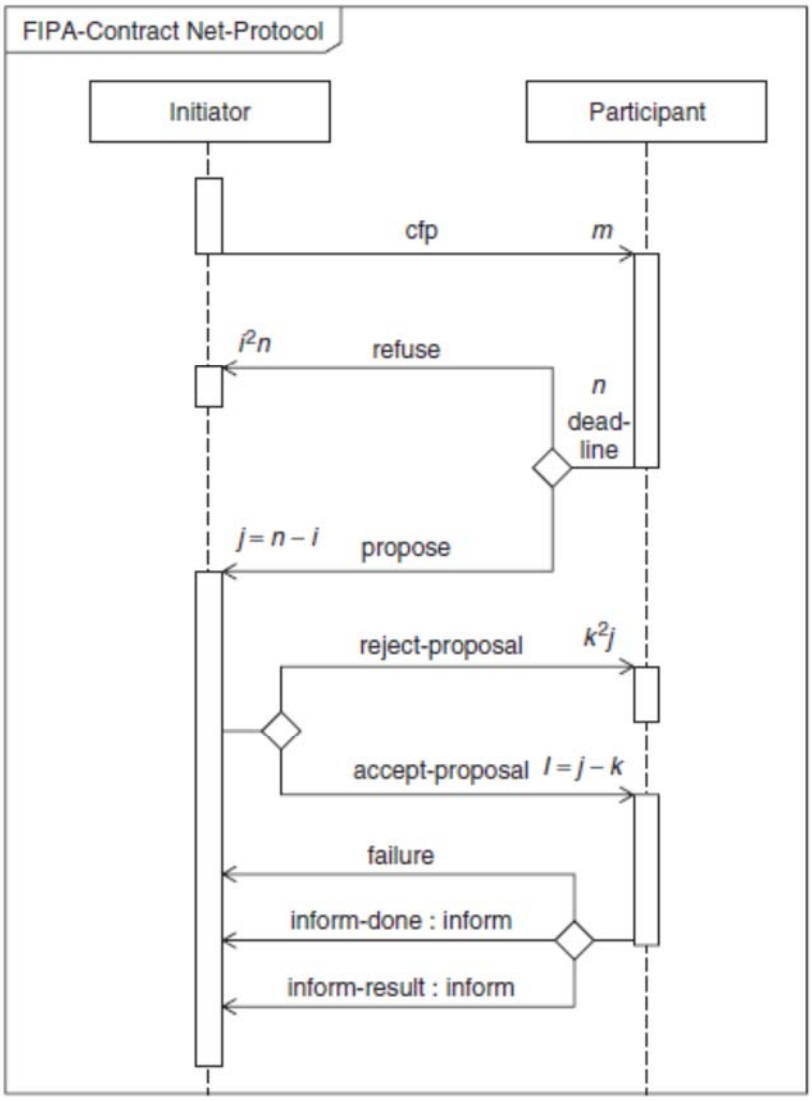

Figure 3.4 The FIPA Interaction Protocol [123]

When using multi-agents, there is no global control action that can be taken by the agents. Each agent is always competing to maximize its utility without considering the other agent's utilities. In some cases, the agent's utility function is private, and in order to perform cooperative control, a negotiation protocol is required to protect the agent privacy.

Cooperation is a decision-making process that needs contributors to evaluate all the alternatives and to consider each offer made by another member. Most of the time, the

agent will need to compromise one of his objectives while searching for optimal value from the negotiation results. The game theory represents the most effective way to actively perform optimal negotiations between agents in order to maximize the agent utility.

3.3 Game Theory

Game theory can be described as the choice of the optimal solution of two or more players acting together in a strategic way [125]. The benefits versus costs of different options for each player depend on the other player's choices. Game theory is an important field to help reach consensus between agents when there are conflicts between objectives.

When a strategic situation involves multiple interacting agents who make decisions while trying to anticipate the actions and reactions of others, there should be an equilibrium or consensus between agents.

Different models have been developed in the literature to solve the equilibrium problem, even if the agent work in simultaneous (Cournot) or sequential (Stackelberg) [126-127].

3.3.1 Stackelberg Model

In the Stackelberg model, a leader agent moves first followed by an agent which moves sequentially; then both the leader and the follower compete on a quantity or a price.

In order to design the Stackelberg model, the total price of the output industry should be a function of the quantity shared by each agent. Then the cost of each agent is calculated and an agent is pronounced as the leader of all agents. Bake word induction is applied to solve for all agents and finally, the reaction of the leader agent is calculated. For example, if two agents are competing for a quantity using the Stackelberg model algorithm 3.1 can be followed to find the value shared by each agent.

Algorithm 3.1 Stackelberg Model

1: Start

Inputs:

$P(q_1 + q_2)$ total price function on the produced quantity by each agent

$C_i(q_i)$ the cost function of each agent

Assume leader agent (e.g. agent number one)

2: Calculate the total profit of non-leader agent : profit = revenue – cost

$$\pi_2 = TR_2 - C_2 = P(q_1 + q_2) \times q_2 - C_2(q_2) \quad (3.8)$$

3: solve for quantity that maximizes the agent profits

$$\frac{\partial \pi_2}{\partial q_2} = \frac{\partial P(q_1+q_2)}{\partial q_2} \times q_2 + P(q_1 + q_2) - \frac{\partial C_2(q_2)}{\partial q_2} = 0 \quad (3.9)$$

4: solve for leader agent

$$\pi_1 = TR_1 - C_1 = P(q_1 + q_2(q_1)) \times q_1 - C_1(q_1) \quad (3.10)$$

$$\frac{\partial \pi_1}{\partial q_1} = \left[\frac{\partial P(q_1+q_2)}{\partial q_1} \times \frac{\partial q_2(q_1)}{\partial q_1} + \frac{\partial P(q_1+q_2)}{\partial q_1}\right] \times q_1 + P(q_1 + q_2(q_1)) - \frac{\partial C_1(q_1)}{\partial q_1} = 0 \quad (3.11)$$

Output: quantity and profits of each agent

6: **End**

3.3.2 Cournot Model

In the Cournot model, agents compete on the amount of output they produce and choose quantities simultaneously. It is based on using the Nash equilibrium to find the reaction function of each agent. Algorithm 3.2 show the steps to design the Cournot model.

Algorithm 3.2 Cournot Model

1: Start

Inputs:

$P(q_1 + q_2)$ total price function on the produced quantity by each agent

$C_i(q_i)$ the cost function of each agent

2: Calculate the total profit of each agent : profit = revenue – cost ; $\pi_{\mathrm{i}} = TR_i - C_i$

$$\pi_{\mathrm{i}} = P(q_1 + q_2) \times q_i - C_i(q_{\mathrm{i}}) \quad (3.12)$$

3: solve for quantity that maximizes the agent profits

$$\frac{\partial \pi_i}{\partial q_i} = \frac{\partial P(q_1+q_2)}{\partial q_i} \times q_i + P(q_1 + q_2) - \frac{\partial C_i(q_i)}{\partial q_i} = 0 \quad (3.13)$$

Output: quantity and profits of each agent

6: **End**

To illustrate the process, assume we have two agents A and B who compete for a quantity. The price set by the market is linear. $P = 100 - 2 \times (q_A + q_B)$, the marginal cost of the unit produced is constant and equal to 4.

The solution starts by solving for maximizing the profit of agent A (π_A),

$arg_{QA} \max(\pi_A) = \max(TR_A - C_A)$

$\frac{d\pi_A}{dQ_A} = \frac{d}{dQ_A}\left(100 - 2Q_A - 2Q_B\right) \times Q_A - 4 \times Q_A = 0$, $Q_A = 24 - 0.5Q_B$

Then solving for agent B:

$arg_{Qb} \max(\pi_B) = \max(TR_B - C_B)$

$\frac{d\pi_B}{dQ_B} = \frac{d}{dQ_B}\left(100 - 2Q_A - 2Q_B\right)Q_B - 4Q_B = 0$, $Q_B = 24 - 0.5Q_A$

Finally the quantity of each agent can be estimated: $Q_A = Q_B = 16\, unit$.

The two oligopoly models (Cournot or Stackelberg) can only be used for non-cooperative actions. They can also be used when either the price or quantity required is pre-set by the market.

3.3.3 Negotiation Strategies and Tactics

The problem of defining an effective negotiation strategy that best fits the context of the negotiation problem is one in which the optimal outcomes of the most tasks are taken in pre-bargaining preparation. This method not only determines a general behavior but also denotes specific actions (e.g. response rules, opening offers).

If a group of agents has the ability to fallback to a sharing option, and they are required to perform a cooperative task, Nash Bargaining (NB) [128] is considered a great method to solve the negotiation problem. In NB, the choice of one agent depends on the choice of another agent. The solution of this type of problem also depends on the need to maximize the payoff function for all agents.

For example, if you have two agents bargaining over an outcome and both have fallback options (V^A, V^B) and utility functions (U^A, U^B), the Nash outcome should maximize the product of the gain which may be represented mathematically as follows:

$$Max_x \left((U^A(x) - V^A)\ (U^B(x) - V^B)\right) \qquad (3.14)$$

When a single agent provides "a take-it-or-leave-it" offer, which imply that this agent is not motivated to give a large share of the surplus to other agents. Ultimatum game theory is the best tactics to be used since the ultimatum game is a simple game that is the basis of a richer model.

In ultimatum game theory the agent that receives an offer have only two options; accept or reject. If the agent rejects the offer, this means the negotiations round is terminated

without an agreement, as all the agents are primarily motivated by economics, it is better to accept a deal even if it is only slightly more attractive than bargaining breakdown.

3.4 Optimal Power Flow

The Optimal Power Flow (OPF) algorithm is a powerful analyzing tool in power system operations. It is used to find the steady state point of operation, which achieves a certain objective like minimizing operating cost, minimizing losses or maximizing the usage of renewable sources. The OPF is a nonlinear optimization problem that has different equality and inequality constraints. Two types of power flow algorithms are used in power systems: The first is deterministic power flow and the second is probabilistic power flow (P-OPF).

Most of the work in OPF includes objectives to solve problems in the PDS. However, little of the previous work investigates the SDS in the optimization procedure.

In deterministic power flow, the algorithm is based on worst case conditions, where other situations cannot be handled. On the contrary, probabilistic power flow can be used in any problem that includes uncertainty.

The P-OPF problem is formulated to include the SDS with PEVs as a stochastic load and DERs as a stochastic source. Fig. 3.5 show the framework for the new P-OPF.

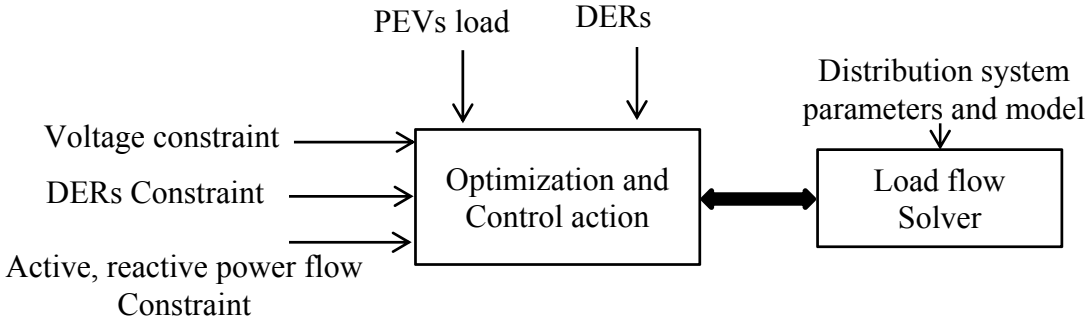

Figure 3.5 Probabilistic Power Flow Architecture

In the distribution system, the load flow solver is used through a robust iterative technique based on a ladder network [129]. This method is used instead of the typical power flow methods (e.g. Newton-Raphson) which are used in the transmission system. The reason of using a ladder network is due to the high resistance to reactance (R/X) ratio of the distribution feeders compared to that of the transmission system. Fig. 3.6 shows the basic steps for applying the ladder network method to solve the load flow problem in the distribution system.

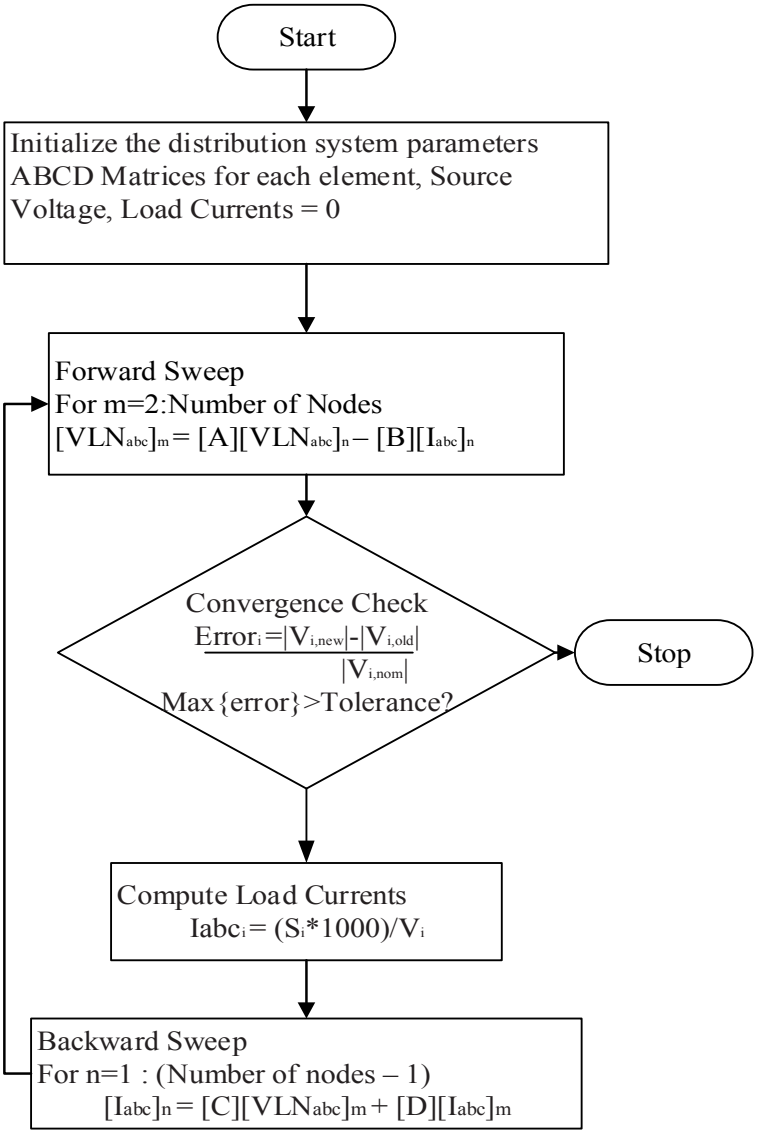

Figure 3.6 Outline of the Backward Forward Algorithm

3.5 Summary

The Transactive Energy (TE) control platform is presented in this chapter, the basic elements required to implement the TE control algorithm are introduced, and the multi-agent system characteristic and mathematical rules are formulated. Moreover, the agent communication protocol is described and discussed. The multi-agent was designed to work in cooperative manner, the cooperative operation of the multi-agent has the advantage of both distributed control (e.g. each agent is capable of taking the optimal decision, and the centralized control (e.g. central agent can transfer data and request action from the local agents).

The sequential Nash bargaining is applied to maximize the payoff of each agent and ensure all agents reach a state of consensus.

The next chapter presents the proposed mathematical modeling for PEVs and DERs. Also, the mathematical formulation for the TE control platform is introduced.

Chapter 4: System Modeling and Mathematical Formulation

4.1 Introduction

In order to achieve the outlined research objectives, proper mathematical modeling of electric power distribution system components needs to be developed.

This chapter will introduce an overview of system modeling including the Plug-in Electric Vehicles (PEV) charging demand, Distributed Energy Resources (DERs) and the load probabilistic model as well as the home and neighborhood management systems involving day ahead load forecasting and multi-agent cooperative control implementation.

4.2 Plug-in Electrical Vehicles Charging Demand Model

PEVs charging can be described as a stochastic process since it involves many uncertainties such as the distance traveled, the time at which the vehicles start charging, the charging level (120 Volt or 240 Volt), and the vehicle location.

Since the charging demand of PEVs contains many uncertainties, a probabilistic approach should be used to accurately determine the most probabilistic solution. In this research, Monte Carlo Simulations will be used to address the uncertainty associated with PEVs charging process.

Monte Carlo methods are one of the most common approaches to provide a probabilistic solution for stochastic problems involving several uncertainties. MC uses a random number generator and applies a sampling technique over a large number of trials (repeating the event that have randomness). The effects of randomness are lessened to an extent where analysis can be drawn to the probabilities of different events.

In the literature [130-131], there are many different methods used to mathematically represent the MC simulation process. In this research, the inversion cumulative distribution function is used [132]. This method is based on sampling of a uniform random number U in the range of (0, 1). If the random variable under investigation is $F_x(X)$, the value of X can be calculated based on (4.1).

$$X = F_X^{-1}(U) \quad (4.1)$$

Fig. 4.1 shows an illustration of this process. The cumulative distribution function of the random variable X is on the right hand side and the cumulative distribution function of U is on the left hand side. Since the CDF of X and the CDF of U is a one-to-one correlation, the probability of U is found then the same probability is used on the right-hand side to evaluate the value of (x).

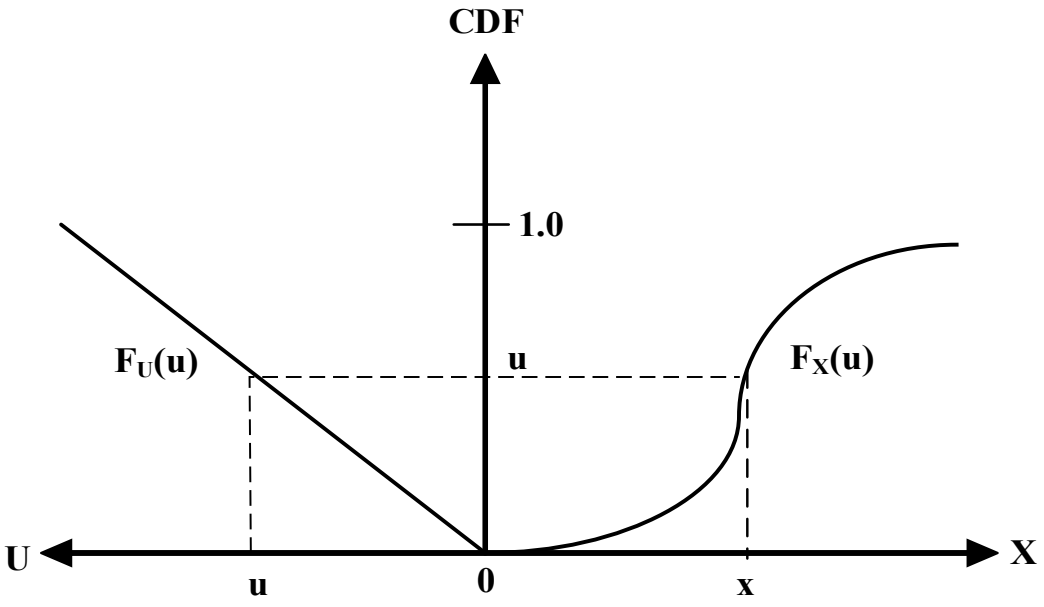

Figure 4.1 MCS Inverse Transform Technique

Different institutions worked to collect data from the vehicles owners to predict the daily distance traveled and the charging time (which can be assumed to be the time when people arrive home from work). The National Household Travel Survey (NHTS) [133]

is one of the institutions that collects these data which is used to generate the cumulative distribution functions shown in Fig. 4.2. The CDFs were sampled in the MCS based on the inverse random number generation explained earlier.

The process to represent the stochastic parameters (e.g. charging daily profile) of the PEVs was calculated in three steps:

1) Sampling the mileage (km) driven using the CDF shown in Fig. 4.2-a.
2) Based on the selected mileage (km) driven the energy required (E_{rec}) from the battery can be evaluated using algorithm 4.1 [27].
3) Then the charging start time can be calculated based on the sampling of home arrival times that are represented by the CDF as shown in Fig. 4.2-b.

Applying these three steps, the vehicle charging profile can be estimated, and added to the house load profile.

In order to estimate the amount of PEVs (N_{veh}), equation (4.2) can be used where P is the PEVs penetration, N_{houses} is the number of residential house, and $\propto$ is the average vehicle per house, which assumes to be two vehicles/house [133].

$$N_{veh} = P \times N_{houses} \times \propto \quad (4.2)$$

Two different charging levels are available in most residential homes in North America, namely level 1 (120 V) AC and level 2 (240 V) AC and are used in this work. Data for the two charging levels are shown in Table 4.1 [134].

Fig. 4.3 shows the connection of PEVs in the distribution system, while Fig. 4.4 shows a sample of the evaluated neighborhood vehicles charging profile seen by the electric distribution utility.

Table 4.1 Plug in Electric Vehicles Charging Station Specification

Charging level	Rated current	Rated power	Miles Added Per Hour
Level 1 (120 volt)	12 A	1.4 kW	5
Level 2 (240 volt)	16/ 32 A	3.3/6.6 kW	11/22

Algorithm 4.1 The Energy Required from PEV Battery [27]

1: **Start**

Inputs: E_b, d, ε, and η

2: The minimum state of charge of electric vehicles constraint

$$SOC_{min} = \begin{Bmatrix} 30\ \% & if\ vehicle\ type\ PHEV \\ 5\ \% & if\ vehicle\ type\ AEV \end{Bmatrix} \quad (4.3)$$

3: energy consumed by electric vehicle battery

$$E_{con} = \frac{d \times \varepsilon}{E_b} \quad (4.4)$$

4: The battery finial state of charge value

$$SOC = \max\{(1 - E_{con}), SOC_{min}\} \quad (4.5)$$

5: The required energy to full charge the electric vehicles battery

$$E_{rec} = \frac{(1 - SOC)}{\eta} \times E_b \quad (4.6)$$

Output: E_{rec}

6: **End**

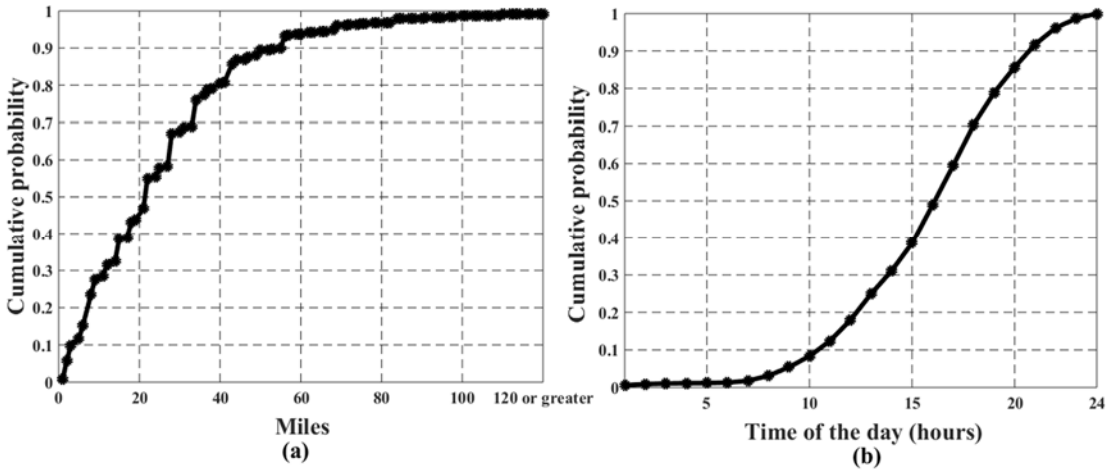

Figure 4.2 Cumulative Distribution Function for (a) Mileage Driven and (b) Home Arrival Time

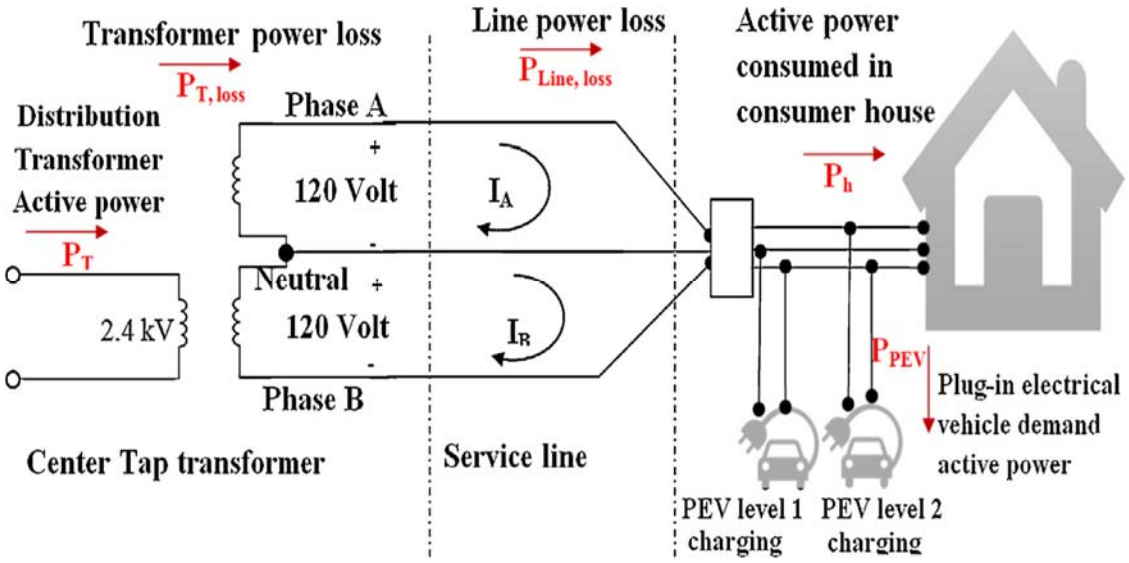

Figure 4.3 Plug-in Electric Vehicles Connected to Secondary Distribution System [29]

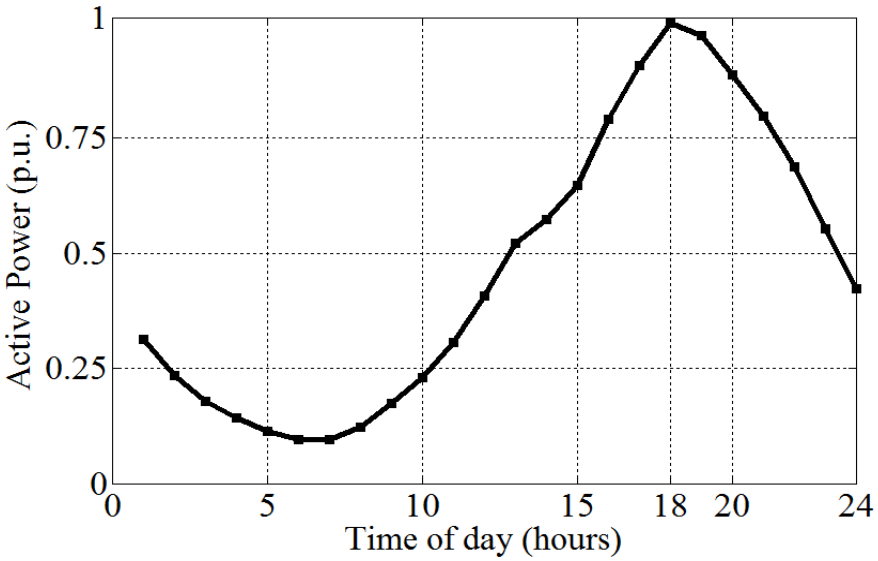

Figure 4.4 Typical Daily PEVs Charging Profile

4.3 Distributed Energy Resources Modeling

In this section, the modeling of the DERs is described. The author selected the most popular types of DERs used nowadays in the distribution system [135], which include Wind DERs, rooftop solar photovoltaic DERs, and Battery energy storage DERs. The modeling, mathematical representation, and implementation are explained in detail in the following subsections.

4.3.1 Wind DERs

The power generated from wind DERs mainly depends on the wind speed profile. The biggest challenge when solving the probabilistic power flow problem is how to select the wind profile as it changes all throughout the year. One of the most suitable solutions is to group days with similar wind speed profiles and to use these data to construct a CDF for the probability of each profile to exist. This CDF can then be used later for sampling in the MCS.

In this work, the days with similar attributes are gathered together using a k-means partitioning clustering technique [136]. The only problem when using k-means is to determine the best number of clusters (days to represent the dataset); therefore, it is important to develop a means to evaluate the goodness of clustering.

The wind DERs model starts with identifying a yearly wind speed dataset. In this work, the wind speed from the "National Climatic Data Center" (NCDC) [137] is used after pre-processing is completed to remove any anomalies.

Then K-means is applied to the dataset. Most previous studies use the sum of the squares errors (SSE) as the main index to identify the quality of the evaluated clusters. However, the SSE does not involve the statistical distribution of wind speed data and significantly increase the number of wind profile clusters.

In order to overcome the problem of using the SSE as the index to determine cluster quality, a new validity index called the cluster distribution validity (CDV) index was developed in this work. The CDV index determines the most suitable number of clusters calculated by k-means, taking into account the distribution of wind speed. The CDV index is different from SSE as it works on improving the goodness of clustering while

aiming to find the smallest number of wind profiles that keeps the statistical characteristics associated with the wind speed data.

The Weibull distribution function [138] has been always used to represent the probability distribution of wind speed data according to (4.7).

$$f(v) = \left(\frac{k}{c}\right)\left(\frac{v}{c}\right)^{k-1} e^{\left(-\frac{v}{c}\right)^{k}} \quad \text{With, } k = \left(\frac{\sigma}{\bar{v}}\right)^{-1.086} \quad \text{and } c = \frac{v}{\Gamma\left(1+\frac{1}{k}\right)} \qquad (4.7)$$

The CDV index computes the corresponding probability distributions and compares between the one found from the k-mean and the parameters found from the original dataset. Algorithm 4.2 outlines the process used to evaluate the quality of clustering using the validity index.

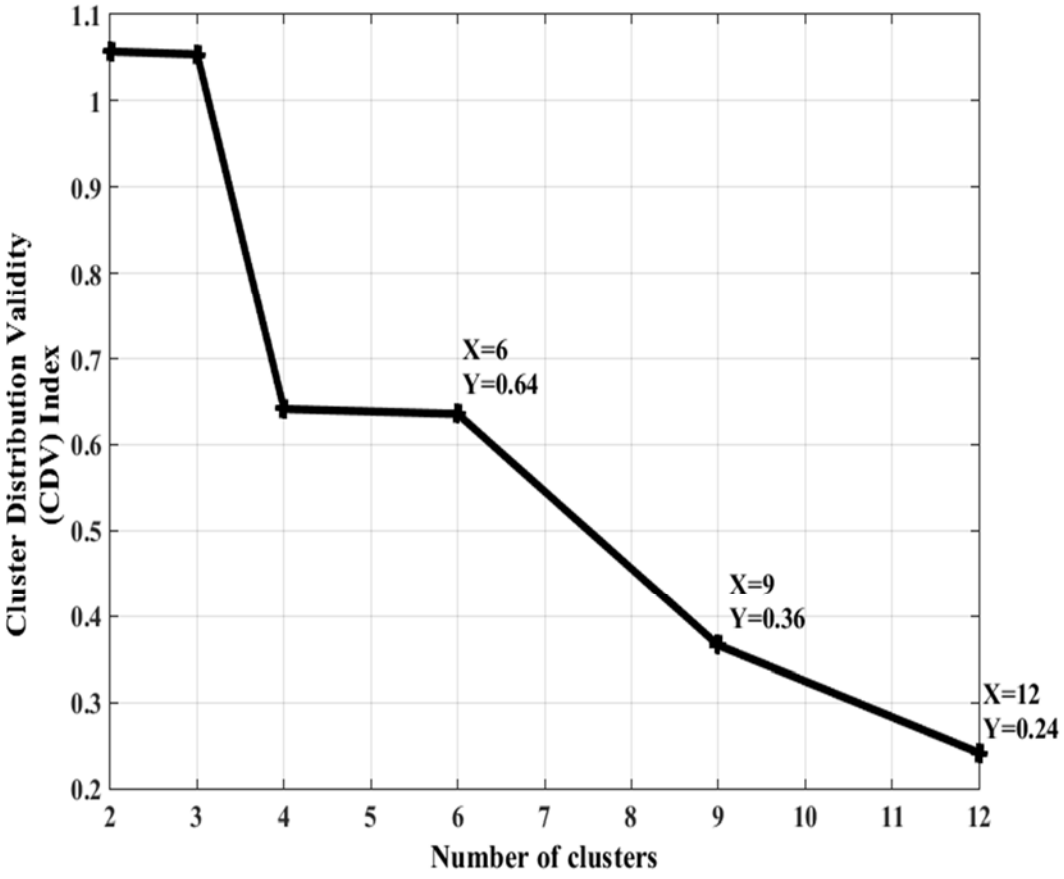

Figure 4.5 Cluster Validity Index for the Wind Speed Dataset

Algorithm 4.2 Representative Wind Speed Profiles Computation [27]

1: Start

Inputs: NCDC wind speed profile dataset (365×24)

N_{min}, N_{max}: minimum and maximum number of cluster (1 and 40, respectively).

J: Trials number 100

2: Calculate (c_0, k_o) Weibull parameters for original wind speed dataset.

3: **For** j = 1 : 1 : J **Do**

4: **For** i = N_{min} : 1 : N_{max} **Do**

5: Apply k-mean algorithm to partition the data set into i clusters

6: Compute Weibull parameters (c_i, k_i) according to (4.7)

7: Calculate the difference between the distribution parameters of cluster group i and the original data set.

$c_{diff,i} = |c_i - c_0|$ and $k_{diff,i} = |k_i - k_0|$

8: **End for**

9: Compute the maximum difference in c and k parameters

$c_{diff,max} = \max\{c_{diff}\}$ and $k_{diff,max} = \max\{k_{diff}\}$. (4.8)

10: Calculate the CDV_i index

$$CDV_i = \left(\frac{C_{diff,i}}{C_{diff,max}}\right)\left(\frac{K_{diff,i}}{K_{diff,max}}\right) \quad (4.9)$$

11: Compute the minimum CDV

$CDVmin_j = \min\{CDV_i\}$ (4.10)

12: **End for**

Output: The numbers of clusters represent the wind profile that corresponds to most frequent minimum CDV over J trial.

13: **End**

Fig. 4.5 shows the CDV index after running Algorithm 2 for 100 trials. The figure reveals that the minimum value of CDV index occurs at 12 clusters. However, at nine clusters a knee can be observed. The use of nine cluster will reduce the number of clusters without losing the goodness of the representative wind profile.

It can be also observed that 40 clusters are needed to bring the SSE to a minimum value if the SSE used as the cluster goodness index as shown in Fig. 4.6.

Fig. 4.7 shows the selected wind speed profiles of the nine clusters which represent the whole dataset. While Table 4.2 lists the wind speed profiles cluster and how many days each cluster represent, and the frequency of occurrence of each cluster (number of days each cluster represents divided by the number of days of one year). The frequency of occurrence will be used in MCS to determine which wind profile should assigned to each trial.

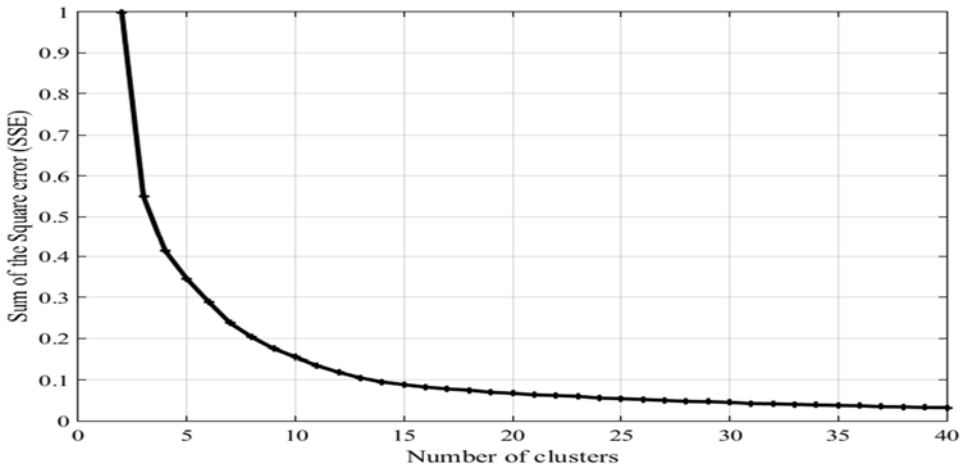

Figure 4.6 Sum of the Square Error for the Wind Speed Clusters

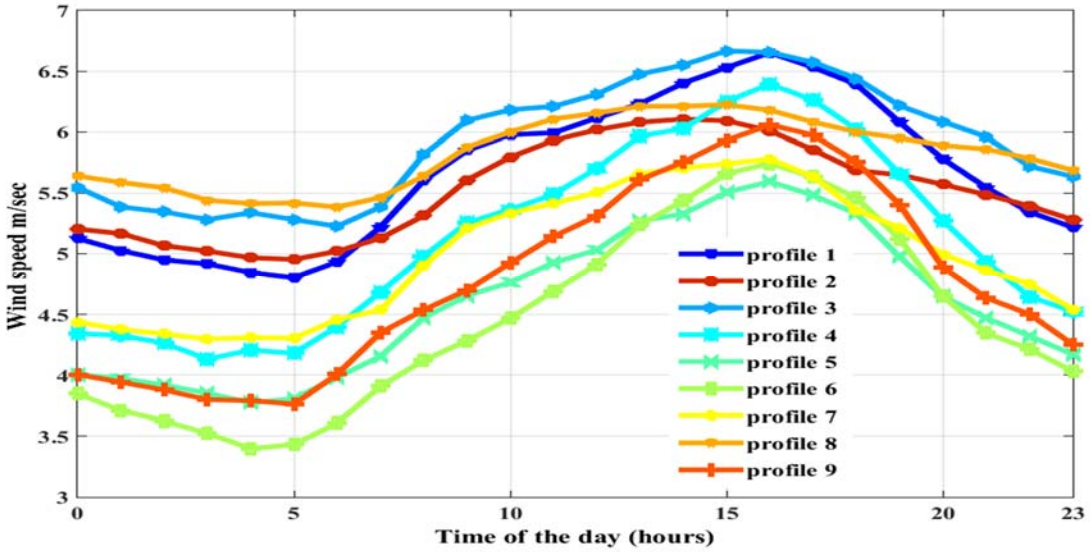

Figure 4.7 Representative Wind Speed Profiles Obtained Using the CDV Index

Table 4.2 Representative Wind Speed Profiles Frequency of Occurrences

Profile number	Number of days	Frequency of occurrence (%)
1	21	5.8
2	28	7.7
3	28	7.7
4	30	8.2
5	30	8.2
6	30	8.2
7	41	11.2
8	68	18.6
9	89	24.4

The evaluated wind speed profiles will be used as an input to equation (4.11) to estimate the injected power from wind DERs to the distribution system.

$$P_i = \frac{1}{2}\,\rho_0 A\, v_i^3 CP \qquad (4.11)$$

Where CP is the power coefficient, v_i is the wind speed, P_i is the power output, A is the swept area of the wind turbine rotor, and ρ_0 is the reference air density.

4.3.2 Rooftop Solar Photovoltaic DERs

The mathematical model of a solar PV is explained in this subsection. Also the model representation and the uncertainty associated with the power generated from the PV are discussed in detail.

According to [139], the power generated from PV (P_{PV}) is given by (4.12). The main factors affect the generated power is the PV array surface area (A_C), solar irradiance ($IR_{s\beta}$), and the PV efficiency η.

$$P_{PV} = A_C \times \eta \times IR_{s\beta} \qquad (4.12)$$

The irradiance can be calculated as follow:

$$IR_{s\beta} = \left[G_{sb} + \left(\frac{1+\cos\beta}{2} - G_{sb}\right) \times X_s + \rho \times \frac{1-\cos\beta}{2}\right] \times R_{st} \qquad (4.13)$$

Once the $IR_{s\beta}$ is calculated, the cell temperature, cell voltage, and current can be calculated which will be used to calculate the total output electric power from the PV.

$$T_c = T_a + IR_{s\beta} \times (\frac{T_{OT} - 20}{0.8}) \quad (4.14)$$

$$I = IR_{s\beta} \times [I_{sc} + k_i(T_c - 25)] \text{ , and } V = V_{oc} - (k_v \times T_c) \quad (4.15)$$

$$P = FF \times V \times I \quad \text{, and} \quad FF = \frac{V_{mpp} \times I_{mpp}}{V_{oc} \times I_{sc}} \quad (4.16)$$

The total installed capacity of the rooftop solar PV (N_{PV}) distribution system is given by the following equation.

$$N_{PV} = \sum_{i=1}^{NHouses} \beta_i \quad (4.17)$$

Where (β) is the PV capacity in kW, in each house. The PV capacity can vary from 10 kW (maximum solar PV rated power per house according to [7]) to 0 kW (no PV) with 2-kW step change in rated PV power. The details of 2 kW, and 10 kW solar PV parameters can be found in appendix A [140].

The other important parameter affecting the PV model is the weather data. The same procedure for the uncertainty in the wind speed profile is followed with the weather temperature and irradiance. First, one year of data is collected and preprocessed to remove any erroneous or missing data, and Toronto weather station data are used in this work [141].

Fig. 4.8 shows the temperature/ irradiance dataset. The k-mean clustering [136] is applied to the preprocessed dataset, and the optimal number of clusters is chosen based on the knee point of the SSE versus the number of clusters curve which shown in Fig. 4.9.

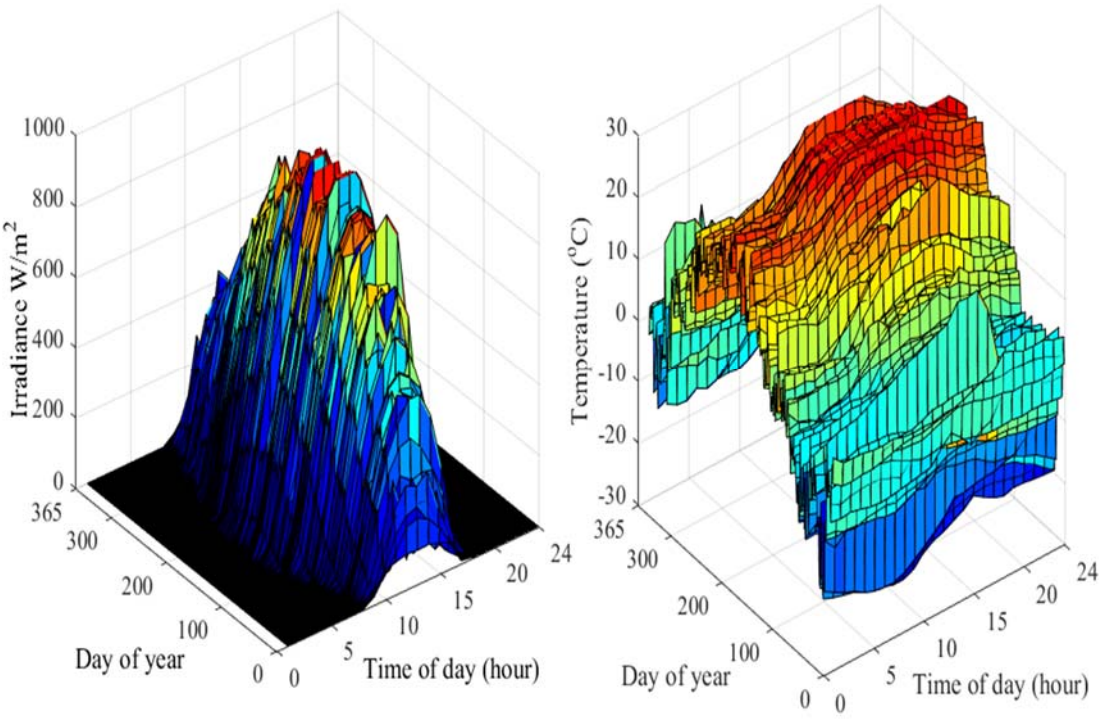

Figure 4.8 Yearly Irradiance and Temperature Profiles

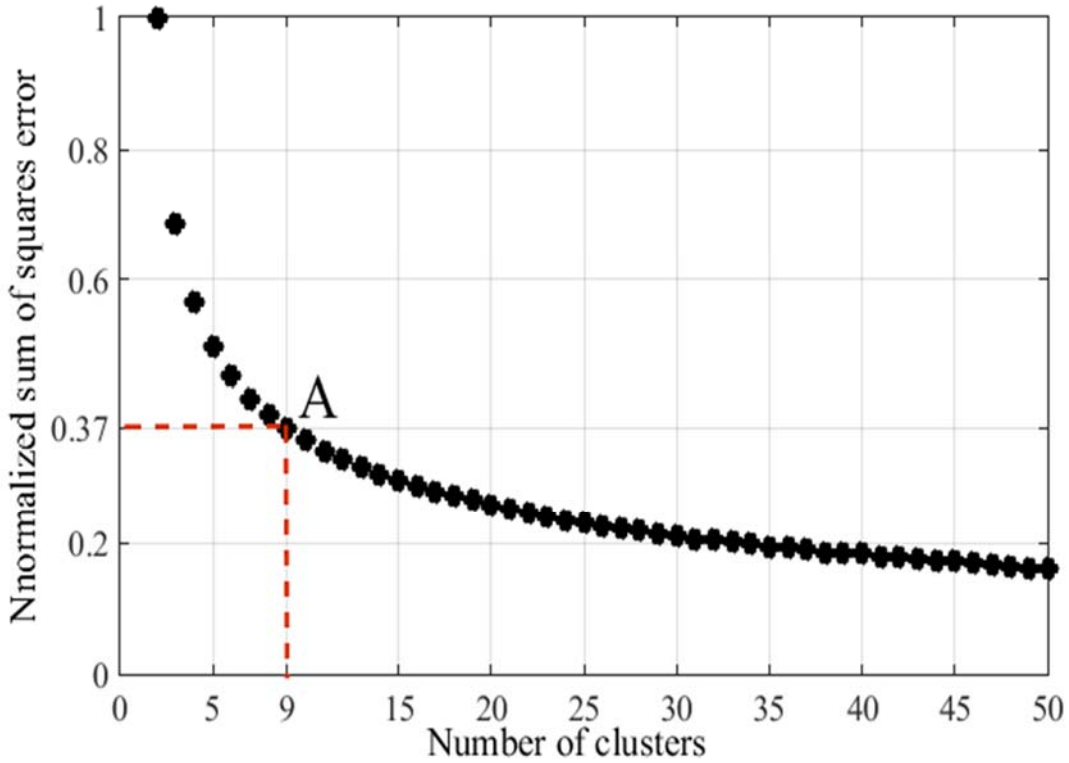

Figure 4.9 Sum of Squares Error (SSE) for Irradiance and Temperature Dataset

The maximum of successive differences [142] of λ_{SSE} (k) is used to find the knee point of the SSE curve.

The three consecutive points on the SSE curve are used to determine the maximum value of λ_{SSE}, the value of λ_{SSE} (k) can be zero (if the three points are aligned), positive or negative (if the three points change the SSE curve slope). The maximum value of λ_{SSE} happens to occur at the knee point of the curve. Once the knee point in SSE curve is determined, the number of cluster at this point will be selected as the optimal number of clusters.

Visual inspection of Fig. 4.9 show that the knee point (labeled A) was found to happen when the SSE have a value of 0.37 that corresponds to the optimal number of cluster (9 clusters). This nine clusters representing the 365 irradiance and temperature data collected from the Toronto weather station.

$$\lambda_{SSE}\,(k) = SSE\,(k-1) + SSE\,(k+1) - 2 \times SSE(k). \qquad (4.18)$$

The details of the nine optimal clusters which will be used in MCS are shown in Fig. 4.10 and Table 4.3.

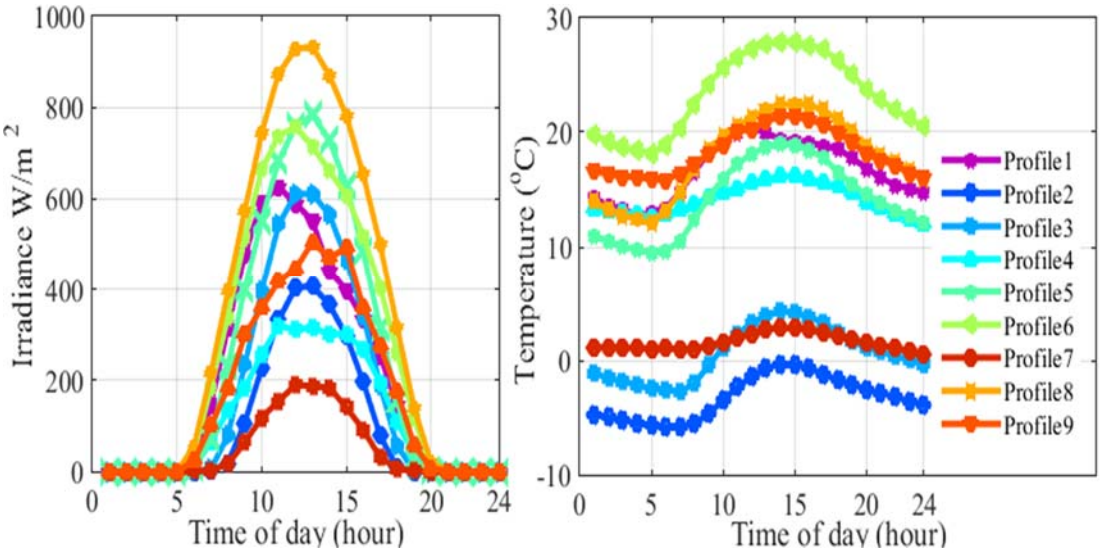

Figure 4.10 Representative Irradiance and Temperature Profiles

Table 4.3 Representative Temperature/ Irradiancy Profiles Frequency of Occurrences

Profile number	Number of days	Frequency of occurrence (%)
1	22	6.1
2	50	13.6
3	32	8.8
4	26	7.1
5	37	10.1
6	37	10.1
7	93	25.5
8	46	12.6
9	22	6.1

4.3.3 Energy Storage System

One of the challenges facing the researchers when using Energy Storage System (ESS) is how to justify the cost of the battery? In order to minimize the cost of the storage system, the optimal battery size should be determined. However, the ESS sizing must be calculated based on the function required from ESS.

Developing new ESS functions could be the best solution to justify the ESS cost either if they installed on homeowners' properties or in the electric utility's system. In this work, the authors investigated different ESS functions (existing and new functions) in order to select the optimal ESS single or multiple functions that should be used in the distribution system to satisfy certain objectives.

In this section, the basic mathematical and parameters of energy storage model are discussed, and as well the mathematical representation of ESS function (objective, constraints) is presented.

4.3.3.1 Mathematical Modelling of Energy Storage System

The lifetime and the performance of ESS are determined based on the battery cycle depth of discharge (DOD). However, the battery state of charge (SOC) determines the remaining energy in the storage system which will affect the decision taken by the

Battery Management System (BMS) in which function should be executed. The SOC is given by [143]:

$$SOC = \frac{S(t)}{S_{reference}(t)} \quad (4.20)$$

where S (t) is the battery capacity at time t, $S_{reference}$ (t) is the battery capacity reference which depends on the required DOD level [144](a limit that storage cannot work behind it), the higher level is the better for the battery life time.

The determination of the SOC is essential to the BMS for real-time operation, the SOC calculation is usually considered a difficult task as it depends on the temperature and the state of the life of the battery system. Coulomb-counting based estimation [145] is a well-known method for determining the SOC and it uses the integration of the measured current over time as given in (4.21). Fig 4. 11 shows the cell voltage versus the measured SOC for lithium-ion battery. It is worth noting that the minimum SOC depends on the temperature and the designed DOD which affects the battery's lifetime.

$$SOC\ (t) = SOC\ (0)\ \pm \frac{1}{Q} \int_0^t I(t)\ dt \quad (4.21)$$

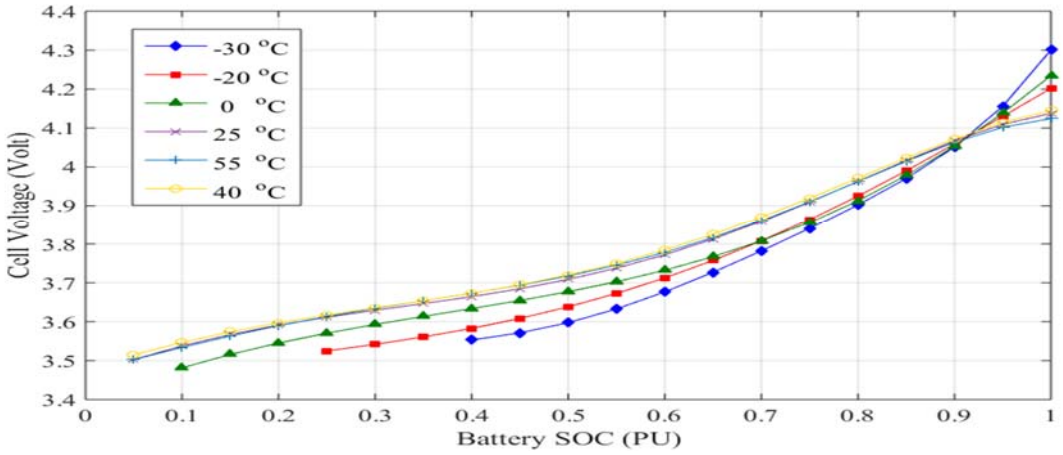

Figure 4.11 Battery State of Charge Characteristics at Different Ambient Temperature

The cost of ESS is given in (4.22)

$$C_{over} = C_s \times S + C_p \times P \quad (4.22)$$

Where P is the power rating for the energy storage, S is the storage system capacity, C_s, C_p indicate the storage cost, the typical values for C_s, C_p is given in [146].

4.3.3.2 Energy Storage Functions

The BMS decision is usually based on the battery SOC calculation, which will determine the optimal charging and discharging time to perform the required functions from the ESS, taking into consideration all system constraints.

Three different ESS functions namely: Home Owner Comfort (HoCom); Peak over Average Power Reduction (PAPR); and System over Load Reduction (SOLR) are considered in this work. The three functions are formulated and discussed to determine the system performance under each function, and as well the electric utility and customer cost/ benefit.

A. Home Owner Comfort (HoCom)

This function is designed to maximize the benefit of homeowners and to ensure his satisfaction by maximizing the savings in the monthly electricity bill and by decreasing the power interruption time in the case of electric utility power system failure. This function can be mathematically formulated as: function can be mathematically formulated as:

$$\max f = \sum_{t=1}^{T} \mathrm{C}_t \times P_{sto_t} \times \Delta t \qquad (4.23)$$

where f is the objective function, C_t is the price of unit energy ($/kWh), T is the total time, t is the instant time, and Δt is the period duration, P_{sto} is the storage power (kW). It is worth noting that the storage has three modes of operation; ideal mode in which the storage power equal to zero, charging mode in which the storage power is negative, and discharging mode in which the storage power is positive.

The objective function is subject to the following constraints:

$$E_{min} \leq E_{sto_t} \leq E_{max} \qquad \forall\, t \in T \qquad (4.24)$$

$$-P_{Rated} \leq P_{sto_t} \leq P_{Rated} \qquad \forall\, t \in T \qquad (4.25)$$

In this work, the energy unit price is set based on the TOU pricing.

B. Peak over Average Power Reduction (PAPR)

In this case the energy storage located in consumers' home and/or pole top transformer, the ESS are working to minimize the ratio between the maximum power seen by the distribution transformer and the average load profile during one day of operation. The battery energy storage will try to shift the load to flatten the load curve seen by the distribution transformer to minimize the transformer loss of life. The PAPR function can be mathematically formulated as following:

$$\min f = \frac{\max[P_{TR}]}{P_{av.}} \qquad \text{With} \qquad P_{av} = \frac{\left(\sum_{t=1}^{T} P_{TR_t}\right)}{T} \qquad (4.26)$$

where P_{av} is the average power over one day of operation seen at the distribution transformer, and P_{TR_t} is the power supplied by the distribution transformer at hour t.

The same constraints in equations (4.24 and 4.25) are applied and are used in the optimization problem formulation. In addition to the previous two constraints, the residential energy storage is working for utility control as any DG in primary or secondary distribution system in this case additional constraints need to be added to the optimization formulation which formulated and given in Eq. 4.27 and 4.28.

These constraints include the service voltage at each house which should be maintained within the limits defined in ANSI standards C84.1 [147], and the power flow constraint:

$$V_{min} \leq V_t \leq V_{max} \qquad \forall\, t \in T \qquad (4.27)$$

$$P_{G_t} + P_{sto_t} - P_{LL_t} - P_{TL_t} - P_{D_t} = 0 \qquad \forall\, t \in T \qquad (4.28)$$

Moreover, after determining the optimal control profile for the residential storage, the negotiation (utility offer money (bids) to customer) between the utility agent and the home agent to reach an agreement in order to allow the utility to execute the designed control action to the home energy resources. The required bids are determined using the ultimatum game theory as explained in section 3.3.3.

C. System over Load Reduction (SOLR).

This newly developed function in this work tries to satisfy both the electric utility and end user by keeping the profits and saving of homeowners and remove the distribution transformer overload while keeping the transformer loss of life in its normal values.

The BMS will optimize the charging and discharging rate and time, to keep the power flow over the secondary distribution at certain permissible limit which is pre-defined by electric utility. The SOLR function can be formulated as follows:

$$\min f = \frac{\max(S_{TR})}{S_{TR_{rated}}} \qquad (4.29)$$

where $S_{TR_{rated}}$ is the rated power of distribution transformer (i.e. 25 kVA or 50 kVA).

The objective function is subject to the constraints given in (4.24- 4.25- 4.27 and 4.28) and the additional inequality constraint:

$$S_{TR_{min}} \leq S_{TR_t} \leq S_{TR_{max}} \qquad \forall\, t \in T \qquad (4.30)$$

$$S_{TR_{min}} = (1 - X) \times S_{TR_{rated}} \qquad (4.31)$$

$$S_{TR_{max}} = (1 + X) \times S_{TR_{rated}} \qquad (4.32)$$

where $S_{TR_{min}}$is the minimum power that should be imported from the distribution transformer to increase the overall efficiency, $S_{TR_{max}}$ is the maximum allowable

overload power, X is permissible overload limit which is pre-defined from electric utility.

4.4 **Distribution Transformer Overload and Loss of Life**

The following three indices need to be calculated in order to assess the impact of PEV on the distribution transformer [27]: the transformer overload, the transformer hotspot temperature, and the transformer loss of life. In this section, the mathematical formulation of the three indices is introduced.

In order to determine the transformer percentage overload ($ST_{Overload}$), the measured power flow on each side of the distribution transformer is compared to the transformer rating. The percentage overload on side A or side B can be calculated using [30] (4.33).

$$S_{Side_{overload}} = \frac{S_{Side_{measured}}}{S_{Side_{rating}}} \times 100 \qquad (4.33)$$

where the subscript 'side' is used to represent either side A or side B of the center-tapped distribution transformer. Fig. 4.12 shows the equivalent circuit of the center-tap transformer which are commonly used in North America.

The transformer overall percentage overload can be calculated by taking the arithmetic mean of the percentage overload on side A, and side B according to (4.34).

$$ST_{overload} = \frac{SA_{overload} + SB_{overload}}{2} \qquad (4.34)$$

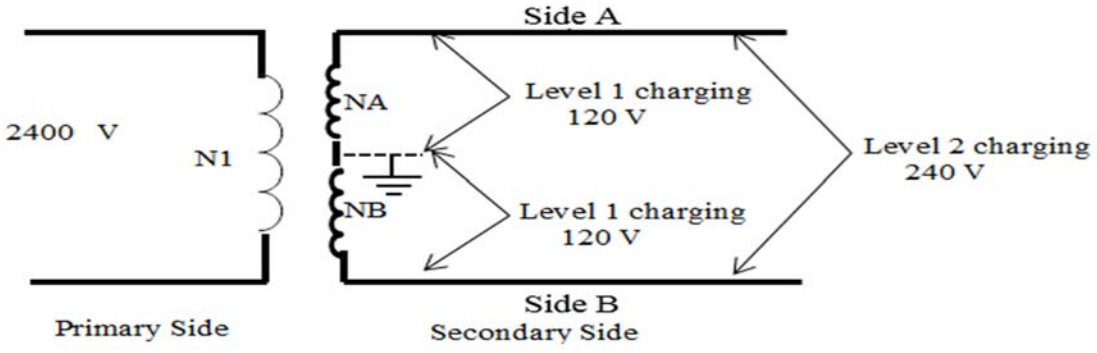

Figure 4.12 Center Tab Distribution Transformer

The transformer lifetime is defined as "the total time between the initial state for which the insulation is considered new and the final state for which dielectric stress, short circuit stress, or mechanical movement, which could occur in normal service, and could cause an electrical failure" [148]. The lifetime of the transformer is highly affected by the loading conditions, which affect the transformer insulation and may lead to early dielectric break-down.

According to the IEEE Std. C57.91 [148], the aging acceleration factor (F_{AA}), and the equivalent aging acceleration factor (F_{EQAA}) of one day of operation need to be calculated to determine the percentage daily loss of life (LOL) as given in (4.35-4.37)

$$F_{AA} = e^{\left(\frac{15{,}000}{110+273} - \frac{15{,}000}{\theta_H+273}\right)} \tag{4.35}$$

$$F_{EQAA} = \frac{\sum_{n=1}^{N} F_{AA_n} \times \Delta t_n}{\sum_{n=1}^{N} \Delta t_n} \tag{4.36}$$

$$\%\ \text{Loss of life} = \frac{F_{EQAA} \times t \times 100}{\text{Normal insulation life}} \tag{4.37}$$

It is clear from (4.35) that the transformer LOL mainly depends on the transformer hot-spot temperature (θ_H). The two parameters that control the change in θ_H are the average ambient temperature θ_A and the top-oil temperature θ_{To}, which can be calculated as follows:

$$\theta_H = \theta_A + \Delta\theta_{To} + \Delta\theta_H \tag{4.38}$$

$$\theta_{To} = \theta_A + \Delta\theta_{To} \tag{4.39}$$

where $\Delta\theta_{To}$ is the top-oil rise over ambient temperature, $\Delta\theta_H$ is the winding hottest spot rise over top-oil temperature in ˚C.

The value of $\Delta\theta_H$ and $\Delta\theta_{To}$ is mainly depend on the thermal and winding time constant, the ratio of the load value to its rated value, and the type of cooling system which is determined by the values of (n and m).

$$\Delta\theta_{To} = \Delta\theta_{To,R} \times \left[\upsilon + \left[\frac{K_i^2 \times R + 1}{R + 1} \right]^n \right] \quad \text{with} \quad \upsilon = \left[\left[\frac{K_U^2 \times R + 1}{R + 1} \right]^n - \left[\frac{K_i^2 \times R + 1}{R + 1} \right]^n \right] \times (1 - e^{-\frac{t}{\tau_{To}}}) \tag{4.40}$$

$$\Delta\theta_H = \Delta\theta_{H,R} \times \left[(K_u^{2m} - K_i^{2m}) \times (1 - e^{-\frac{t}{\tau_w}}) + k_i^{2m} \right] \tag{4.41}$$

It is worth noting that the transformer daily LOL should not exceed 0.0134% as recommended in [148]. Once the transformer LOL calculated the transformer life time can be calculated (e.g. if the yearly LOL equal 5% the transformer life time will be 20 years). Table 4.4 lists the thermal parameters of the 50-kVA transformer used in estimating the LOL [149].

Table 4.4 Thermal Parameters for 50 kVA Transformer

Parameters	Value
Top-oil rise over ambient at rated load	53 ^{o}C
Hottest-spot conductor rise over top-oil temperature, at rated load	27 ^{o}C
Ambient temperature	30 ^{o}C
Oil thermal time constant for rated load	6.86 hours
Ratio of load loss at rated load to no-load loss	4.87
Exponent of loss function vs. top-oil rise	0.8
Exponent of load squared vs. winding gradient	0.8

4.5 Optimal Management of HEMS and NAEMS Resources

One of the main component when designing the Home energy management system is to pre-schedule the home demands and determine the required control action for the energy

resources. The high accuracy load forecasting model can ensure the best performance of HEMs.

Once the day-ahead load forecast is determined the management system in both the home and the neighborhood will start to communicate and perform the optimal operation based on the TE multi-agent decisions execution.

In this section, the methodology used to predict a day ahead load of individual households is identified, and the multi-agent predefined functions and rules are described.

4.5.1 Day Ahead Load Forecasting

Due to the diversity of applications and business needs of load forecasting process, the process of predicting the load can be classified into three categories: short-term forecasts (i.e. one hour to one week), medium forecasts (i.e. a week to a year), and long-term forecasts (longer than a year).

Forecasting, by nature, is a stochastic problem rather than deterministic. The output of a forecasting process is supposed to be in a probabilistic form.

Most forecasting methods in the literature used statistical techniques or artificial intelligence algorithms such as regression, or neural networks [150]. A good forecasting model has to capture the features of the electric load data series.

The major factors driving the load profile are economy, climate, weather, human activities, and salient features of electric load series.

The accuracy of the load forecasting model mainly depends on two factors; the size of the historical load dataset; and the selected attributes (featured) used by the forecasting model.

4.5.1.1 Data Base

In order to build accurate load forecasting model, it needs to have enough database that will help to improve the forecasting accuracy. In addition to the electric load database, the proposed forecast model should include weather database and holidays.

In this research the hourly electric load data collected from six different loading segments from 2009 to 2015 are used [151]. The different load segments are used to represent the house load profiles with different consumption patterns (i.e. residential houses with non-electric heat, residential houses with electric heat, and residential houses applying time of use price, etc.). However, the load database extracted from [151] is not the same as the typical Canadian residential dwellings [152]. In order to adjust the load database to match the peak load given in [152]. The load profile given in [151] is normalized by dividing the daily load profiles by the peak annual demand. Then, the daily load profile is multiplied by the Canadian residential dwelling peak loads given in [152]. The weather data including the dry bulb temperature and the dew point temperature are included to complete the input set of the load forecast model. Fig. 4.13 shows a sample of the house electric load data for January 2015.

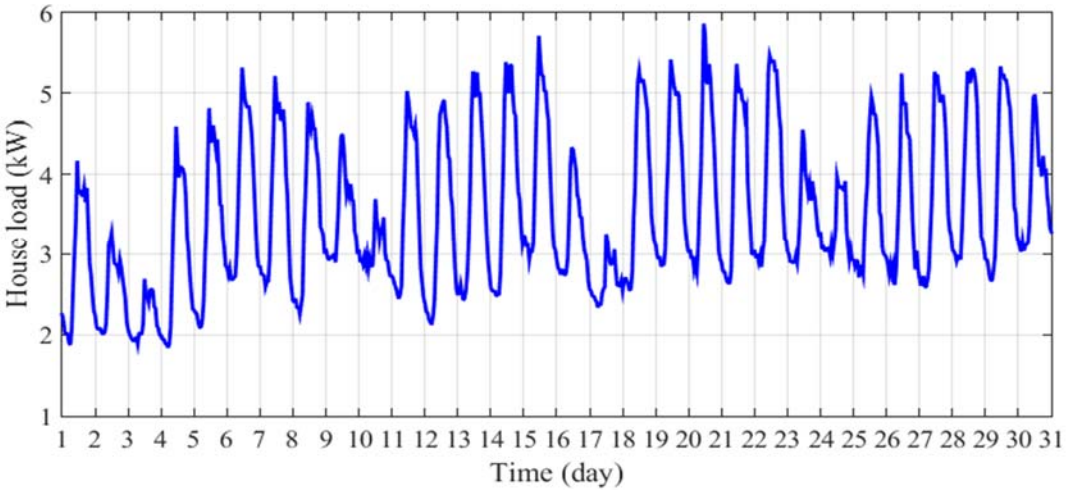

Figure 4.13 Sample of Historical Load Dataset (01-01-2015 to 01-31-2015)

4.5.1.2 Predictors Attributes

The load forecast model accuracy is based on the selection of the attributes. For each record in the database, ten different attributes are selected to be used by the forecasting algorithm. The attributes were selected to extract the maximum suitable future of the dataset to improve the load prediction accuracy. As explain earlier, the weather has a large impact on the people electric load consumption (heating or cooling unit) so that the temperature are selected to be the first two attributes for the load forecast model. The other attributes were selected to extract the pattern of the customers load consumption, which was done by correlating the demand with the time of the day and the day of the week and either if its weekday or holiday. Table 4.5 shows an example of the artificial neural network predictor output for Monday, February the 2nd, 2015. The selected attributes used in the load forecast model are listed below:

a) Dry bulb temperature

b) Dew point temperature

c) Hour of day

d) Day of the week

e) Holiday/weekend indicator

f) The previous 168 hours (previous week) lagged load (PWLL)

g) The previous 24 hours lagged load (PDLL)

h) Previous 24-hr average load (PDAL)

i) The previous hour average load (PHAL)

j) The most similar weather condition lagged load (SWLL)

Table 4.5 ANN Predictor Output

Dry bulb	Dew point	Hour	Day	holiday/ weekend	PWLL	PDLL	PDAL	PHAL	SWLL
-0.6	-8.9	1	2	1	1.94	2.90	3.03	2.73	2.56
-0.6	-8.3	2	2	1	1.95	2.96	3.02	2.69	2.89
0	-7.8	3	2	1	1.89	2.88	3.01	2.63	2.11
0	-6.7	4	2	1	1.89	2.97	2.99	2.57	2.01
0	-6.1	5	2	1	1.84	2.87	2.97	2.51	1.96
-1.1	-6.1	6	2	1	1.88	2.99	2.95	2.44	1.96
-1.1	-5.6	7	2	1	2.10	2.82	2.94	2.49	3.92
-1.1	-5	8	2	1	2.75	2.93	2.96	2.61	3.61
0.6	-4.4	9	2	1	3.43	2.85	2.99	3.32	3.56
2.2	-3.3	10	2	1	3.84	2.85	3.06	3.76	3.97
5	-2.8	11	2	1	4.59	3.16	3.14	4.39	4.92
5	-2.2	12	2	1	4.23	3.69	3.19	5.03	3.91
6.7	-1.7	13	2	1	3.96	3.44	3.24	4.92	3.57
6.1	-1.1	14	2	1	4.09	3.36	3.29	4.76	3.90
6.7	-1.1	15	2	1	4.09	3.18	3.35	4.58	2.63
7.2	-0.6	16	2	1	4.06	3.30	3.40	4.58	4.21
7.2	0	17	2	1	3.99	3.31	3.46	4.51	3.39
8.3	0.6	18	2	1	3.73	3.47	3.50	4.60	2.97
7.8	0.6	19	2	1	3.22	3.03	3.53	4.41	3.02
7.2	0.6	20	2	1	3.04	2.92	3.55	3.84	2.58
6.7	0.6	21	2	1	2.74	2.91	3.54	3.32	2.74
6.7	0	22	2	1	2.51	2.78	3.54	2.82	2.65
6.1	0	23	2	1	2.32	2.71	3.53	2.64	2.38
6.1	0	24	2	1	2.30	2.73	3.51	2.46	2.34

4.5.1.3 Model Implementation

The artificial intelligent algorithm is used to implement the load forecasting model. The outline of the procedure used in [153-154] are followed in this work, The Levenburg-Marquardt algorithm [155] is used to initialize and to train of the neural network, where the first six-year were used for training. However, the last year was used to test the model accuracy.

4.5.1.4 Model Accuracy

In order to estimate the model accuracy, the mean absolute error (MAE), mean absolute percent error ($MAPE$) [156] are used to quantify the performance of the forecaster as following.

$$MAE = \frac{\sum_{t=1}^{Y} |P_{Ac_t} - P_{Fc_t}|}{Y} \tag{4.42}$$

$$MAPE = \frac{\left[\sum_{t=1}^{Y} \frac{|P_{Ac_t} - P_{Fc_t}|}{P_{Ac_t}} \times 100\right]}{Y} \tag{4.43}$$

Where P_{Ac_t}, P_{Fc_t} are the actual and forecasted load, Y is the number of hours per year (8760).

Figs. 4.14-a and 4.14-b show a comparison between the actual load and the predicted load for one year, visual inspection of Figs. 4.14-a and 4.14-b show that the load forecasting model is always capable to achieve accurate predication and follow the actual loads in normal operating conditions. However, the model is unsuccessful when unexpected event in the power consumption occurred such as power interruption, for example in mid-March, the demand drops to zero this event the load forecast model was not able to recognize and predict it.

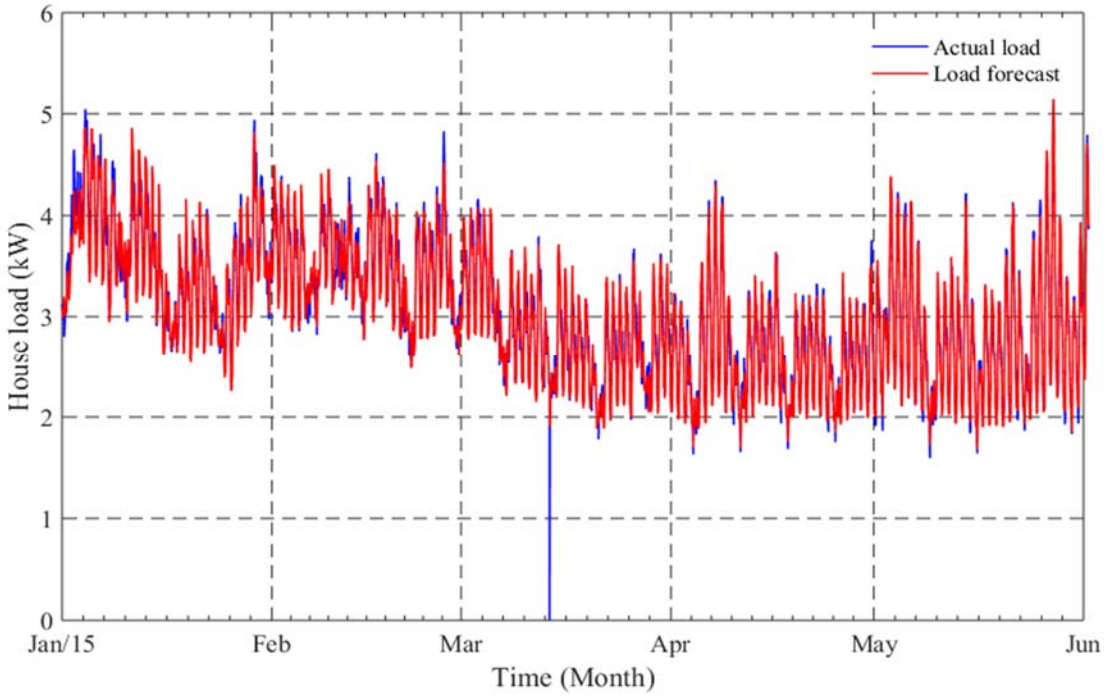

(a)

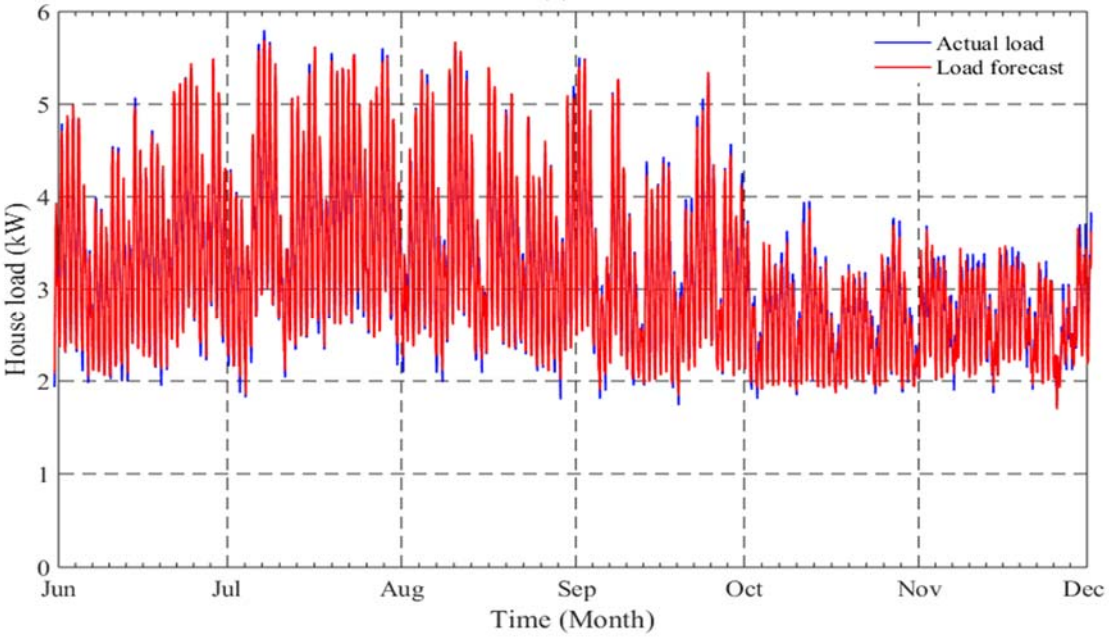

(b)

Figure 4.14 House Load Forecast against the Actual Load, a) Jan. 2015 to Jun. 2015, b) Jun. 2015 to Dec. 2015

Fig. 4.15 shows the box plot showing the median, the 25th percentile and the 75th percentile of the statistic percent forecast errors by hour of day for year 2015. The figure reveals that the maximum value of the median percent forecast errors over the hours of

day is 2%, and it is found that the hour 9 AM, 10 AM, 6 PM, 7 PM, and 8 PM have the highest percent forecast errors (i.e. when people leaving to their work and come back to their homes). Fig 4.16 shows the box plot of statistical percent forecast errors breakdown by the day of the week, and it can be noticed that Monday is the highest day had percent forecast errors due to the consumption change from weekend to the regular weekday. Fig 4.17 also shows the box plot of statistical percent forecast errors for the month of the year, and again it can notice that the median percent forecast errors is below two percent.

The analysis performed over the load forecast model and the result shown in Figs. 4.15, 4.16, and 4.17 prove that the load forecast model is reliable and all the required control action can be scheduled over the output of the model.

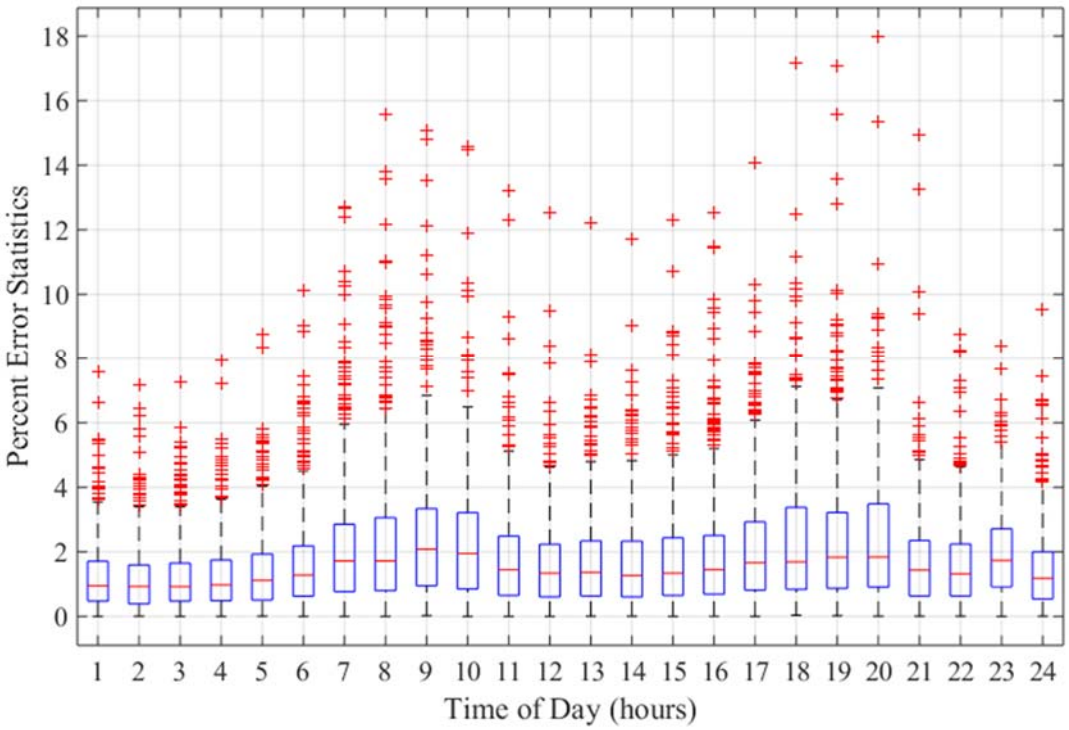

Figure 4.15 Breakdown of Forecast Error Statistics by Day Hour

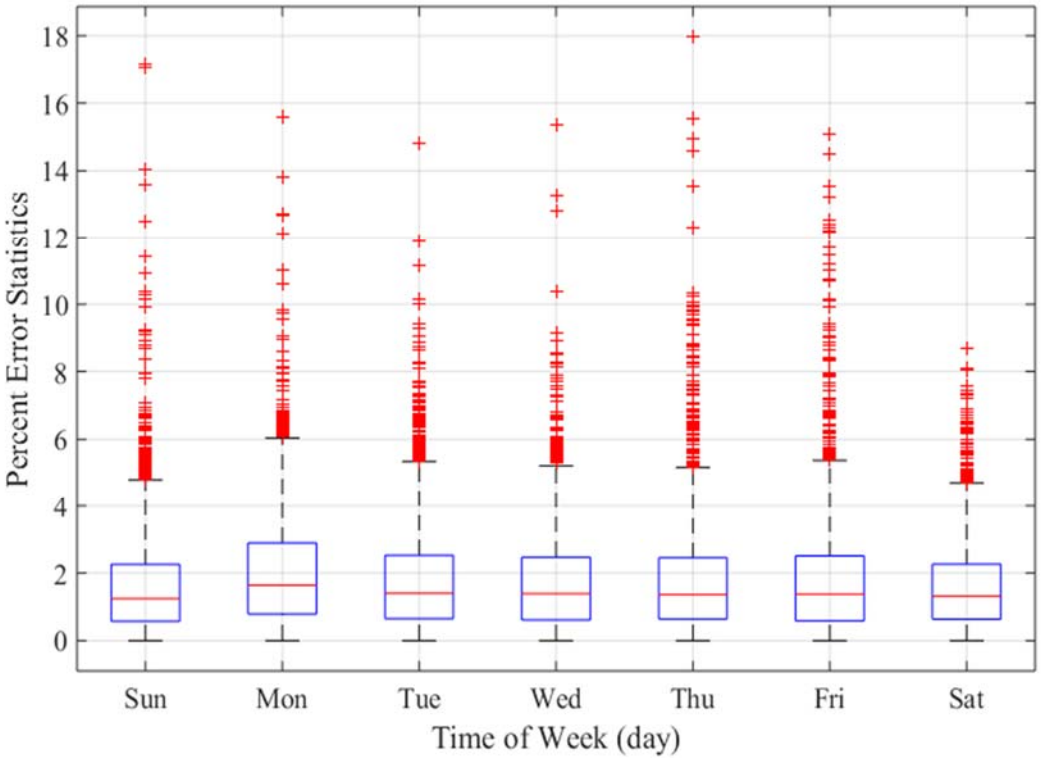

Figure 4.16 Breakdown of Forecast Error Statistics by Day of Week

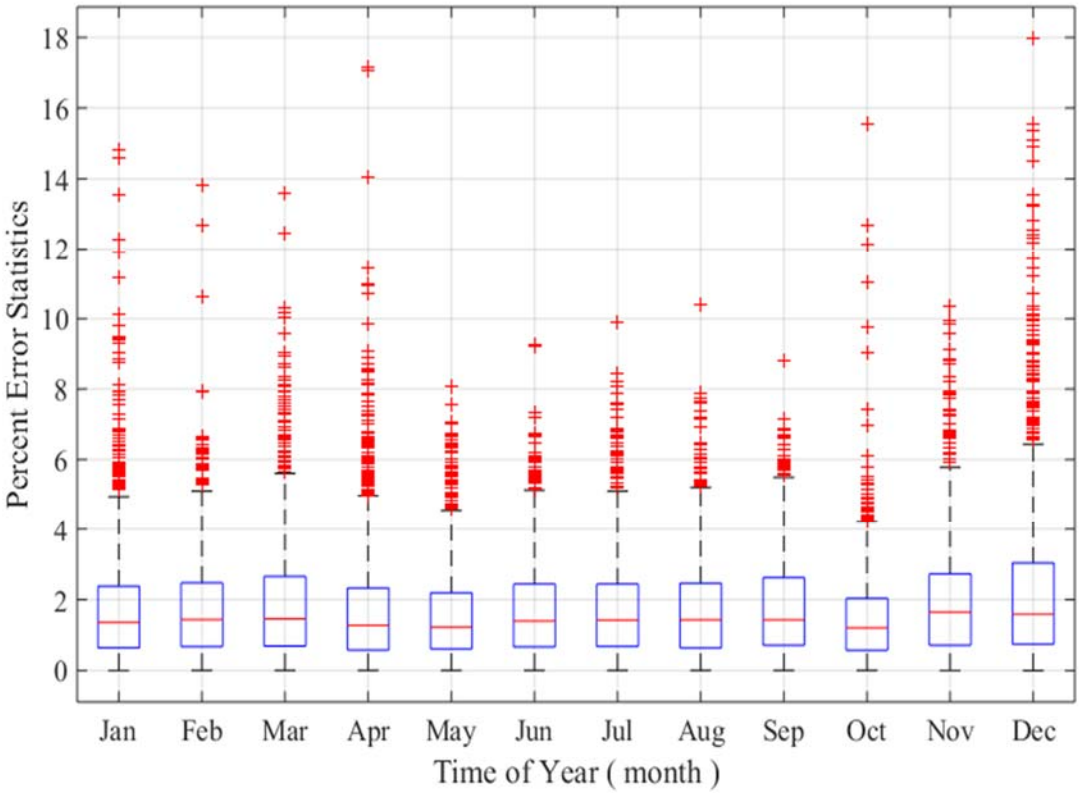

Figure 4.17 Breakdown of Forecast Error Statistics by Month

4.5.2 Implementation of the Transactive Energy Control Concept

The problem of changing the consumers' role in the smart grid operation is not a trivial task due to the conflict between the consumers' objectives (e.g., energy cost minimization, homeowners comfort maximization), and the electric utility's objectives (e.g., profit maximization, infrastructure upgrade cost minimization).

The proposed Transactive Energy (TE) control concept aims to coordinate the different agents that have a set of different objectives and requirements in an optimal way to satisfy both electric utility and homeowners.

As described earlier, the TE concept is implemented in this work by developing cooperative control between the multi-agents involved in the entire distribution system. For implementing TE control actions, three levels of agents are used in this work, namely electric grid agent, Neighborhood area energy management agent (NAEM agent), and home energy management agent (HEM agent).

The electric grid agent sends the electricity pricing and the required ancillary service and receives data and information from the NAEM agents.

NAEM agent is responsible for the neighborhood management (SDS) which includes a certain number of houses (e.g., 6 or 10 houses) that are supplied from a distribution transformer. The role of this agent is to coordinate between the agents in the residential area and reach an agreement between the grid agent and the HEM agents.

HEM agent is responsible for monitoring and controlling the consumer's devices (appliances and resources) to maximize the homeowners' objective.

In the agent initialization stage, each agent is registered and add itself to the Agent Management System (AMS) file for the communication purpose and add all the service

that he can perform in the directory facilitator (DF) file. The agents can communicate using the FIPA protocol and the ACL message form. Fig. 4.18 shows the agents architecture while Fig. 4.19 shows an example of the communication between the agents in different levels while. It can be observed from Fig. 4.19 that two type of HEM agents exists; an active and a passive agent. The HEM active agent is the prosumer (i.e. customer that own DERs), while the HEM passive agent is the consumer (i.e. customer without any power generation capabilities).

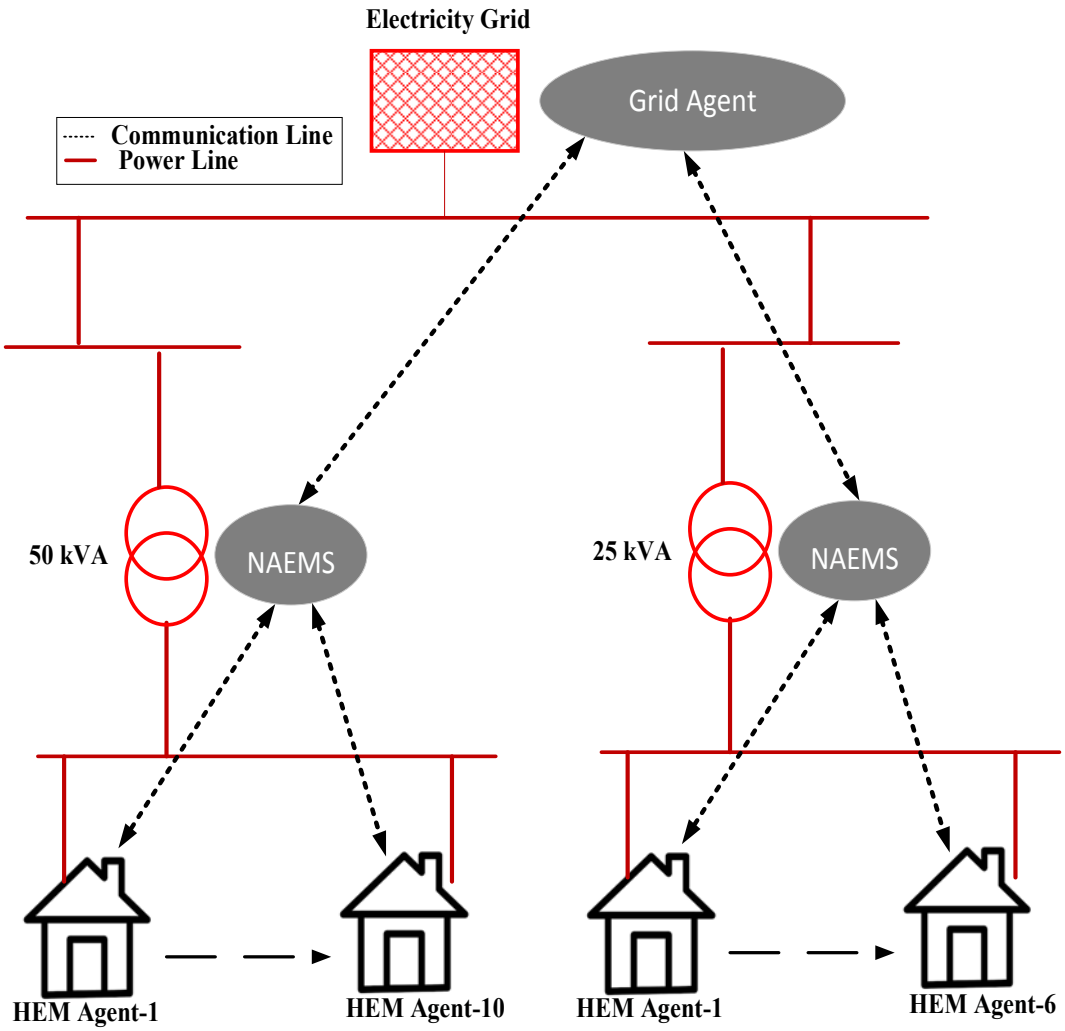

Figure 4.18 Architecture of the Transactive Energy Control of MAS

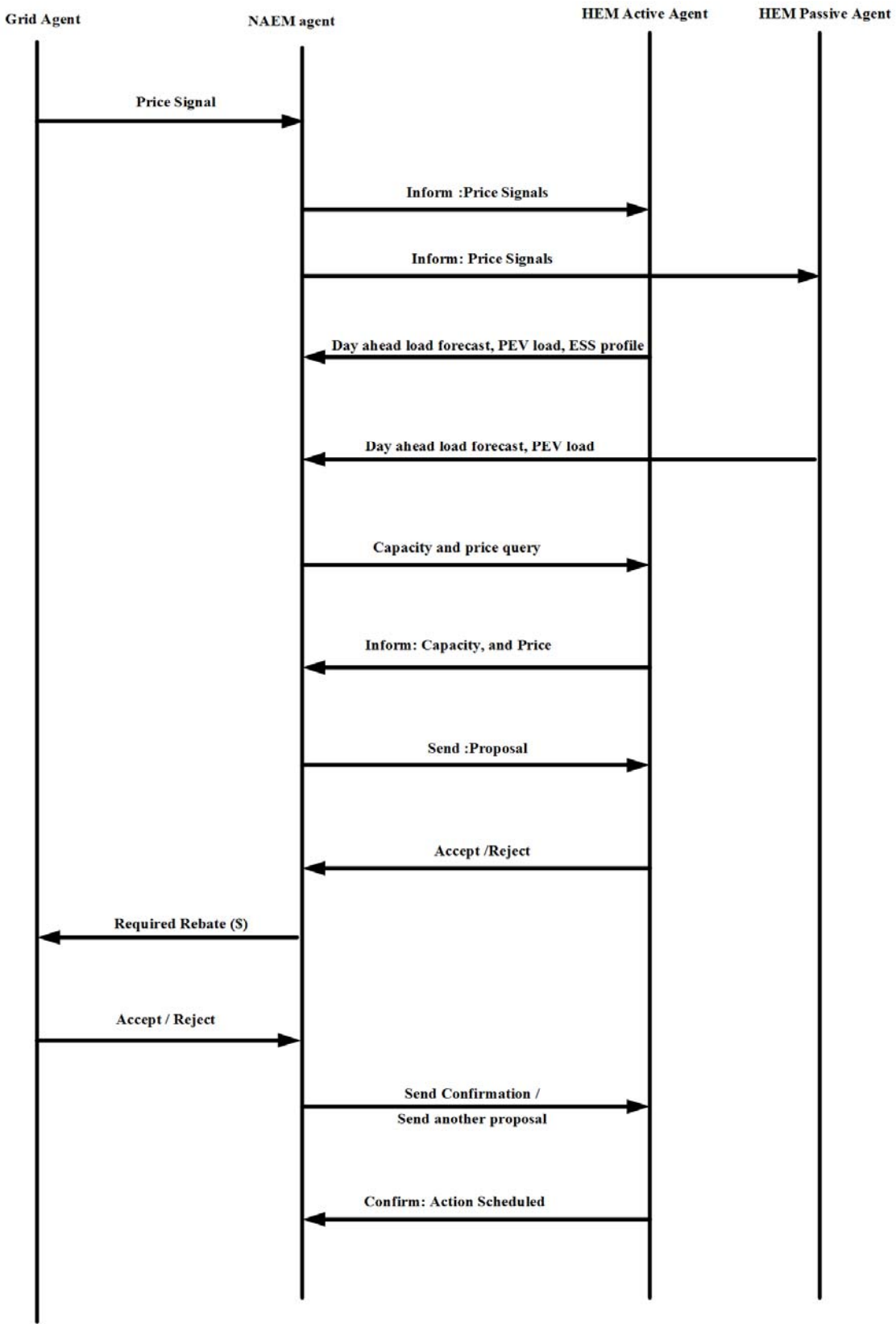

Figure 4.19 Message Exchange between Agents

The HEM agent can perform the HoCom function to maximize the homeowners' profits. However, the NAEM agent will place a bid value corresponding to the economic cost of rescheduled the energy storage profile provided by the HEM agent. The NAEM agent will perform either the PAPR or SOLR function to reschedule the residential energy storage profile in order to balance the utilities and the consumers' objectives as closely as possible while satisfying any required constraints.

In order to evaluate the optimal solution for each objective, the mixed integer linear (MILP) optimization algorithm [157] was implemented and was used in this work. The MILP algorithm is formulated as following:

$$\min/\max: f(x, y) \tag{4.44}$$

With quality constraints

$$g(x, y) = 0. \tag{4.45}$$

And inequality constraints

$$h(x, y) < 0. \tag{4.46}$$

Equations (4.44) - (4.46) represent the general formulation of the optimization algorithm. These equations will be arranged and modified based on the energy storage optimization function (e.g. the objective function *f* will be HoCom, PAPR, or SOLR, and x is the dependent control variable (storage power P_{sto}), and y is independent controllable variable).

The procedure of applying the TE control management between the NAEM and HEM agents to reach consensus state is explained using the flowchart in Fig. 4.20.

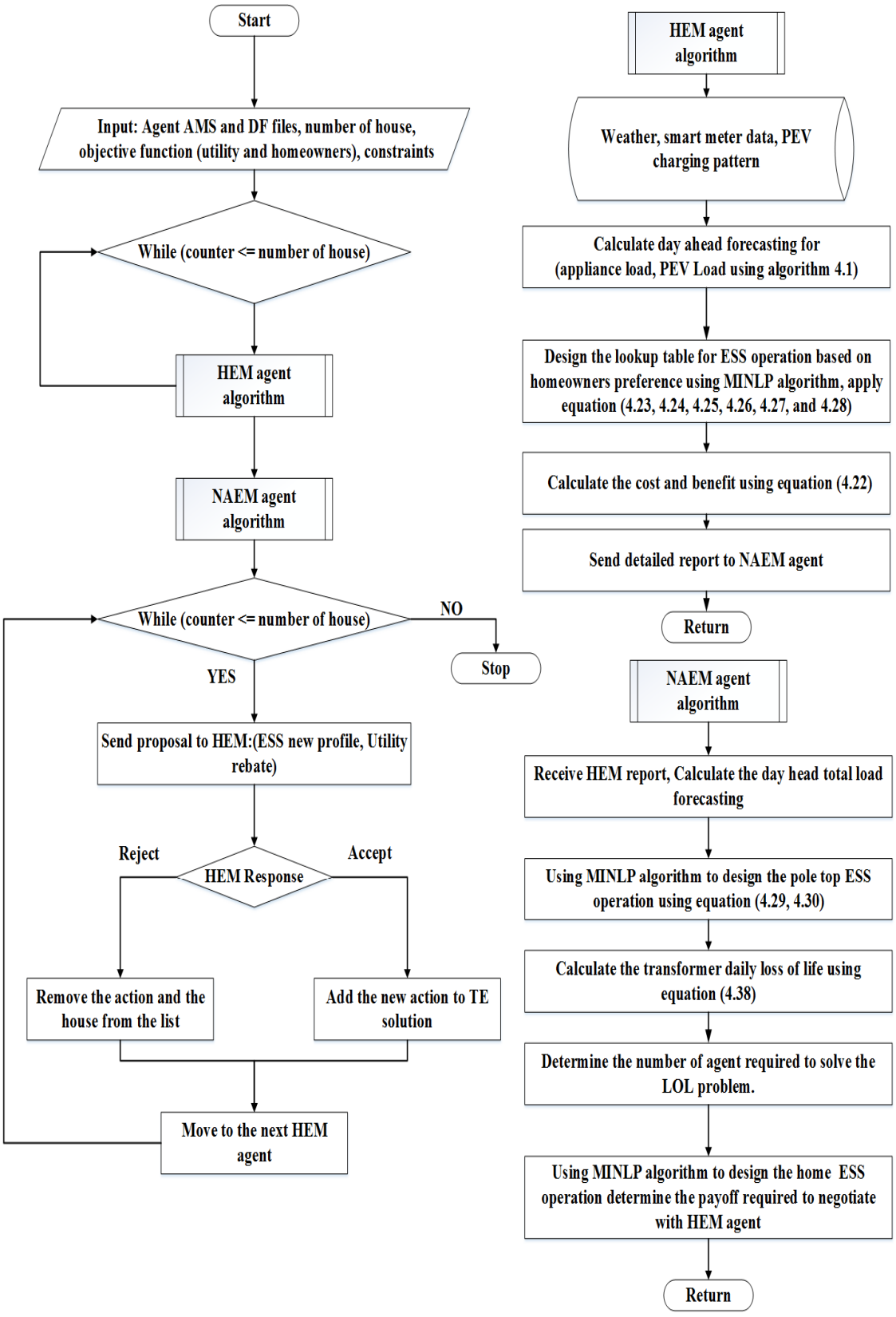

Figure 4.20 Transactive Energy Control Algorithm

4.6 Summary

This chapter presents the modeling and mathematical representation of the distribution system components. The home arrival time and the mileage driven are sampled to determine the Plug-in Electric Vehicles (PEVs) daily charging profile. The Monte Carlo simulation (MCS) technique is used to address the uncertainties in the PEVs charging demand.

The national house travel survey database is used to extract the data required from the vehicle owners driving pattern (e.g. daily driven distance, home arrival time). The extracted data are used to evaluate the cumulative distribution function for both the mileage driven and the charging time which will be used in the MCS.

The chapter also presents the modeling of wind distributed generation (DG) and rooftop solar photovoltaic (PV). The model performs an accurate estimation of wind speed, temperature, and irradiance profile to determine the exact amount of power generated from wind DG or solar PV. The k-mean clustering technique is used to reduce the number of profiles representing the whole dataset. The cluster distribution validity (CDV) is a new index introduced in this chapter to determine the optimal number of wind speed profiles while the knee point of the sum of square error (SSE) curve is used to determine the optimal number of temperature and irradiance profiles.

The impact of PEVs charging demand, the power generated from wind DG and solar PV on distribution transformer overload, loss of life are mathematical formulated and presented in this chapter.

The chapter also introduces the mathematical formulation of energy storage system functions. Three function are presented namely, Homeowner Comfort, Peak over

Average Power Reduction, and System Overload Reduction. The artificial neural network is used to predict the customers' loads which will be involved in a day ahead energy storage operation design.

The Transactive Energy (TE) control platform is presented for the optimal operation of the energy storage system and to coordinate the customers' and electric utilities objectives to ensure reliable operation of the electric distribution system.

The Transactive Energy control platform was presented for optimal operation of energy storage system and to coordinate the customers and electric utility objectives to ensure reliable operation of the electric distribution system.

The next chapter presents the simulation results of including PEVs, wind DGs, solar PVs, and energy storage system in the distribution system.

Chapter 5: Simulation Results and Analysis

5.1 Introduction

This chapter presents the analysis and results of including the Plug-in Electric Vehicles (PEVs) and distributed energy resources (DERs) to distribution system, the analysis is divided into main three sections, each section represent different case study: in the first case study the author investigates the impact of increasing the penetration of PEVs in distribution system embedded with wind DERs on PDS and SDS.

The second part investigates the effectiveness of using rooftop solar photovoltaic as a potential solution to mitigate the impact of PEVs charging demand in SDS; the last case study investigates the use of the Transactive Energy cooperative control of energy storage not only to mitigate the impact of PEVs charging demand, but to perform ancillary service to benefit both the electric distribution utility, and the homeowners. The outcome of implementing such approach is to improve the existing conservation program offered by the Canadian Independent Electricity System Operator (IESO).

The presented analysis in the three case studies focused on evaluating the overload of distribution system components, transformer loss of life, the power flow in the distribution system, the cost-benefit for utility and homeowners.

5.2 Case 1: Distribution System Including PEVs and Wind DGs

This case study aims to address the synergy between PEVs charging at secondary distribution system and the active and reactive power generated from wind-DGs in terms of energy flows, the amount of energy not supplied, and the adequate wind-DG penetration required to fulfill the PEVs charging demand.

5.2.1 Test Distribution System Description

The original IEEE 123-bus standard test PDS [158] is modeled using OpenDSS [159]. The topology of the system is radial with voltage level 4.16 kV. Fig. 5.1 shows the test system after modification by adding four wind DGs the size and location of which are set based on the result published in [160].

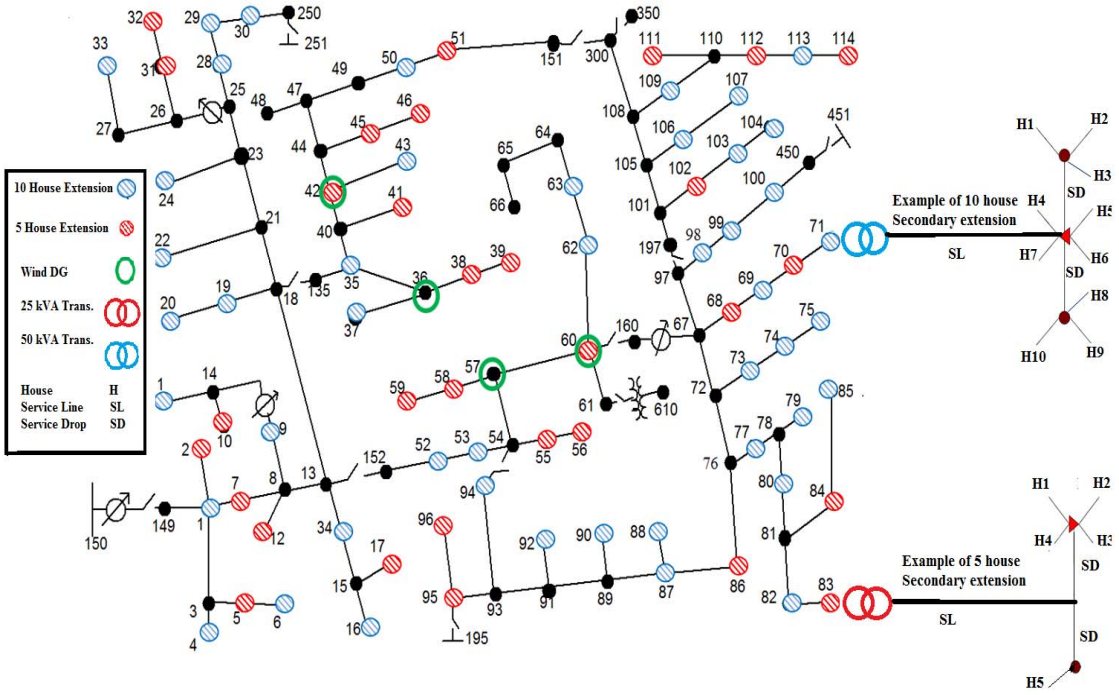

Figure 5.1 IEEE 123-Bus Standard Test with the Addition of Wind DG and SDS.

The SDS components are modeled and replaced the spot loads at the nodes in the original IEEE 123 bus system. As depicted in Fig. 5.1 the primary nodes with spot loads in the range between 44 and 72 kVA are replaced by SDS components consisting of a 50 kVA center-taped distribution transformer and two service lines and ten service drops, so that this SDS can host 10 houses. The other primary nodes with peak loads range between 22 to 36 kVA replaced by SDS feed 6 houses from 25 kVA distribution transformer using one service line and five service drop.

The peak load for the modeled house in any of the SDS (25 or 50 kVA) is set to 5.1 kW and 2.6 kVAR, the power setting is chosen to match the original spot load as possible. The simulation of the test distribution system is verified by solving the power flow using the backward-forward sweep technique after adding the SDS. The simulation results show that the voltage at each node matches the benchmark results published by the IEEE Power and Energy Society (PES) for this distribution system.

The IEEE reliability test system [161] is used in this work to present the load profiles for the residential sector. The load profile given in [161] represent the daily, weekly, monthly, yearly maximum demand. The remaining spot loads were kept as primary nodes and set to host commercial loads with the profiles given in [162]. The data for the IEEE 123 bus and the SDS modification are given in appendix B.

5.2.2 Considered Scenarios

The MCS is designed to include a different set of what-if scenarios which include different penetration levels of PEVs up to (50%) with different charging level (120 volts, 240 volts), this penetration was selected to match the expected PEVs deployed in Canada by 2030 [4]. On the other hand, the wind-DGs penetration is set up to (35%) [27], the indicated previous scenarios are listed in Table 5.1.

The mean and the standard deviations of bus voltage are used to assist and verify the choice of MCS runs. Based on our observation that no change in the bus voltages and the standard deviation occurred after 1000 run, the maximum number of MCS trials is set to 1,000 which found to be sufficient for convergence [163].

In each MCS run, the number of PEVs connected to the secondary nodes is calculated based on the penetration level, while the required charging demand is calculated based

on sampling the CDF of home arrival time and mileage driven as explained in section (4-2). Also, the nine representative wind speed profiles were evaluated as described in section (4-3-1), then the profiles are sampled based on their probability of occurrence. Finally the selected wind profile is assigned to each wind DG. Fig. 5.2 shows a flowchart outline the implementation of MCS algorithm to perform the designed scenarios.

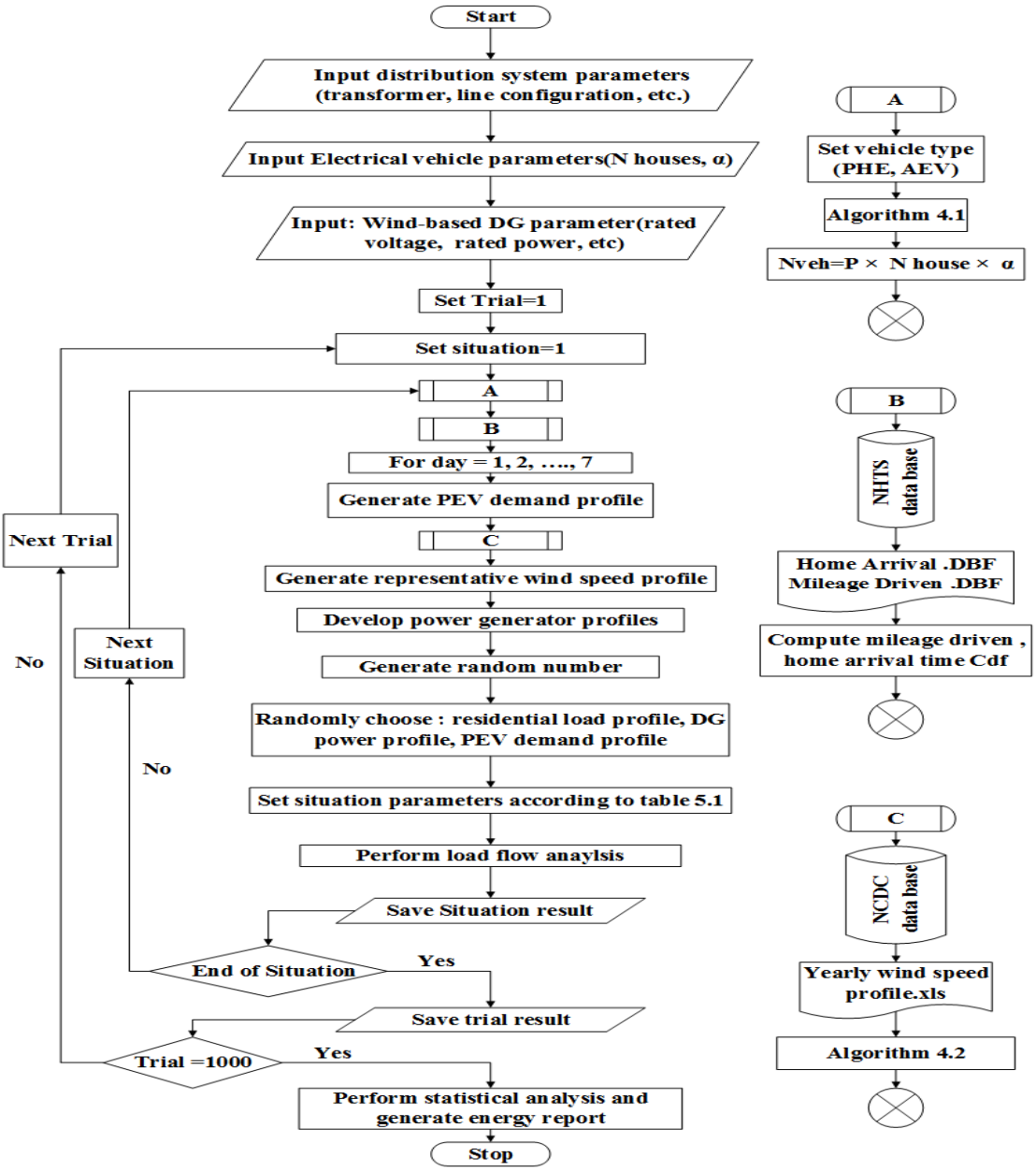

Figure 5.2 MCS Algorithm

Table 5.1 PEV & DG Penetration Scenarios Used in MCS

Scenario	Charging	PEV	DG	Scenario	Charging	PEV	DG
1	NA	0 %	0 %	25	Level 2	30%	0 %
2	NA	0 %	3.5 %	26	Level 2	30%	3.5 %
3	NA	0 %	17 %	27	Level 2	30%	17 %
4	NA	0 %	35 %	28	Level 2	30%	35 %
5	NA	0 %	0 %	29	Level 1&2	30%	0 %
6	NA	0 %	3.5 %	30	Level 1&2	30%	3.5 %
7	NA	0 %	17 %	31	Level 1&2	30%	17 %
8	NA	0 %	35 %	32	Level 1&2	30%	35 %
9	NA	0 %	0 %	33	Level 1	30%	0 %
10	NA	0 %	3.5 %	34	Level 1	30%	3.5 %
11	NA	0 %	17 %	35	Level 1	30%	17 %
12	NA	0 %	35 %	36	Level 1	30%	35 %
13	Level 2	10 %	0 %	37	Level 2	50%	0 %
14	Level 2	10 %	3.5 %	38	Level 2	50%	3.5 %
15	Level 2	10 %	17 %	39	Level 2	50%	17 %
16	Level 2	10 %	35 %	40	Level 2	50%	35 %
17	Level 1&2	10 %	0 %	41	Level 1&2	50%	0 %
18	Level 1&2	10 %	3.5 %	42	Level 1&2	50%	3.5 %
19	Level 1&2	10 %	17 %	43	Level 1&2	50%	17 %
20	Level 1&2	10 %	35 %	44	Level 1&2	50%	35 %
21	Level 1	10 %	0 %	45	Level 1	50%	0 %
22	Level 1	10 %	3.5 %	46	Level 1	50%	3.5 %
23	Level 1	10 %	17 %	47	Level 1	50%	17 %
24	Level 1	10 %	35 %	48	Level 1	50%	35 %

5.2.3 Synergy Analysis

The following are the key findings of applying MCS to the modified IEEE 123 bus distribution system considering the scenarios listed in Table 5.1.

The synergy between the wind DGs and PEVs is quantified using three different indices: excess of wind active power generation; Reverse Power Flow; active and reactive power loss, and transformer overload.

i. Excess of Wind Active Power Generation (EWAPG):

The excess of wind active power generation (EWAPG) can be calculated by comparing the power generated from wind DG and the PEV charging demand at different penetration level during a typical day of operation. The EWAPG is mathematically formulated as following:

$$EWPG_{A,h} = P_{DG,h} - P_{PEVs,h} \quad (5.1)$$

where h is the day hour (i.e. 1, 2,..., 24), $P_{DG,h}$ is the active power generated from the wind DGs at hour h, $P_{PEVs,h}$ is the plug-in electrical vehicle active absorbed power at hour h.

Fig. 5.3 shows the wind DGs active power generation profiles and PEVs load at different penetration. The figure reveals that the maximum charging demand of PEVs fleet occurs at 6 PM, and it can be noticed that a penetration of 35% wind DGs may suffice to supply the PEVs fleet, without requiring any need to import additional power from the substation.

Fig. 5.4 shows a trend of the EWPGA in the case of 50% PEV penetration at different wind DGs penetrations, the figure reveals that, the adequate wind DGs penetration

required to fulfil the PEVs charging requirement is in the range between (17- 35%), and it was found to be exactly at 30% wind DGs penetration.

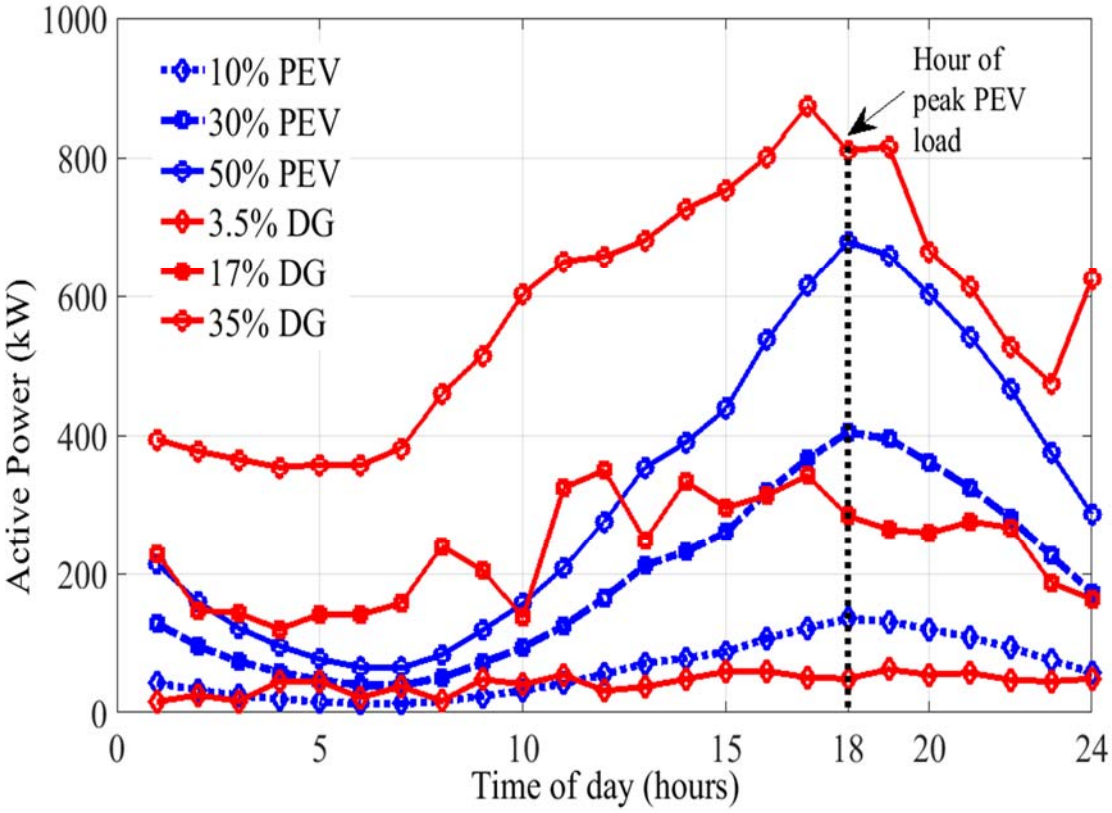

Figure 5.3 Daily Wind DG Power Generation and PEVs Demand Profile

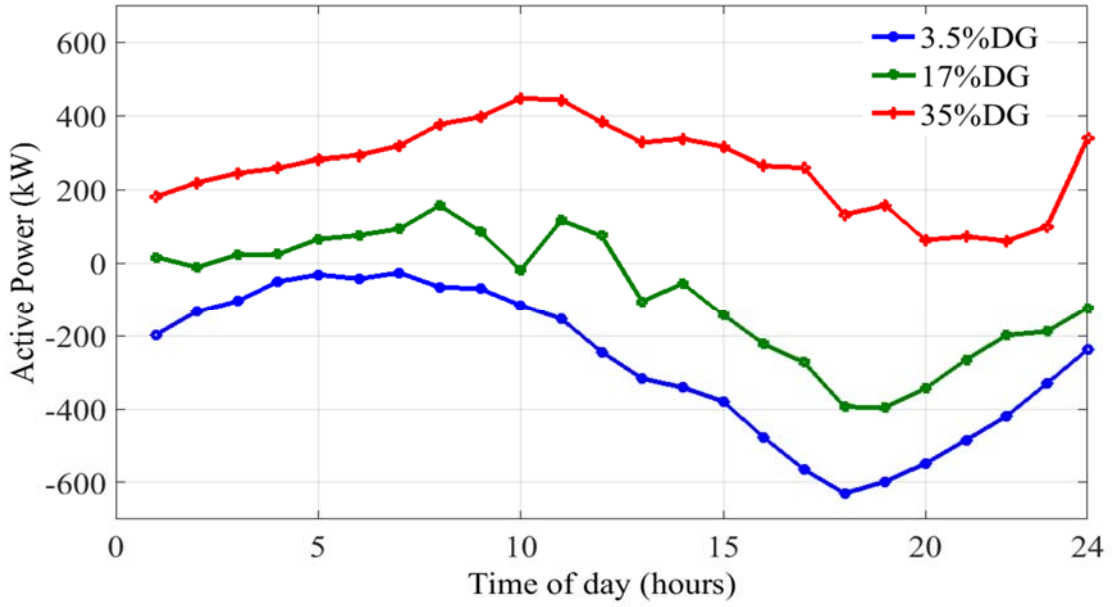

Figure 5.4 Trend of Excess Wind-Based DG Active Power Generation

ii. **Reverse Power Flow (RPF):**

Figs. 5.5 and 5.6 show the daily trend of active and reactive power flow at the substation level in the case of no PEV and at 35% wind DGs penetration. Visual inspection of Fig 5.5 reveals that the active power measured at the substation level is always greater than zero, which indicate that there is no chance to have reverse active power flow under the maximum wind DGs penetration level (35%). However, this is not the same with the reactive power flow as shown in Fig. 5.6. The figure reveals that there is a chance to have reverse reactive power flow at 17% and 35% wind DGs penetration specifically at the early morning hours between 12:00 AM to 7:00 AM. The Reverse reactive power flow (RPFR) at hour h can be calculated as following:

$$RPF_{R,h} = Q_{DG,h} - (Q_{PEVs,h} + Q_{Remload,h}) \quad (5.2)$$

where $Q_{Remload}$ is the total reactive power of the remaining load in the system at hour h, $Q_{DG,h}$ is the reactive power generated from the wind DGs at hour h, and $Q_{PEVs,h}$ is the plug-in electrical vehicle reactive absorbed power.

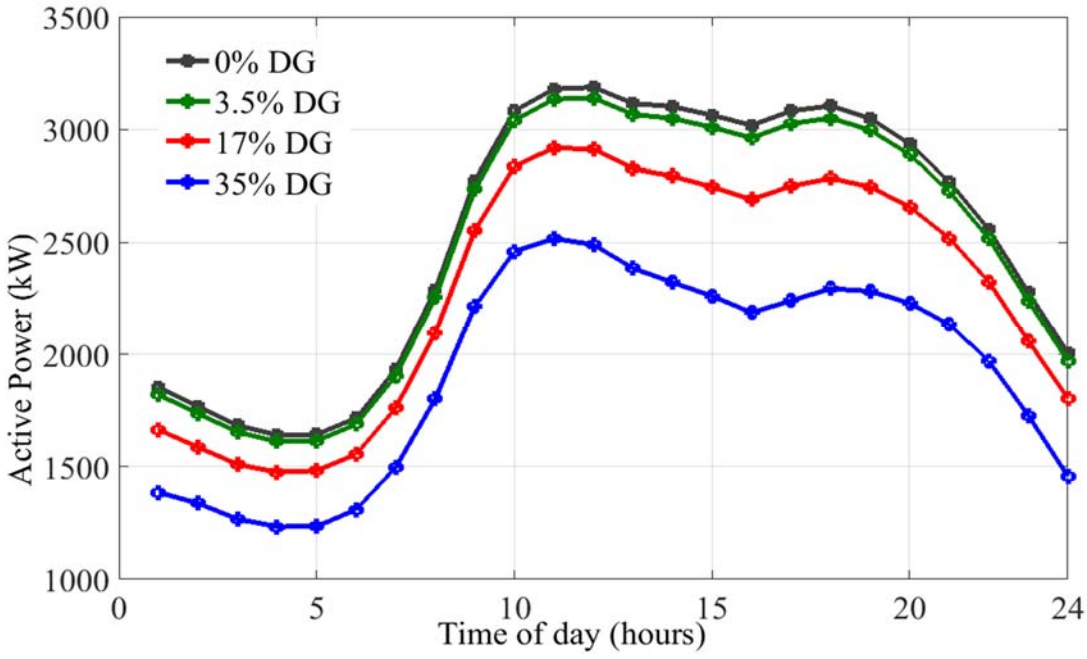

Figure 5.5 Substation Daily Active Power at Different Wind DG Penetration

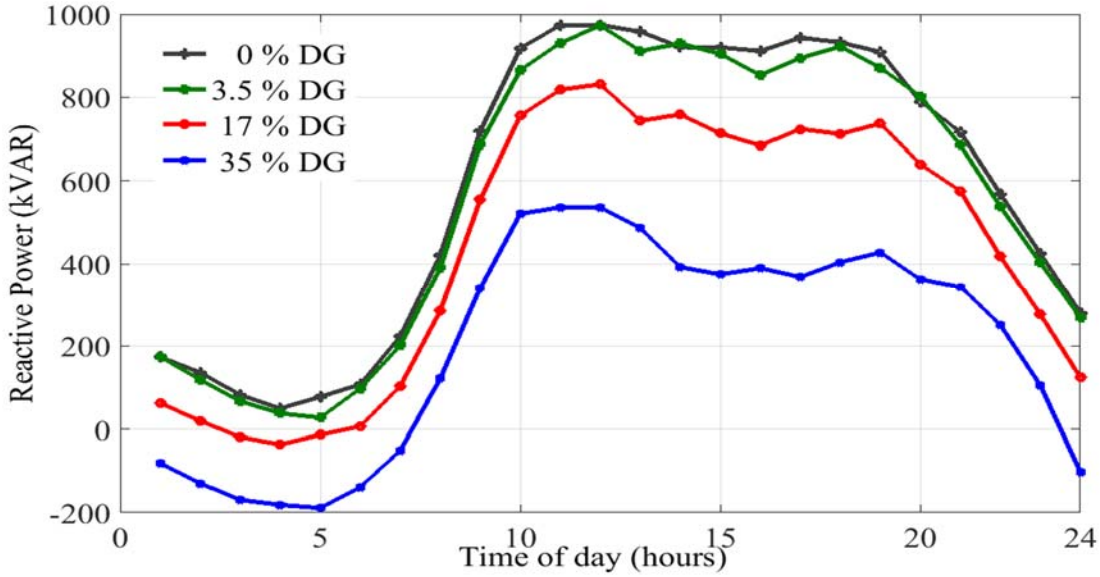

Figure 5.6 Substation Daily Reactive Power at Different Wind DG Penetration

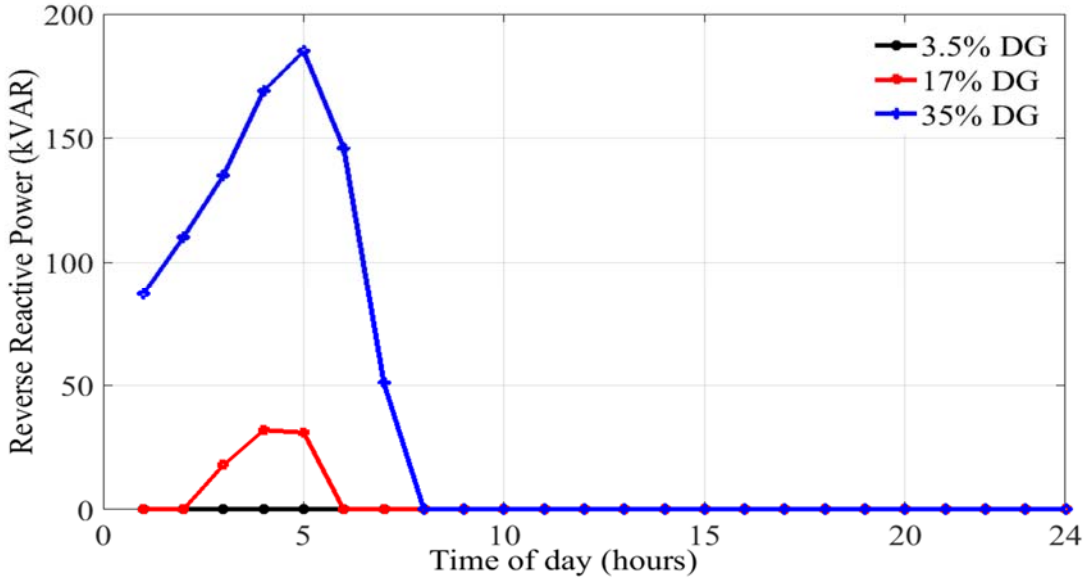

Figure 5.7 Substation Reverse Reactive Power Trend at 50% PEV

Fig. 5.7 shows the reverse reactive power flow daily trend measured at the substation level, in the case of 50% PEV penetration. The figure reveals that the peak RPFR occurs at 5 AM, in the case of 17% and 35% wind DGs penetration.

It can be noticed that during the off-peak periods and in the case of 17% wind DGs penetration (or higher), there might be a significant amount of reverse reactive power at

the substation which may increase the voltage beyond the acceptable limit at the buses and feeder in the neighborhood of the DGs location.

iii. **Energy Losses:**

Figs. 5.8 and 5.9 show the system active and reactive energy losses at different DG penetrations. The figures reveal that the active and reactive energy loss can be reduced by 6% and 12%, respectively in the case of increasing the DG penetration from 3.5% to 35%.

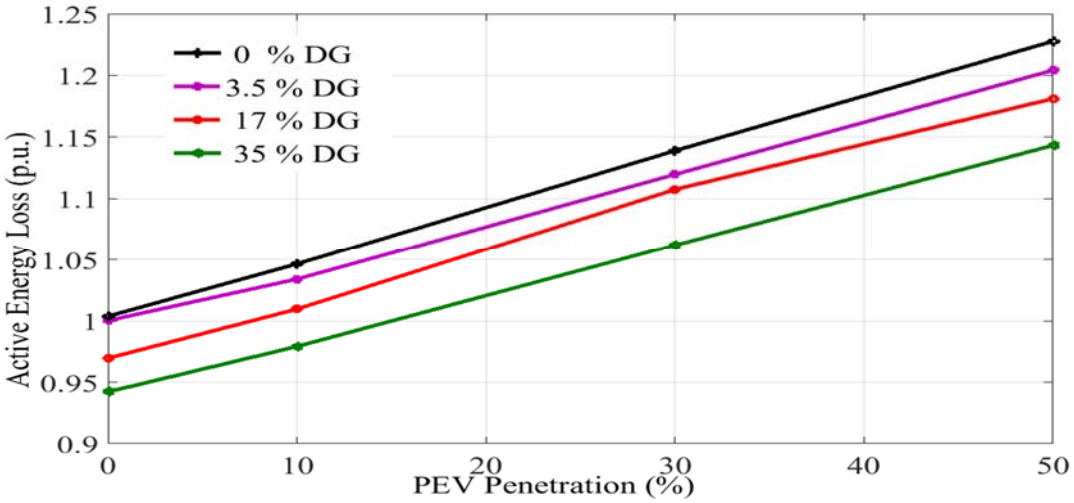

Figure 5.8 System Active Power Losses

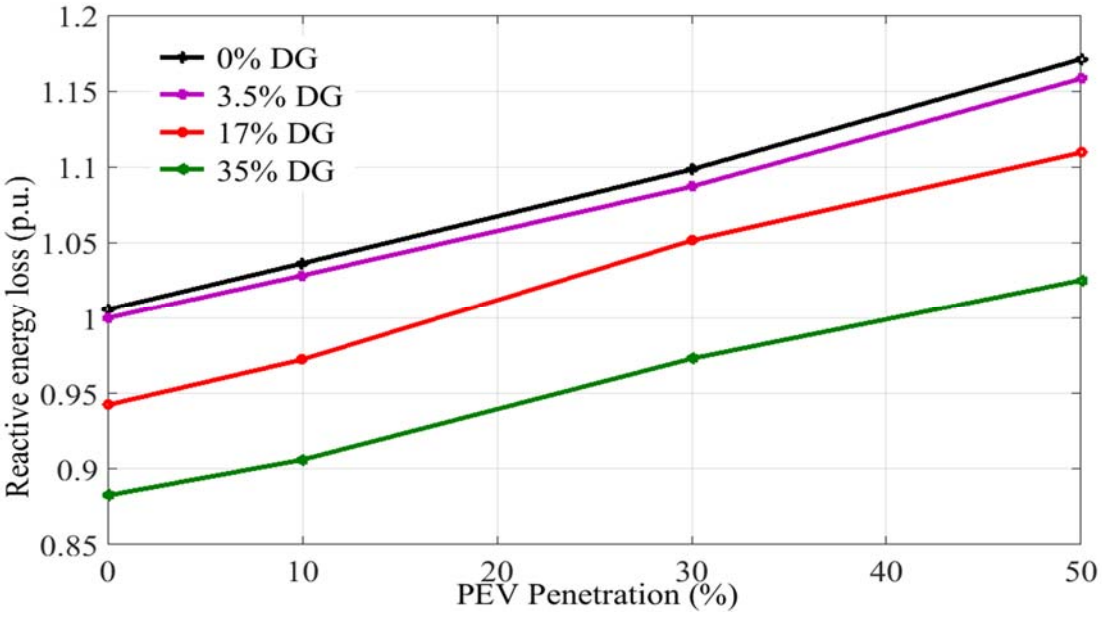

Figure 5.9 System Reactive Power Losses

iv. Distribution Transformer Overload:

Fig. 5.10 show the number of transformers experiencing overload during one representative day for the selected scenarios at the time of PEV maximum charging demand. The transformer overload is calculated using equation (4.34) as explained earlier in section (4-4).

The figure reveals that all the transformers (78 transformers) are overloaded at 7 PM and 8 PM. The figure also reveals that at any wind DGs penetration there is no effect on the number of transformers experiencing overload at the PEVs peak charging demand.

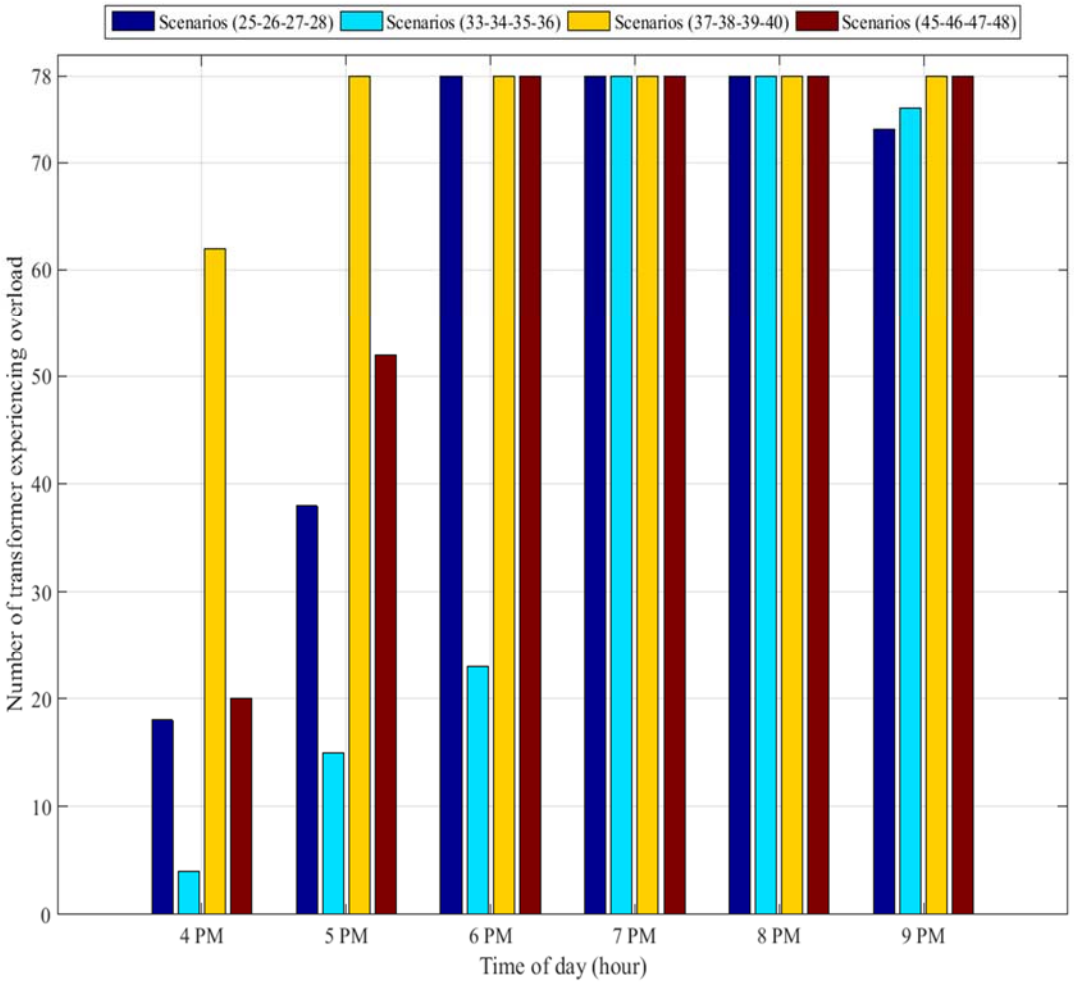

Figure 5.10 Number of Transformers Experiencing Overload during Representative Day

5.3 Case 2: Distribution System Including PEV and Solar PV DG

As shown in the previous case study the wind DGs are able to completely supply the PEVs charging demand locally without increasing the stress over the central generation and distribution substation. However, due to the presence of wind DGs in the primary distribution system, it is not able to reduce the overload of the distribution transformer (either the 25 kVA or the 50 kVA) and the overload on the service line and service drop. In this case study, the potential of rooftop solar PVs to mitigate the PEVs impact on the secondary distribution system is presented.

The IEEE 123 bus used in the previous case study is re-used in this case study after removing the wind DGs and adding the rooftop solar PVs in the SDS houses based on the selected penetration.

5.3.1 PEVs and Solar PVs Scenarios

The solar PVs output power is calculated based on the representative irradiance and temperature profiles obtained in Section (4-3-2). The power profiles are randomly assigned to all the installed PVs units in the residential sector.

Different PEVs and solar PVs penetration are considered in the MCS. Table 5.2 list the selected scenarios to be performed in the MCS.

Table 5.2 PEV-PV Scenarios Considered in the Second Case Study

Scenario	Charging level	PEV penetration	PV penetration
1	NA	0 %	0 %
2	NA	0 %	10 %
3	NA	0 %	30 %
4	NA	0 %	50 %
5	Level 2	30 %	0 %
6	Level 2	30 %	10 %
7	Level 2	30 %	30 %
8	Level 2	30 %	50 %
9	Level 1	30 %	0 %
10	Level 1	30 %	10 %
11	Level 1	30 %	30 %
12	Level 1	30 %	50 %
13	Level 2	50 %	0 %
14	Level 2	50 %	10 %
15	Level 2	50 %	30 %
16	Level 2	50 %	50 %
17	Level 1	50 %	0 %
18	Level 1	50 %	10 %
19	Level 1	50 %	30 %
20	Level 1	50 %	50 %

5.3.2 Scenarios Result Evaluation

The results of the scenarios listed in Table 5.2 are discussed in this section in terms of the PEV-PV active power flow, distribution transformer overload, transformer hot spot temperature and the transformers' loss of life.

Fig. 5.11 shows the charging demand of PEVs at 30% and 50 % penetration, and the rooftop solar PVs generated active power profiles. Visual inspection of Fig. 5.11 reveals that the solar PVs are capable of supplying the PEVs battery demand without importing any power from the distribution transformer during the day sun hours (i.e. 7 A.M. to 6 P.M). However, this is not the case during the evening and overnight.

i. Distribution Transformer Overloads:

Fig. 5.12 shows the transformer loading in percent, and visual inspection of the figure reveals that the maximum percentage transformer loading during PEVs charging in the case of 50% is 140%. The transformer loading can be significantly decreased during the sun hours in the presence of 50% PV penetration.

Fig. 5.13 quantifies the number of transformers experiencing overload during one day of operation, the figure reveals that in scenarios 3, 4, 11, 12, 19 and 20 (when changing the solar PVs penetration from 30% to 50%), the number of transformers experiencing overload decreases and the overloads occur only between 5 P.M. and 10 P.M. Table 5.3 lists 50 kVA transformers overloading hours during one day of operation.

The results in Table 5.3 show that all the 78 distribution transformers are overloaded during the typical day operation for 16 hours, in the absence of solar PV (scenarios 1, 5, 9, 13, and 17). However, a significant reduction in the number of hours transformer

overloaded (40% to 50% reduction) when the distribution system have 50% PV penetration (scenarios 4, 8, 12, 16, and 20).

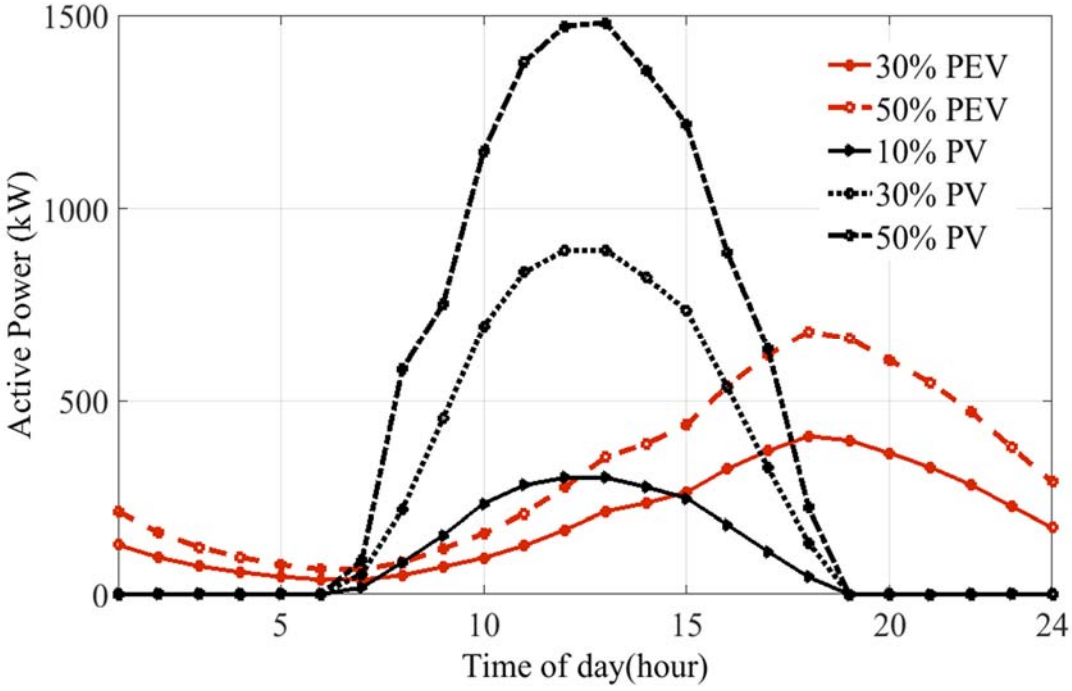

Figure 5.11 PEV Charging Demand & PV Generation Power

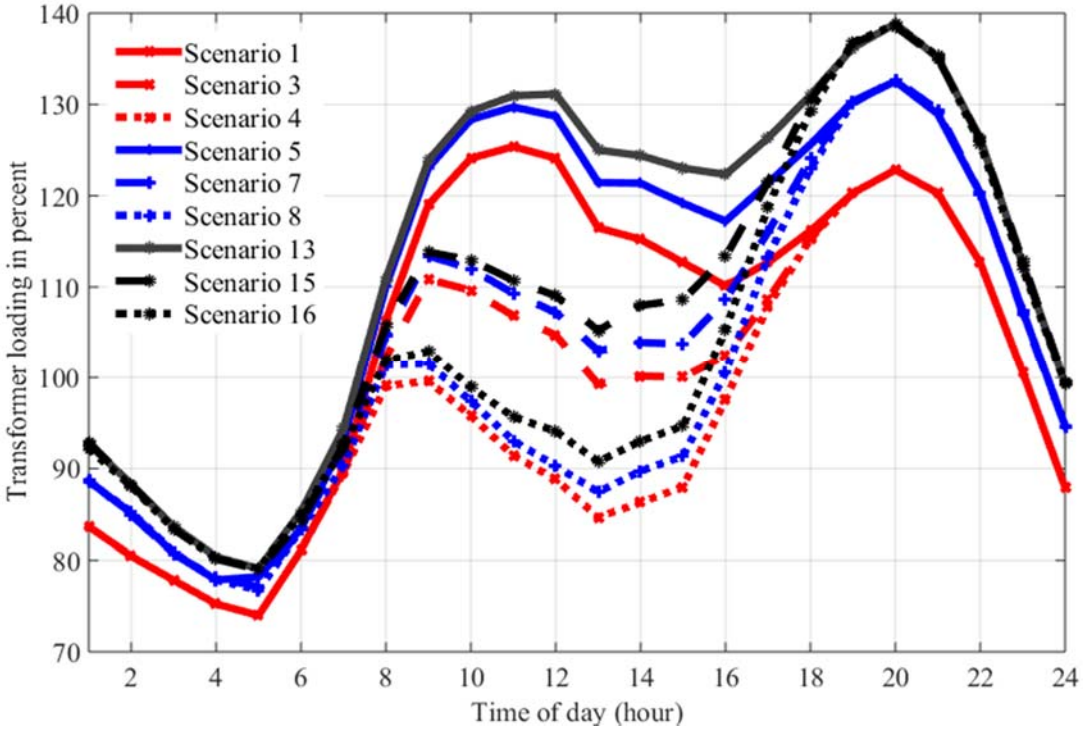

Figure 5.12 Transformer Loading during One Day

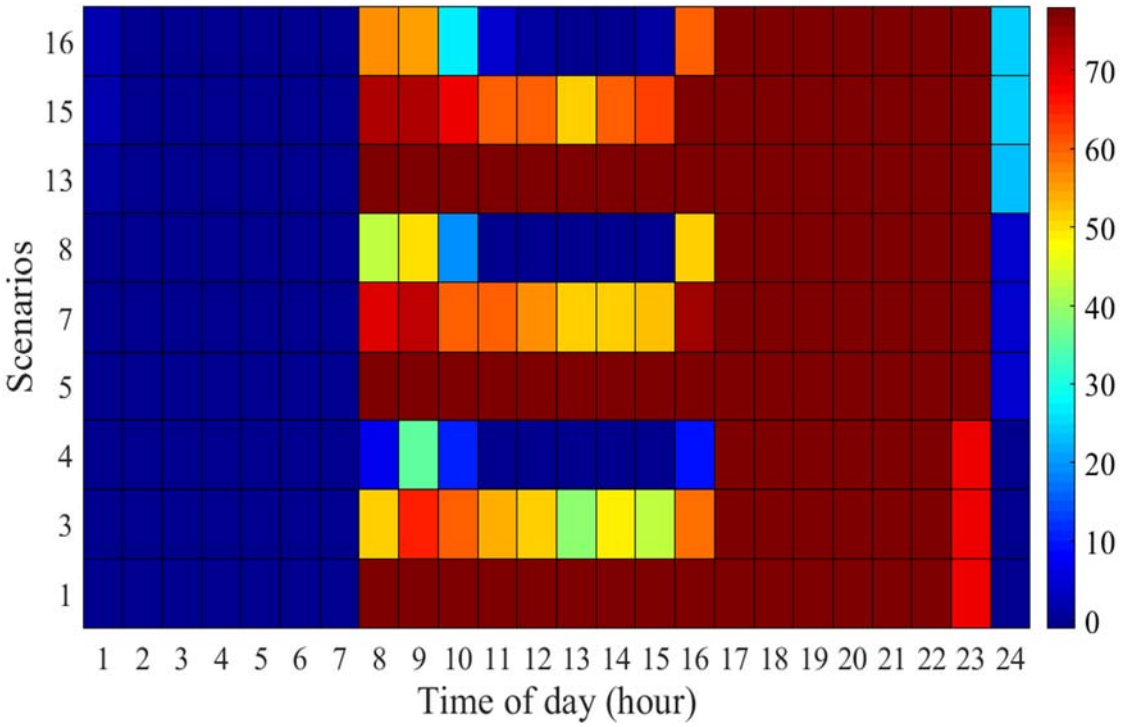

Figure 5.13 Number of Transformers Experiencing Overload

Table 5.3 Number of Hours Transformers are Experiencing Overload

Scenario	50 kVA transformer		
	Minimum	Median	Maximum
1	16	16	16
4	7	8	10
5	16	16	16
8	7	9	11
9	16	16	16
12	7	10	11
13	16	16	16
16	8	11	14
17	16	16	17
20	9	10	12

ii. Distribution Transformer Hotspot Temperature:

Fig. 5.14 shows the trend of the hot spot temperature of 50 kVA transformers calculated by applying equation (4.38). The figure reveals that in scenario 1 (no PEV and no PV) the temperature may reach 132ºC. It is worth to note that the hot spot temperature of transformer should not exceed 110ºC. It can be noted that in the case of scenarios (13, 17) at PEV penetration of 50% and 0% PV penetration the temperature increased from 152ºC to 159ºC when using level 2 charging instead of level 1. Significant improvement to the hot spot temperature can be noticed in the case of 50% solar PVs (scenario 16), a reduction of 37.5% can be observed at 1 P.M. (i.e., when PV is generating its peak power).

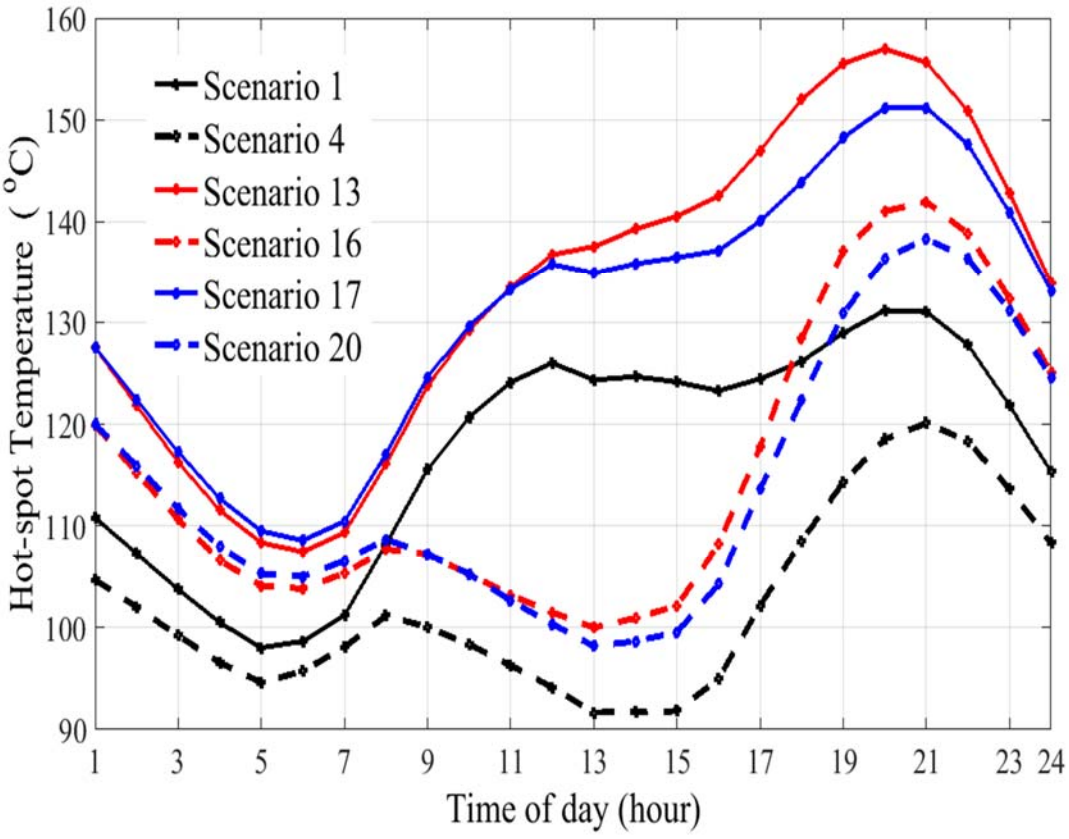

Figure 5.14 Transformer's Winding Hot-Spot Temperature

iii. Distribution Transformer LOL:

Fig. 5.15 shows the 50 kVA transformer loss of life during one day of operation for the two selected 50-kVA transformers; transformer number 47, and 72 (labeled Txf. 47, and Txf. 72) connected to node 71 and 106 of the modified IEEE 123-bus. The two transformers are selected because they represent transformers that experience maximum and minimum loss of life.

Visual inspection of Fig. 5.15 reveals that, the transformer LOL reach to 0.2677% and 0.1200% for the two representative transformers in the case of 50% PEV charging using level 2 with 0% solar PV (scenario 5). However, the transformer LOL can be improved to 0.0588% and 0.0423% for the two selected transformer in the case of 50 % PV penetration (scenario 16). This reduction in transformer LOL due to PV contribution will increase the transformer's lifetime by 37,602 hours (4.3 years) and 13,986 hours (1.6 year) for Txf. 47 and Txf. 72, respectively compared to scenario 5.

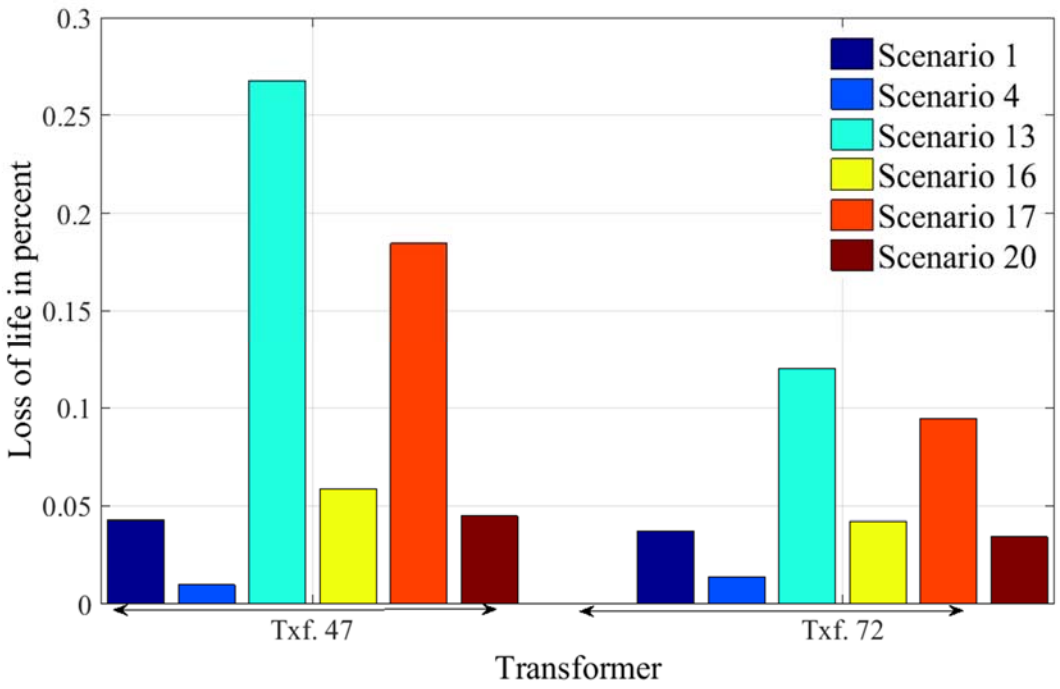

Figure 5.15 Transformer Loss of Life

5.4 Case 3: Distribution System Including PEV and Energy Storage

The results given in the previous two sections shows that relying only on DERs (wind DGs, or solar PVs) is not enough to fully mitigate the PEVs impact on the distribution system. Moreover, in some cases, the DERs may create an additional problem either in the PDS and/or SDS (e.g. solar PVs can overload the distribution transformer in the reverse direction in the case of light load cases).

Moreover, relying only on DERs are not a viable solution due to their intermittency, and therefore the use of energy storage system (ESS) is crucial to completely mitigate the impact on the distribution system.

In this case study, the author investigates the use of multi-agent in the neighborhood and in the home level, to monitor and manage the ESS in SDS. The predefined three objective functions described in section (4-3-3) are investigated to determine the optimal operation of distribution system resources.

The negotiation technique and the Transactive Energy (TE) concept explained in section (4-5-2) are applied to the agents in different levels to choose the optimal operation status of energy storage that maximizes the payoff for the homeowners while satisfying the electric utility objectives.

5.4.1 System Setup and Scenarios

The IEEE 34-bus test system [164], was selected to perform the analysis of testing the TE control platform to mitigate the PEV impact on distribution system, instead of the IEEE 123 bus (i.e. small system that will decrease the required time to perform the required simulation for applying and testing the proposed control platform).

The primary node of the IEEE 34 bus system was modified to have SDS by adding the distribution transformer, secondary line, and service drops. Fig 5.16 shows the original

IEEE 34 bus with two modified node one hosting 10 houses with 50 kVA transformer and the other node equipped with 6 houses powered from 25 kVA transformer. The data for the test system can be found in appendix C.

The residential house loads are calculated for a day ahead forecast using ANN approach discussed in section (4-5-1).

The forecasted loads are used for day ahead planning for the control action of the ESS given by either the HEM or NAEM agent.

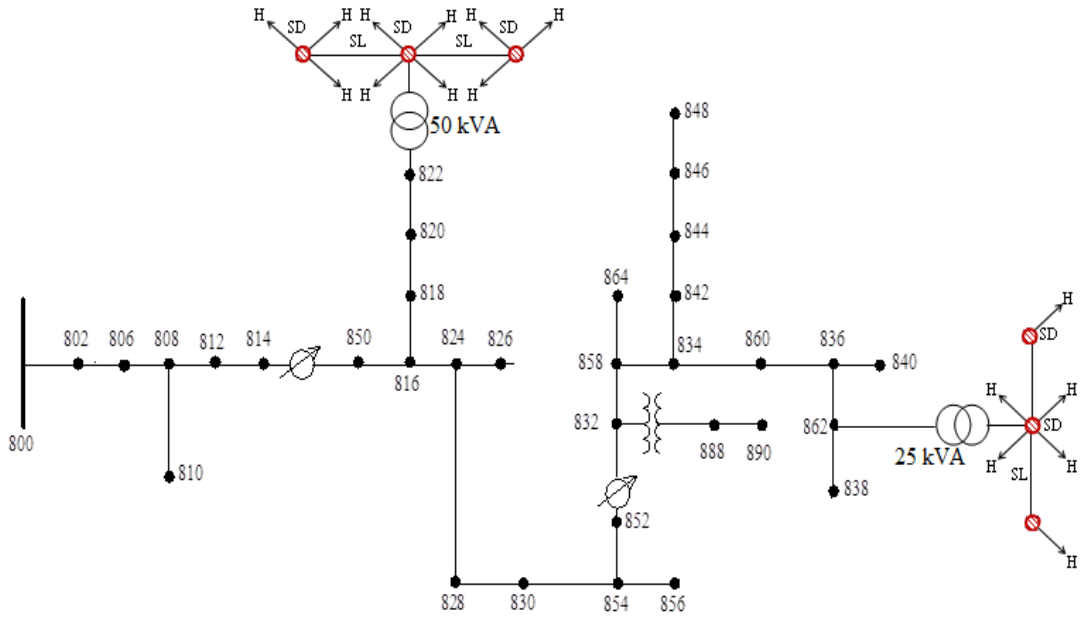

Figure 5.16 IEEE 34 Bus System

Different ESS sizes and locations are used to determine the optimal size, location, and function to maximize the benefit for both electric utility and homeowners.

Three different scenarios are considered for home ESS: 33%, 66%, and 100% (i.e., in 25 kVA SDS the three scenarios will be 2 house or 4 houses or six house have ESS).

Table 5.4 Shows the selected scenarios of the ESS to be tested in this case study, the parameter and cost of the ESS used in this work is available at [165] and given in Appendix A.

The Time of use (TOU) electricity pricing scheme is used to calculate the benefit gained by homeowners for installing ESS. While the transformer loss of life and the cost of replacement are used to assess the cost/benefit for electric utilities. Fig 5.17 shows the TOU for different season.

Three PEV penetration levels are used; 0% (no PEV), 50% (i.e., in 25 kVA SDS mean three houses each have one PEV) and 100% (i.e., in 25 kVA SDS mean six houses each have one PEV).

The charging time is chosen based on home arrival time [133], and the driven distance selected to be the median driven distance by Canadian driver [4]. Table 5.5 shows the PEVs scenarios used in this case study.

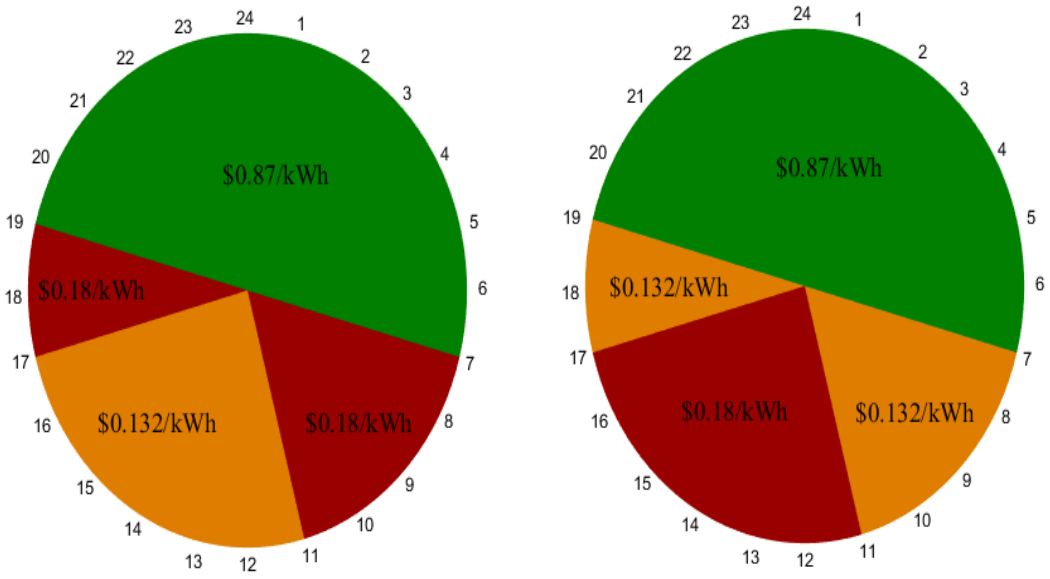

Figure 5.17 Time of Use Price

Table 5.4 Energy Storage System Used in the Simulation Process

Scenarios.	Location – Penetration	Size	Functions
1	Home (owned by customer)- 100%	2 kW- 12kWh	HoCom
2			PAPR
3			SOLR
4	Home (owned by customer)- 100%	3.3 kW- 6.4kWh	HoCom
5			PAPR
6			SOLR
7	Home (owned by customer)- 100%	6.6 kW- 12.8kWh	HoCom
8			PAPR
9			SOLR
10	Home (owned by customer)- 66%	2 kW- 12kWh	HoCom
11			PAPR
12			SOLR
13	Home (owned by customer)- 66%	3.3 kW- 6.4kWh	HoCom
14			PAPR
15			SOLR
16	Home (owned by customer)- 66%	6.6 kW- 12.8kWh	HoCom
17			PAPR
18			SOLR
19	Home (owned by customer)- 33%	2 kW- 12kWh	HoCom
20			PAPR
21			SOLR
22	Home (owned by customer)- 33%	3.3 kW- 6.4kWh	HoCom
23			PAPR
24			SOLR
25	Home (owned by customer)- 33%	6.6 kW- 12.8kWh	HoCom
26			PAPR
27			SOLR
1 to 27	Pole top mounted (owned by utility)	5kW- 16 kWh	PAPR

Table 5.5 PEV Simulation Cases

Simulation case	PEV Penetration	Charging voltage	Charging power
1	50%	240 Volt	3.3 kW
2	100%	240 Volt	3.3 kW

5.4.2 Simulation Results Evaluation

The impact of 50 % PEV penetration (i.e. first simulation case in Table 5.5) is discussed in terms of the transformer loss of life and the cost/benefits for homeowners and electric utilities.

Fig. 5.18- 5.19 show the active power consumed by each house for the 25 kVA SDS, and the total power measured at the distribution transformer, respectively. From Fig. 5.19 it is demonstrated that in the case of 50% PEV penetration, the peak power seen by the 25 kVA distribution transformer reaches 42 kW. This increases the transformer daily loss of life (LOL) from 0.006% (i.e. 0% PEV) to 0.023%. It is worth noting that the normal daily LOL should not exceed 0.0134%. This increase in transformer LOL means that the electric utility is obliged to replace the distribution transformer after 11.9 years compared with 20 years (i.e. normal transformer lifetime) in the case of 0% PEV penetration.

The following section demonstrate the effect of applying the Transactive Energy (TE) control in the distribution system in the case of using ESS 12 kWh, after the NAEM agent and the HEM agents reach to the state of consensus.

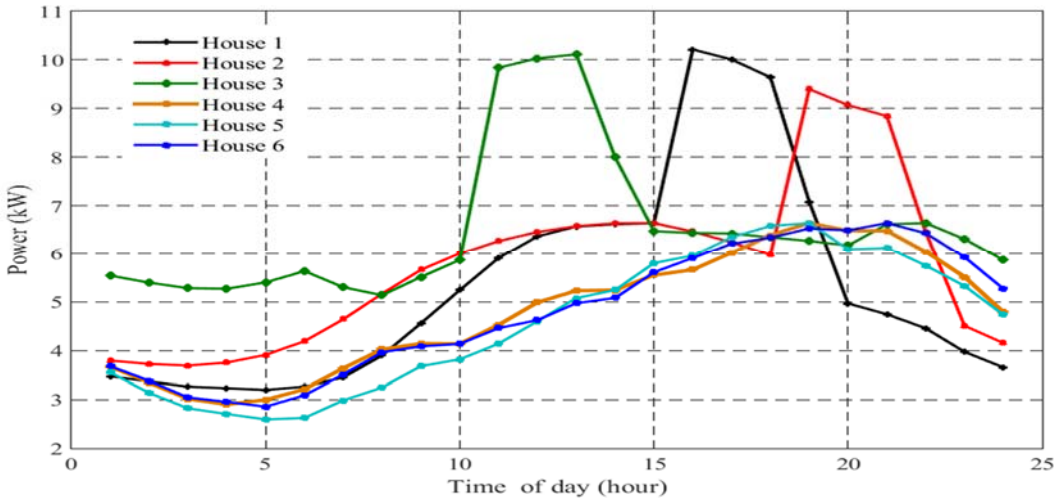

Figure 5.18 Residential Home Forecasted Load

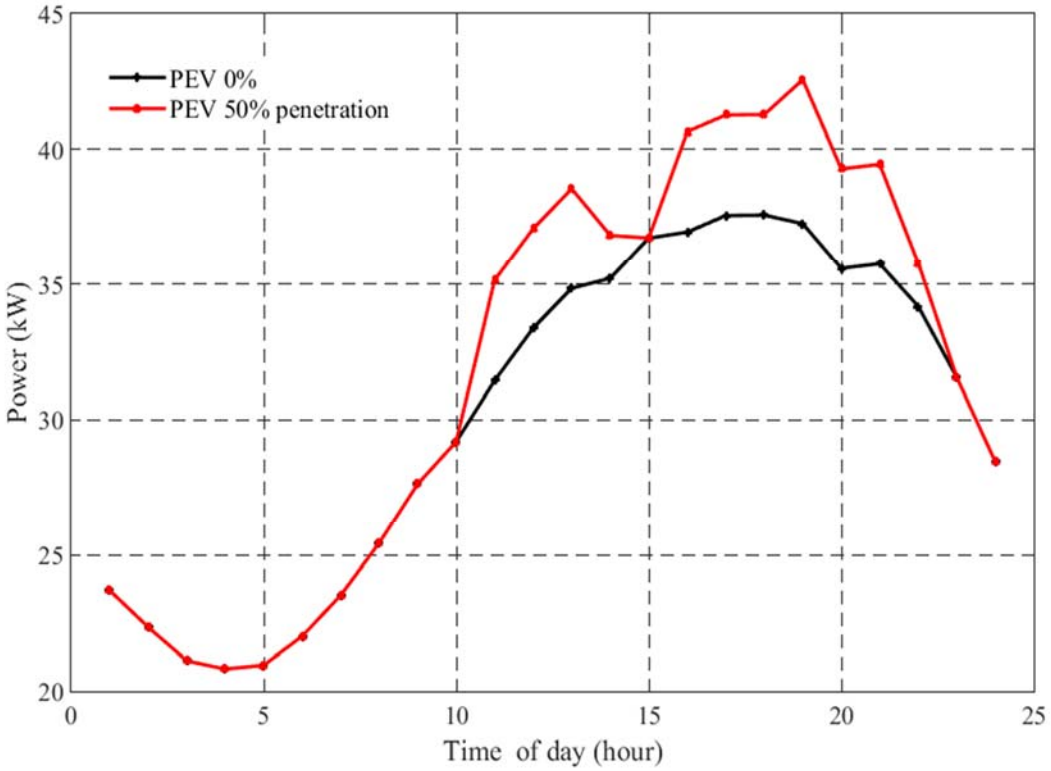

Figure 5.19 25 kVA Transformer Loading

5.4.2.1 Evaluation of ESS 12 kWh HoCom Function

The results for operating the energy storage system (ESS) in Home Comfort (HoCom) function mode with different penetrations is shown in Fig. 5.20.

Visual inspection of Fig 5.20 reveals that, when the HEM decides to operate the ESS based on the HoCom function (equation 4.23- 4.24), the transformer overload reaches to unacceptable limit, which will result in a failure of operation of the distribution transformer. This phenomenon is quantified in Table 5.6, and it was found that the transformer needs replaced after 0.7 years in the case of 100% ESS penetration (i.e. scenario 1). The transformer replacement is required after 2.8 and 7.1 years in the case of 66% and 33% of ESS penetration (i.e. scenario 10, 19), respectively.

As outlined in Fig 4.20, the HEM agents will send the consumed load and the optimal operation of ESS to the NAEM agent.

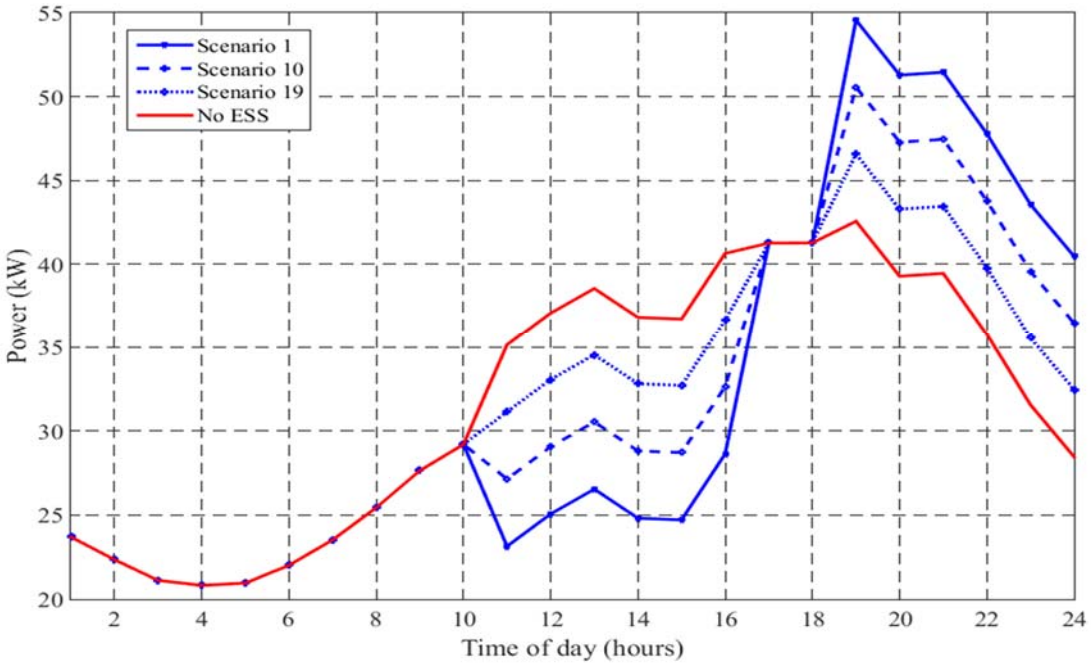

Figure 5.20 Power Seen by 25 kVA Transformer in the Case of 12kWh ESS, HoCom Function

5.4.2.2 Evaluation of ESS 12 kWh PAPR Function

Based on the received report from the HEM agents the NAEM agent will estimate the expected transformer loss of life (LOL). If the calculated LOL exceed the normal LOL the NAEM agent rejects the ESS operation proposed by the HEM agents, and will then start a negotiation round with the HEM agents Fig 5.21, shows the impact of ESS operation when the NAEM agent decide to choose the Peak over Average Power Reduction (PAPR) function (best option to reduce transformer LOL). Fig. 5.21 reveals that the transformer peak demand decreases to 35.5, 33.5, and 31.75 kW at 33%, 66%, and 100% ESS penetration, respectively.

This reduction in transformer peak power will maintain the transformer lifetime at 20 years in the three scenarios (2, 11, and 20). However, the HEM agent can only perform the proposed action from the NAEM agent if the distribution system operator (DSO) need to pay a rebate for home owners to take the control over their energy storage unit

to help electric utility increase the transformer life time. This rebate is calculated as \$4.1, \$2.6, and \$1.3 per day for scenarios 2, 11 and 20, respectively for all the houses equipped with ESS in the secondary distribution system (SDS). The DSO payment breakdown for each house is shown in Fig 5.23. The DSO payment (D_P) required for each house and the electric utility total payment (U_p) can be calculated as follows:

$$D_P = H_{sto/Hocom} - H_{sto/PAPR} \tag{5.3}$$

$$H_{sto/HoCom} = \sum_{t=1}^{T_{charging}} C_t \times (P_{ch_t})_{HoCom} \times \Delta t - \sum_{t=1}^{T_{discharging}} C_t \times (P_{disch_t})_{HoCom} \times \Delta t \tag{5.4}$$

$$H_{sto/PAPR} = \sum_{t=1}^{T_{charging}} C_t \times (P_{ch_t})_{PAPR} \times \Delta t - \sum_{t=1}^{T_{discharging}} C_t \times (P_{disch_t})_{PAPR} \times \Delta t \tag{5.5}$$

$$U_p = \sum_{H=1}^{N_{houses}} D_{P_H} \tag{5.6}$$

where $H_{sto/Hocom}, H_{sto/PAPR}$ are the total home savings when the ESS performs the HoCom and PAPR optimization functions, respectively.

P_{ch}, P_{disch} are the ESS charging and discharging power in kW, and $T_{charging}$, $T_{discharging}$ is the ESS charging and discharging periods decided by the HEM or NAEM agent.

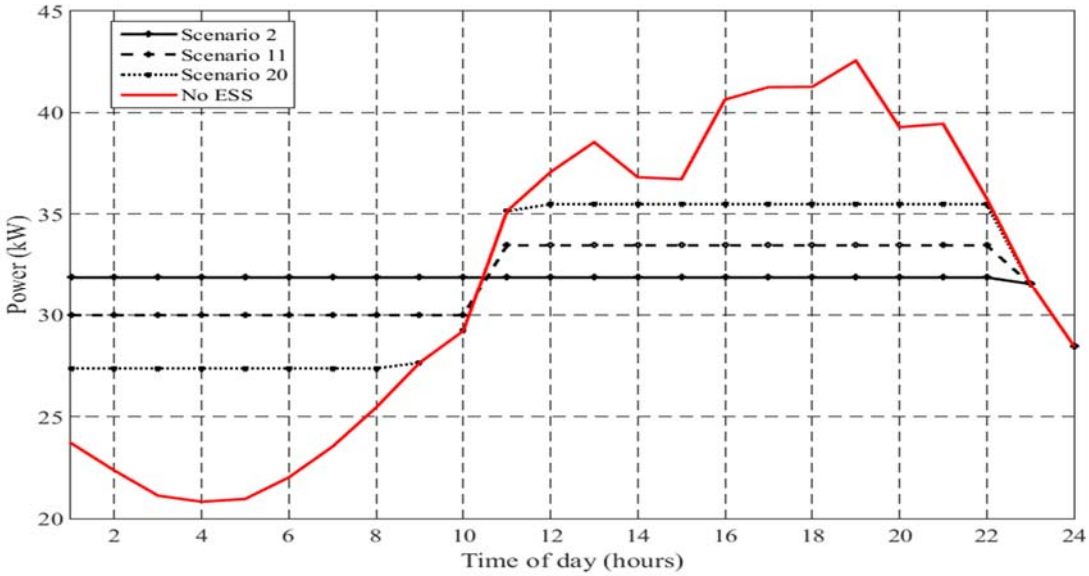

Figure 5.21 Power Seen by 25 kVA Transformer in the Case of 12kWh ESS, PAPR Function

5.4.2.3 Evaluation of ESS 12 kWh SOLR Function

In this work, a new storage function (SOLR) is proposed that is able to reduce the utility payments to homeowners' for utilizing their ESS, and increases the transformer lifetime, while keeping the HEM agent objective at its maximum value.

The TE control solution will operate only to satisfy the required amount of ESS using the SOLR optimization function (equation 4.30 to 4.33) and will release the remaining ESS to perform the HoCom optimization function. The NAEM agent first identifies the required power needed from the customers' ESS to limit the transformer overload to the predefined limit given by the electric utility. Once the required power is calculated, the NAEM agent starts a sequential negotiation with each HEM agent to buy the available capacity of the customers' ESS. Once the action is approved by the HEM agent, the NAEM checks to see if more power is required when no more power is required to remove the distribution transformer overload, the NAEM agent will schedule the second home to perform the HoCom function (no payment is required from electric utility for this function).

Fig 5.22 shows the proposed TE solution, which reveals that the transformer peak demand reaches 34, 36 and 38 kW for scenarios 3, 12, and 21, respectively. This means the transformer lifetime is remain at 20 years, as quantified in Table 5.6. Finally, the required payment from utilities can be reduced to \$3, \$2.6, and \$0.7 per day in the case of scenarios 3, 12, and 21, respectively. The values of utility payment under the TE control action (U_{TE}) are given below and can be calculated as following:

$$D_{TE} = H_{sto/Hocom} - H_{sto/TE} \tag{5.7}$$

$$H_{sto/TE} = \sum_{t=1}^{T_{charging}} \mathrm{C}_t \times \left(P_{ch_t}\right)_{TE} \times \Delta t - \sum_{t=1}^{T_{discharging}} \mathrm{C}_t \times \left(P_{disch_t}\right)_{TE} \times \Delta t \tag{5.8}$$

$$U_{TE} = \sum_{H=1}^{N_{houses}} D_{TE_H} \quad (5.9)$$

where D_{TE} is the DSO's required payment in order to satisfy the customers, and $H_{sto/TE}$ is the customers savings when the ESS is operating in TE mode. Results show that the TE solution is capable of maximizing the objectives of the HEM agent and NAEM agents.

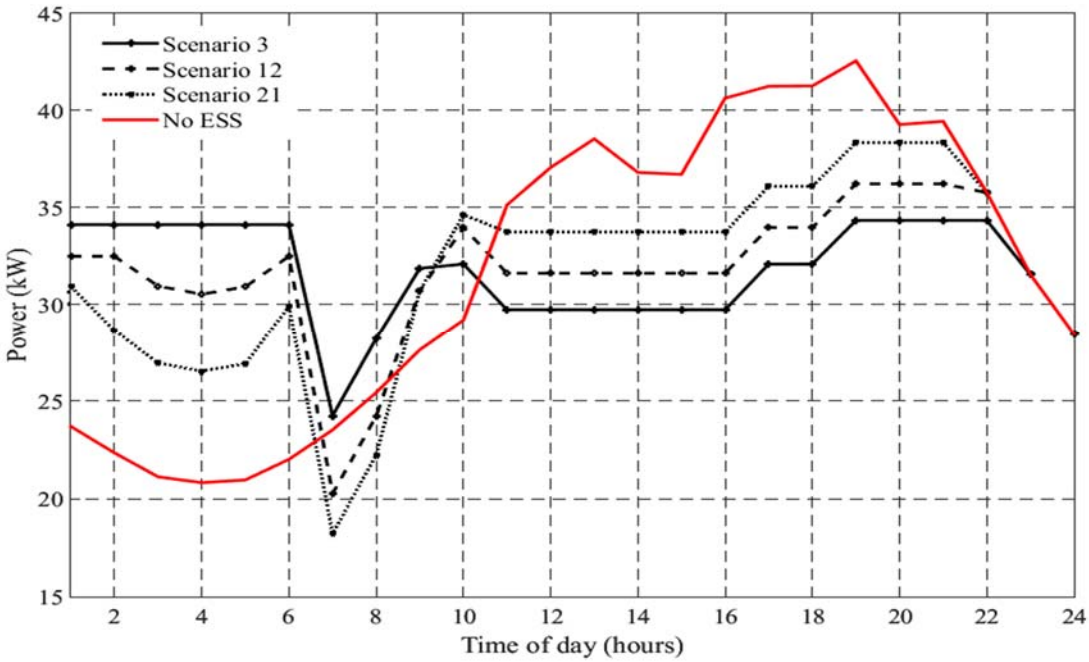

Figure 5.22 Power Seen by 25 kVA Transformer in the Case of 12kWh ESS, SOLR Function

5.4.2.4 Summary of Results for ESS 12 kWh Case Study

Fig 5.23 shows the homeowners savings per day and the electric utility payment required for each home in order to make all the agents reach a state of consensus. The results show that under any ESS operation, homeowners can save $1.10 per day on their electricity bill. With the average ESS lifetime of 15 years [165], homeowners can save $6,022 over that period. This saving is enough to cover the cost of the ESS ($6000) seen in [165].

The results in Table 5.6, reveal that when the electric utility applies the optimal TE solution (Scenario 21), they will required to pay a total of $3,800 ($0.7 per day × 365 × 15) to ensure the transformer lifetime will be kept at 20 years. The electric utility payment of $3,800 will be divided between customers involved in the TE solution (in this scenario 2 homes) with different portions going to each customer based on the amount of power requested from the customers ESS.

If the electric utility pays $3,800 to their customers, this will save them the cost of three replacements of the distribution transformer, that would be required if the utility lets the customers operate their ESS independently (scenario 19).

The cost of replacing a 25 kVA transformer is approximately $2,500, which means the electric utility will save $ 3,700 (2500×3 – 3800) when applying the TE solution. Moreover, even if the electric utility upgrades the transformer to 50 kVA, the cost becomes $3,000. However, upgrading the transformer to a 50 kVA transformer requires replacement of cables and protection devices, it also increases the power losses in the system, which will increase the operating cost of the distribution system. As a result of this discussion, the TE solution is still found to be the optimal solution compared with transformer replacement or transformer upgrade.

To determine the adequate penetration and size of ESS, this work investigated two different sizes of storage. The first size of storage used is 6.4 kWh, since it matches the rating of a Tesla Powerwall home storage system [165]. The second storage size used in this work is 12.8 kWh, this matches the rating of two Tesla Powerwall home storage systems [165].

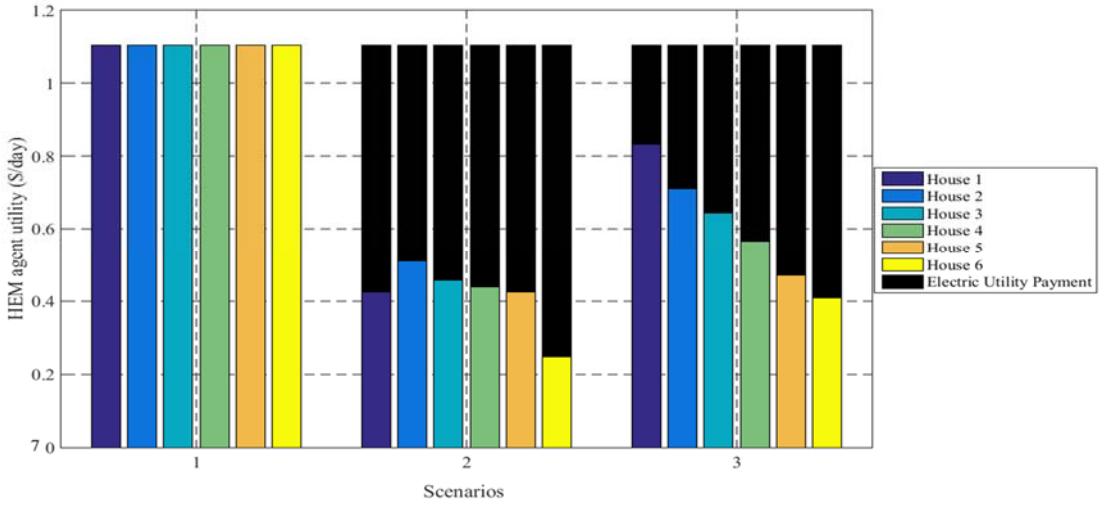

Figure 5.23 Agent Consensus for Different Proposal in Case of 12kWh ESS

Table 5.6 Summary Results for Simulation Case 1.

Scenarios	Transformer daily LOL (%)	Transformer life time (years)	Electric utility rebate ($/day)
1	0.295	0.9	0.0
2	0.002	20.0	4.1
3	0.003	20.0	3.0
4	0.194	1.4	0.0
5	0.004	20.0	2.0
6	0.005	20.0	1.2
7	0.626	0.4	0.0
8	0.002	20.0	4.6
9	0.003	20.0	3.4
10	0.098	2.8	0.0
11	0.003	20.0	2.6
12	0.004	20.0	1.7
13	0.069	4.0	0.0
14	0.005	20.0	1.4
15	0.006	20.0	0.8
16	0.157	1.8	0.0
17	0.003	20.0	2.8

18	0.004	20.0	1.7
19	0.038	7.1	0.0
20	0.005	20.0	1.3
21	0.007	20.0	0.7
22	0.032	8.5	0.0
23	0.007	20.0	0.7
24	0.009	20.0	0.3
25	0.047	5.8	0.0
26	0.005	20.0	1.4
27	0.006	20.0	0.7

5.4.2.5 Evaluation of ESS 6.4 kWh

The impact of changing the storage size from 12kWh to 6.4 kWh is investigated in terms of the cost/benefits for homeowners and the transformer LOL.

Fig 5.24 reveals that with a storage rating of 6.4 kWh, the transformer peak power can reach to 58 kW, which will require transformer replacement after 1.4 years. By reducing the ESS penetration to 66% and 33% (scenarios 13 and 22) the transformer lifetime increased to 4 and 8.5 years, respectively.

Fig 5.25 shows the proposal sent from the NAEM agent to the HEM agents to change storage operation. The figure demonstrate that in the case of scenario 5, the transformer peak power is reduced by 40% when compared with scenario 4, which keeps the transformer lifetime at 20 years. The HEM can accept the proposed operation if the electric utility total payment is $2/day for all of the customers who provide their ESS to be used by the DSO. This solution will be rejected by the NAEM agent due to the high cost to be paid by the electric utility.

Another proposal sent by the NAEM agent to the HEM agents is to change the ESS operation as exposed in Fig 5.26. When an agreement is reached between all agents, the transformer lifetime will be maintained within 20 years, while the total payment required from the electric utility is only $1.20/day in the case of scenario 6.

Fig. 5.27 shows the breakdown for each HEM agent and the required payment by the electric utility to reach an agreement between all agents. The benefit for each homeowner will be $3,220 based on the lifetime of the ESS. This saving is more than the cost of the storage as given in [165] (i.e. $3,000).

The results in Table 5.6 show that with a 6.4 kWh ESS, only 33% penetration is adequate to keep the transformer LOL below the normal LOL values (scenario 24). In this case, the electric utility will require paying a total of $1,642 ($0.3 per day) to the customers in order to apply the TE solution. Again the required payment of the utility is less than the cost of either replacement ($7500 for a total of 3 replacements) or upgrading the distribution transformer to 50 kVA ($3000).

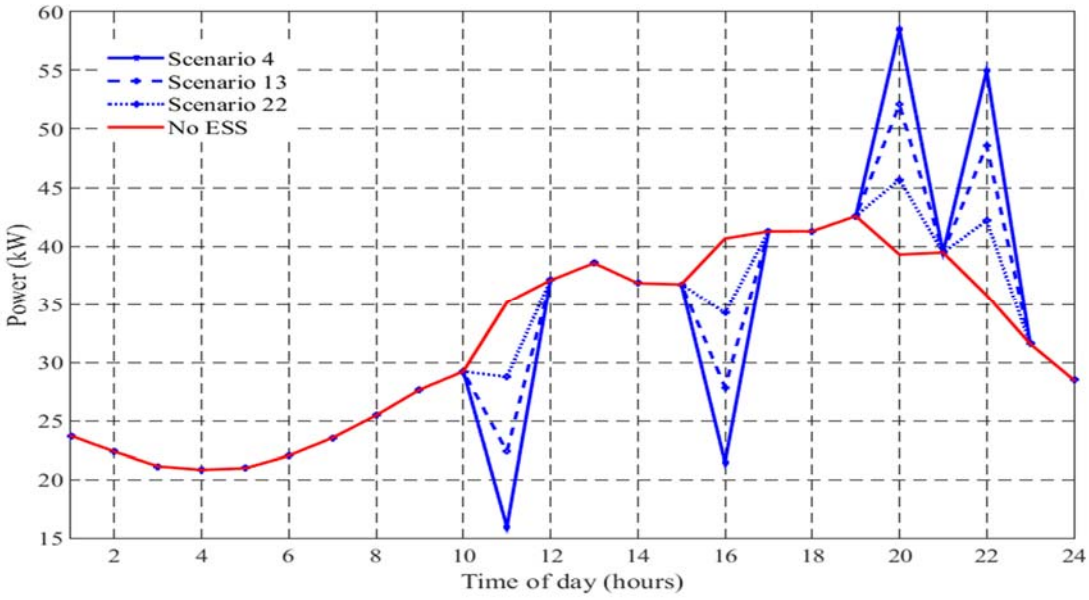

Figure 5.24 Power Seen by 25 kVA Transformer in the Case of 6.4kWh ESS, HoCom Function

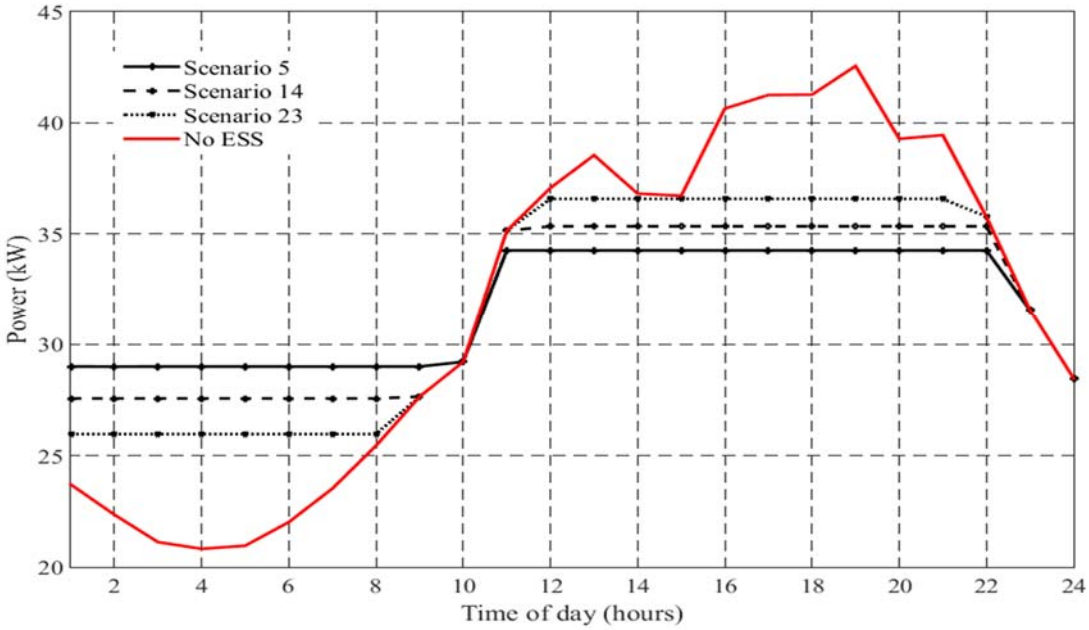

Figure 5.25 Power Seen by 25 kVA Transformer in the Case of 6.4kWh ESS, PAPR Function

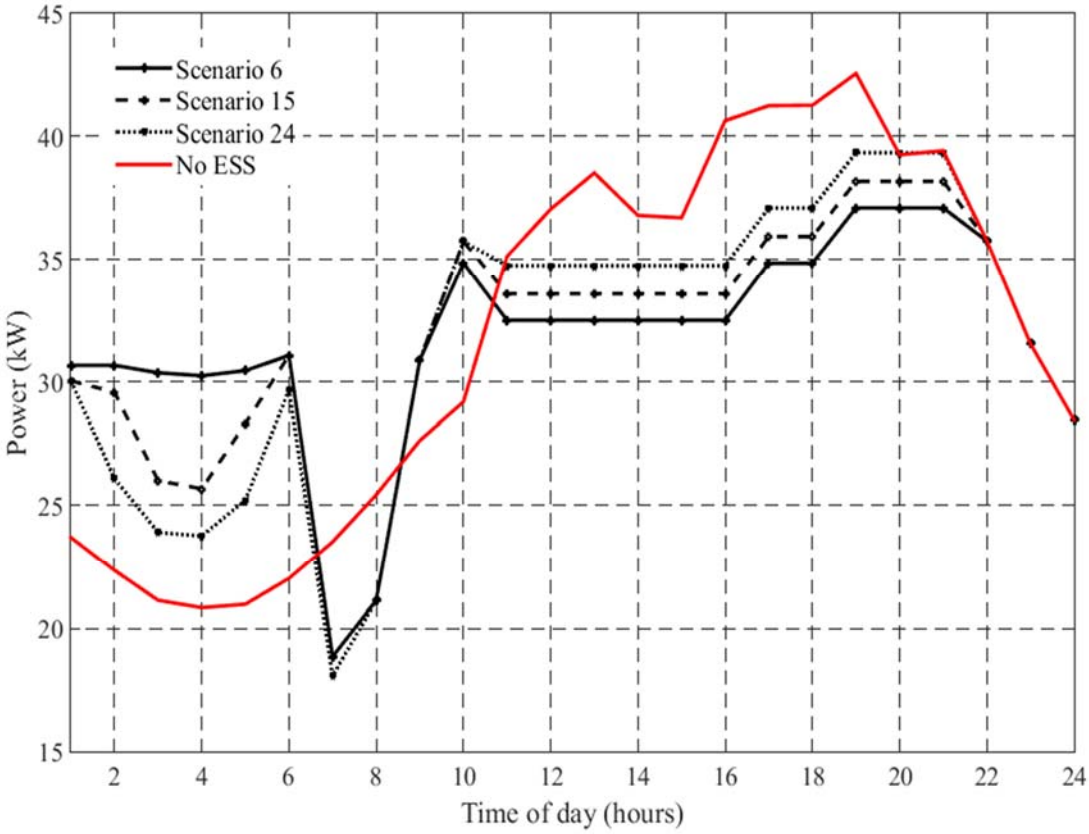

Figure 5.26 Power Seen by 25 kVA Transformer in the Case of 6.4kWh ESS, SOLR Function

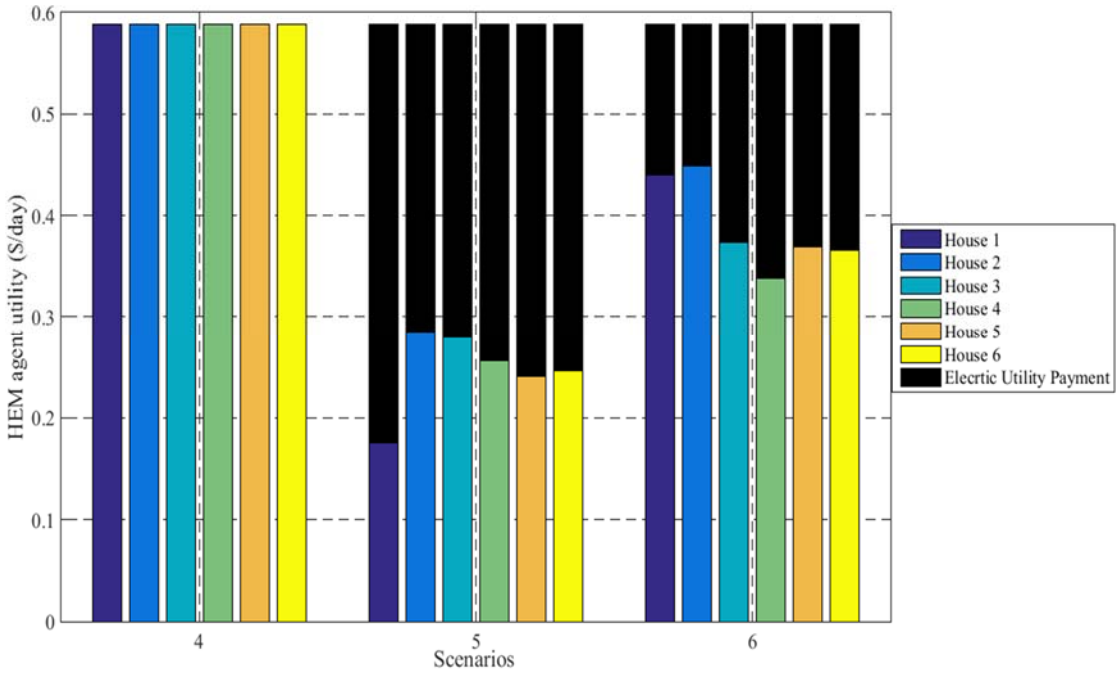

Figure 5.27 Agent Consensus for Different Proposal in Case of 6.4kWh ESS

5.4.2.6 Evaluation of ESS 12.8 kWh

The last ESS size under investigation is 12.8 kWh. Visual inspection of Fig 5.28 reveals that the transformer peak power in the case of scenario 7 reaches 62 kW. This will require the transformer to be replaced after 0.4 years when compared with 1.8 and 5.8 years in the case of 66% and 33% ESS penetration (scenario 16, and 25), respectively.

Fig. 5.29 shows the proposed ESS profile sent from the NAEM agent. This solution will increase the lifetime of the distribution transformer to 20 years for all ESS penetration levels (scenarios 8, 17, and 26). This solution requires the electric utility to pay $4.60, $ 2.80, and $1.40 per day for the pre-mentioned scenarios, meaning the required payment will not satisfy the electric utility and it will be rejected.

The optimal TE solution is shown in Fig. 5.30, which keeps the transformer lifetime at 20 years. However, the required payment will be reduced to $3.40, $1.70, and $0.70 per day in the case of scenarios 9, 18 and 27, respectively.

Fig 5.31 shows the HEM agents savings per day for each home in the case of ESS 12.8 kWh. The savings gained by homeowners will be $6,450, which exceeds the cost of the ESS installation ($6000). The optimal TE solution (scenario 27) will require the electric utility to pay $3800 ($0.70 per day) to reach an agreement with the HEM agents.

Fig 5.32 shows the objective solution for the 27 developed scenarios, in terms of the transformer lifetime and the required utility payment. Visual inspection of Fig 5.32 reveals that many scenarios of ESS operation can maintain the transformer lifetime at 20 years. However, the optimal TE control solution is selected to minimize the rebate that is required from the electric utility to reach an agreement with their customers.

Table 5.7 presents statistical summary for the 27 developed scenarios. The scenarios are organized based on the ESS size, then minimum, maximum and median of transformer lifetime, electric utility payment are calculated. It can be noticed that, the median transformer lifetime is 20 years, which means any of the ESS size is capable of relieve the transformer overload. On the other hand, in the case of 6.4 kWh ESS the median value of the utility payment is $0.70/day, which represent the best value of the cost over the median of all scenarios.

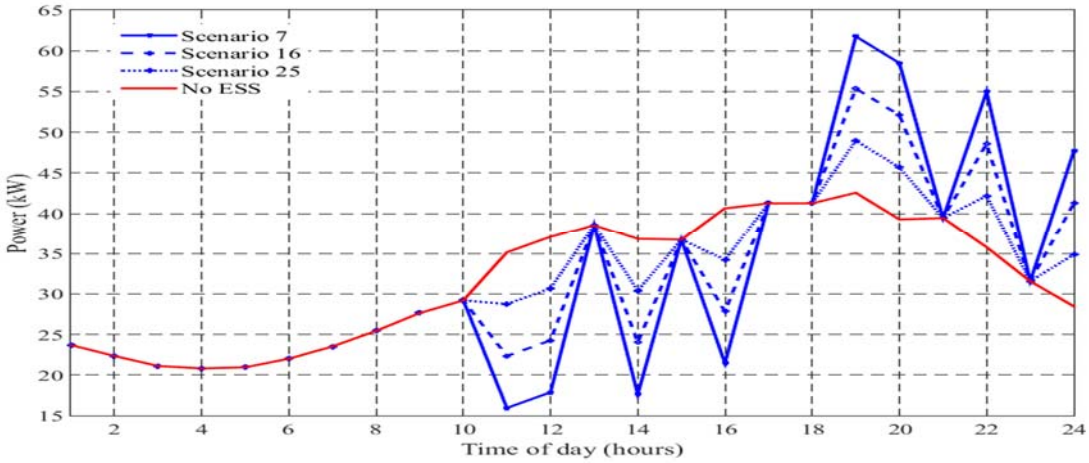

Figure 5.28 Power Seen by 25 kVA Transformer in the Case of 12.8kWh ESS, HoCom Function

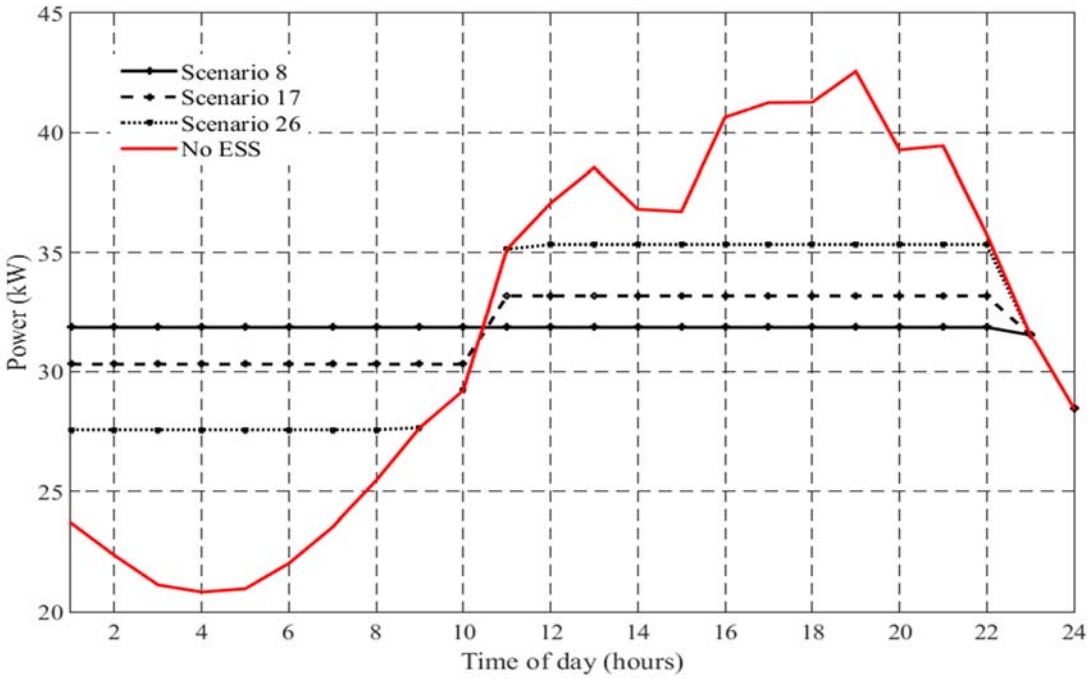

Figure 5.29 Power Seen by 25 kVA Transformer in the Case of 12.8kWh ESS, PAPR Function

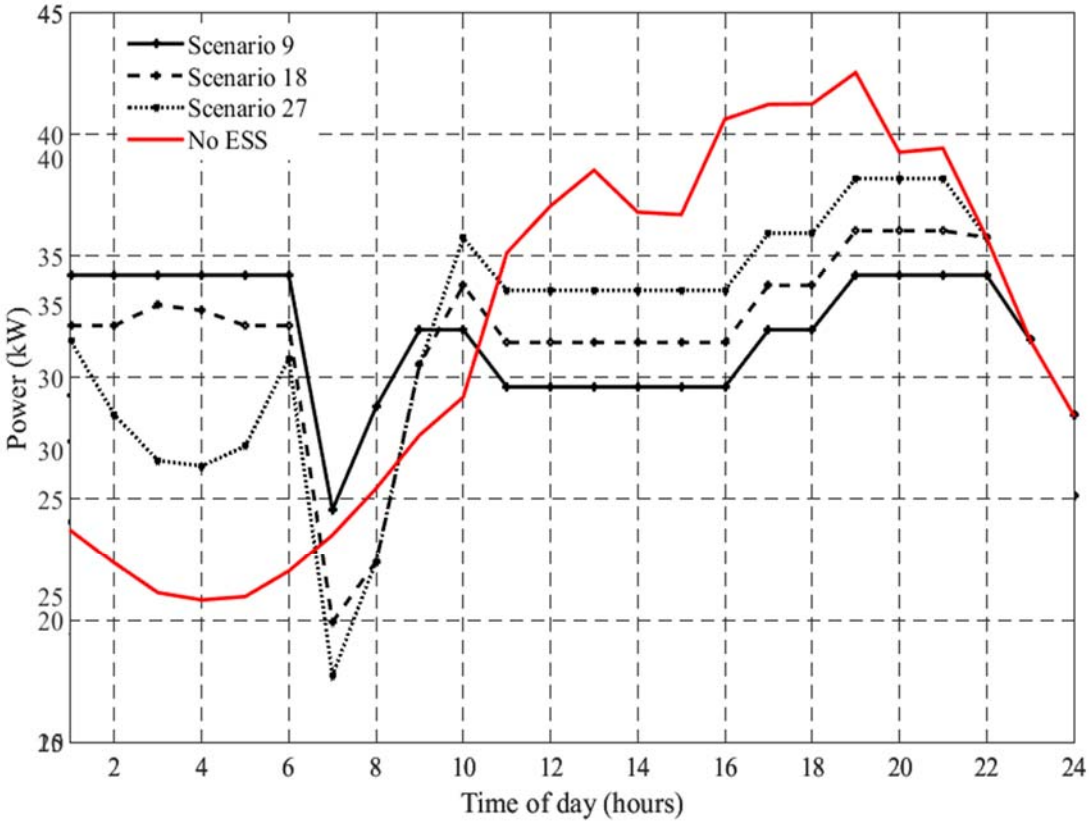

Figure 5.30 Power Seen by 25 kVA Transformer in the Case of 12.8kWh ESS, SOLR Function

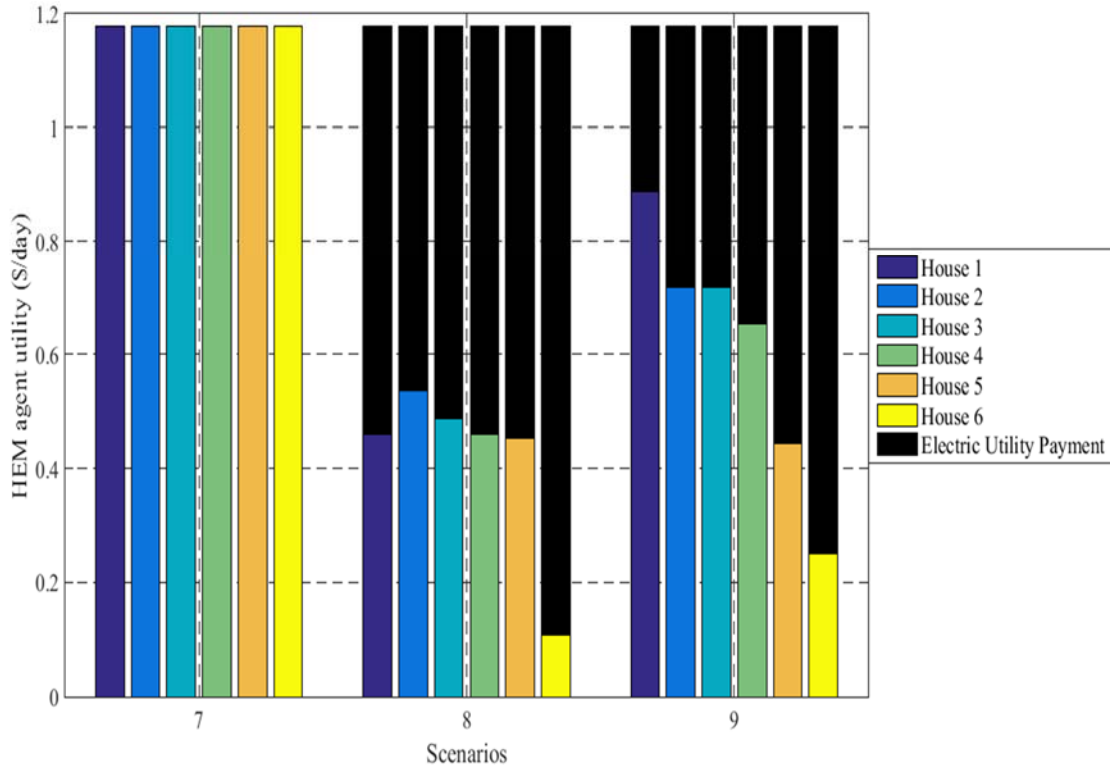

Figure 5.31 Agent Consensus for Different Proposal in Case of 12.8kWh ESS

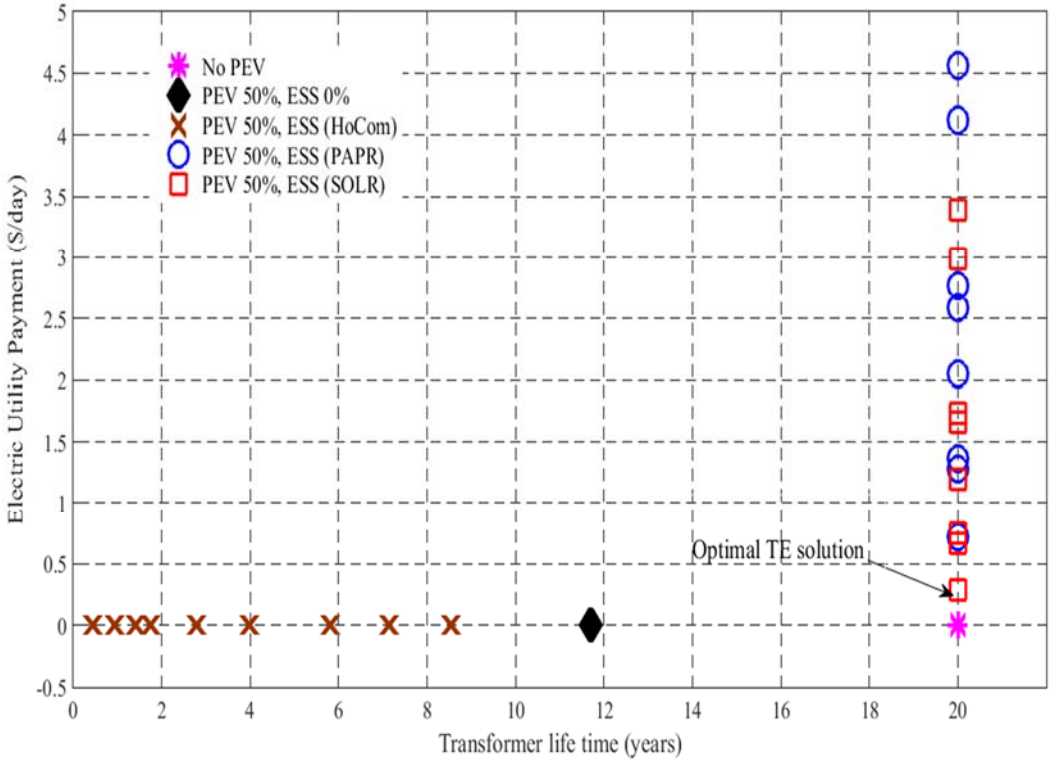

Figure 5.32 Final Solutions Found by HEM, NAEM Agent in the Case of the First Simulation Study

Table 5.7 Statistical Analysis for the Developed Scenarios

Case\ statistical measure		Minimum	Median	Maximum
12 kWh	Transformer life time (years)	0.9	20	20
	Electric utility rebate ($/day)	0	1.3	4.1
6.4 kWh	Transformer life time (years)	1.4	20	20
	Electric utility rebate ($/day)	0	0.7	2
12.8 kWh	Transformer life time (years)	0.4	20	20
	Electric utility rebate ($/day)	0	1.4	4.6

Based on the previous analysis at 50% PEVs penetration with level 2 (3.3 kW) charging power, the adequate ESS storage which satisfies both HEM agents and the electric utility agent is 6.4 kWh. It is found that the optimal TE solution is to operate the ESS using the SOLR objective function. It can also be noted that any of the penetration levels (100%, 66%, or 33%) is capable of mitigating the PEVs impact.

The adequate ESS size (6.4 kWh) will be used to analyze higher penetration of PEVs, and ensure the TE control system will be able to reach an agreement with homeowners and mitigate the PEVs impact at different circumstances.

5.4.2.7 Plug-in Electric Vehicles 100% Penetration Case Study

The PEVs penetration is increased to 100% penetration while keeping the charging level at 240 Volt, 3.3 kW.

Fig. 5.33 shows the transformer loading during a typical day, it can be noticed that the transformer peak power reach to 50kW, which increase the transformer LOL to 0.173% (replacement required after 1.5 years).

Fig 5.34 shows the TE solutions for different ESS penetration 100%, 66%, and 33% (scenarios 6, 15, and 24), the figure reveals that the transformer peak power was reduced to 36.8, 38.9, and 41.5kW for the three selected scenarios.

This reduction will increase the transformer lifetime to 19.5, 13, and 7.6 years in the case of scenarios (6, 15, and 24), respectively.

Fig 5.35 shows the saving for each homeowner, and the required utility payment to reach an agreement with HEM agents.

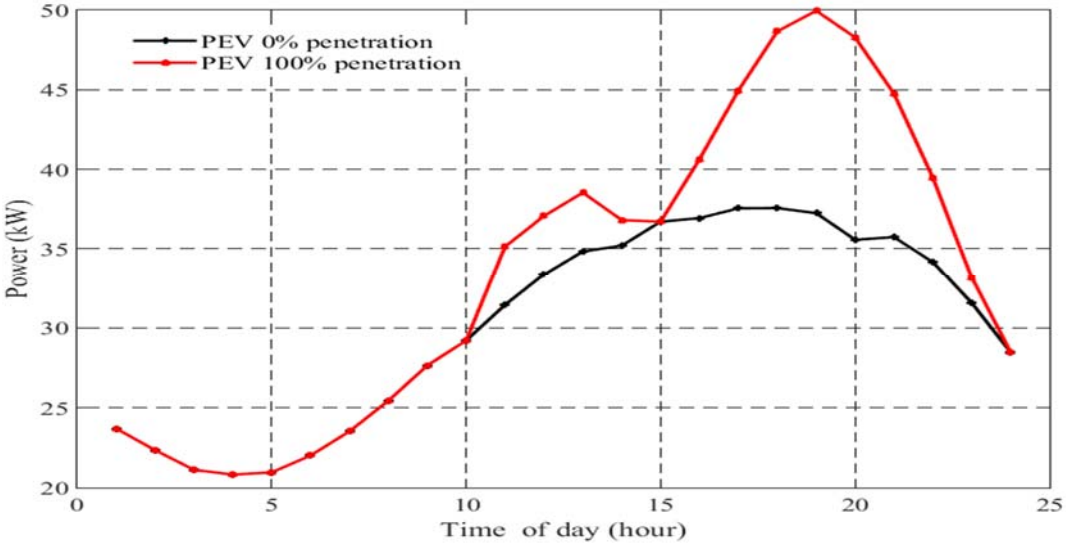

Figure 5.33 Transformer Loading for 100% PEV Penetration

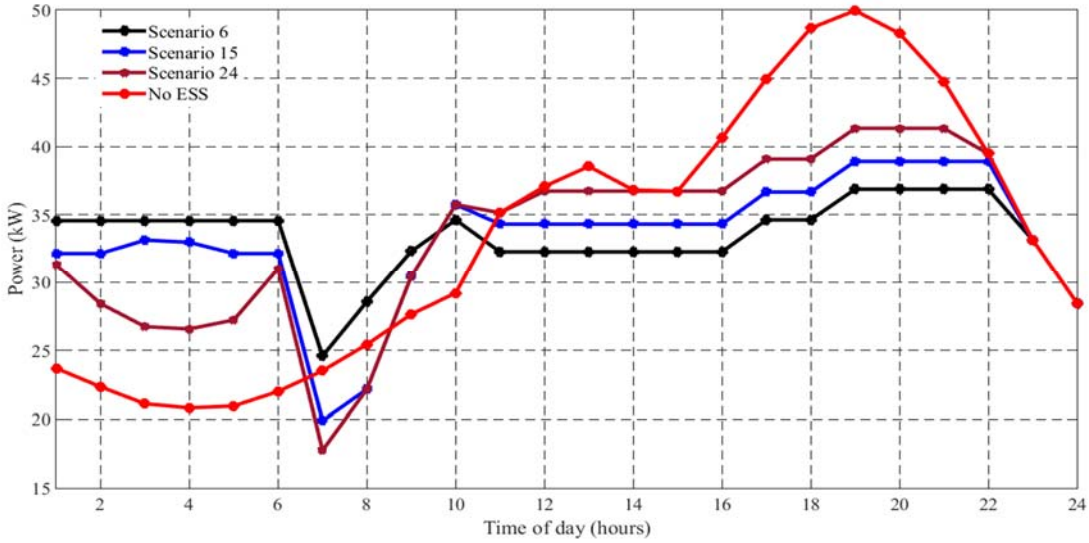

Figure 5.34 Transactive Solutions for 100% PEV Penetration

The optimal TE solution was found to be scenario 6 which will require the utility to pay $10,400 to save 18 replacement of distribution transformer.

Table 5.8 illustrates the results of all the 27 scenarios in terms of transformer LOL, transformer lifetime, and the electric utility payment.

Fig 5.36 shows the layout of all possible solutions during the negotiation rounds between the NAEM agent and HEM agents.

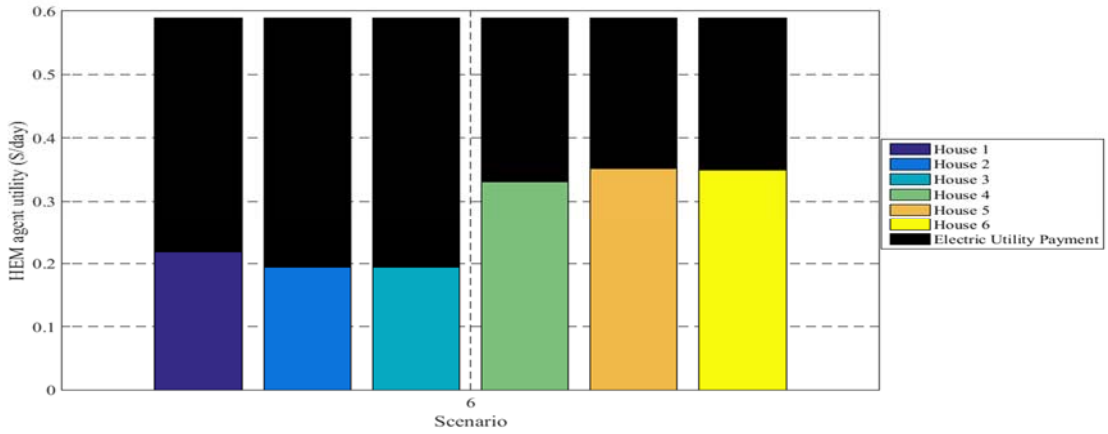

Figure 5.35 Agent Consensus for Different Proposal in Case of 6.4kWh ESS

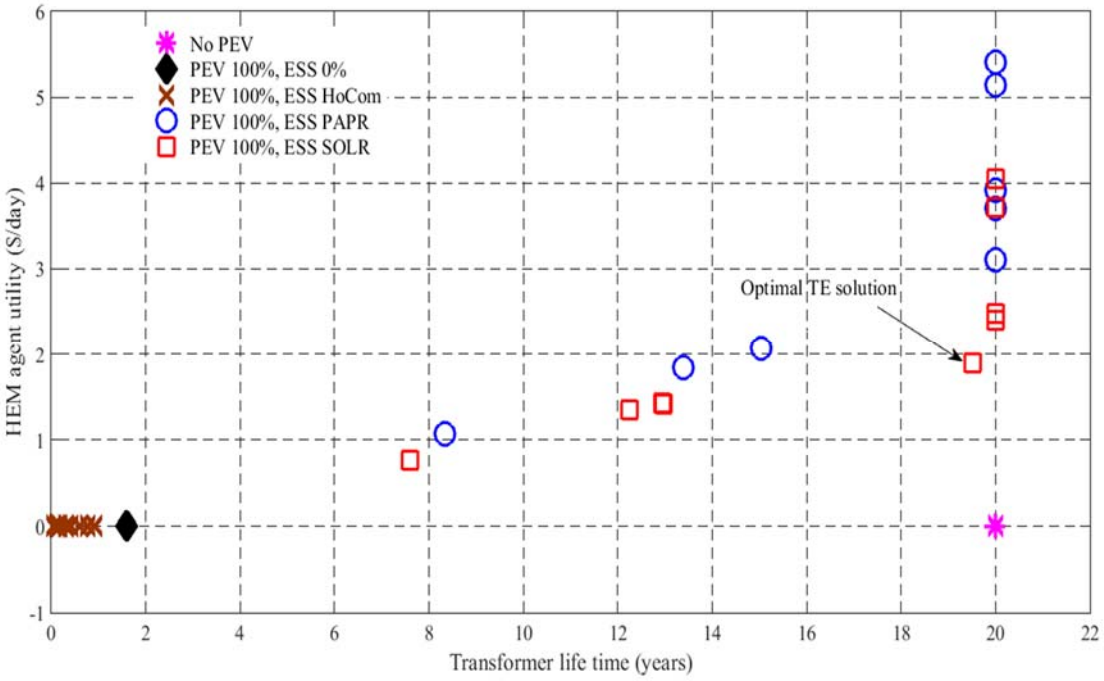

Figure 5.36 Finial Solutions Found by HEM, NAEM Agent in the Case of 100% PEV Penetration

Table 5.8 Summary Results for Simulation Case 2.

Scenarios	Transformer daily loss of life in %	Transformer lifetime (years)	Electric utility rebate ($/day)
1	2.352	0.1	0.0
2	0.005	20.0	5.1
3	0.007	20.0	3.7
4	1.735	0.2	0.0
5	0.011	20.0	3.1
6	0.014	19.5	1.9
7	5.291	0.1	0.0
8	0.005	20.0	5.4
9	0.006	20.0	4.1
10	0.871	0.3	0.0
11	0.009	20.0	3.7
12	0.011	20.0	2.4
13	0.659	0.4	0.0
14	0.018	15.0	2.1
15	0.021	13.0	1.4
16	1.470	0.2	0.0
17	0.008	20.0	3.9
18	0.010	20.0	2.5
19	0.353	0.8	0.0
20	0.020	13.4	1.8
21	0.022	12.3	1.4
22	0.295	0.9	0.0
23	0.033	8.3	1.1
24	0.036	7.6	0.8
25	0.451	0.6	0.0
26	0.018	15.0	2.1
27	0.021	12.9	1.4

5.5 Summary

The result of three case studies are presented in this chapter. The first case study investigates the synergy between wind DGs and PEVs. The simulation results show that the 30% wind DGs penetration is adequate to locally supply the PEVs at 50% penetration. This will reduce the stress over the central generation station. However, the wind DGs are unable to remove the transformer overload. Moreover, at light loading conditions, the reverse reactive power flow is noticed which produces overvoltage in the neighbourhood feeders.

The second case study investigates the use of the rooftop solar photovoltaic as potential solution to mitigate the PEVs impact on the distribution transformer. The results show that solar PVs peak generated power does not coincide with the PEVs peak charging demand therefor the PVs will be able to partially mitigate the PEVs charging demand impact on the distribution system.

The last case study focuses on testing the Transactive Energy (TE) control solution for optimal distribution system operation. Different storage sizes and penetrations are used. It is found that 6.4 kWh is the adequate size of the energy storage system. However, other penetrations of energy storage (e.g., 33%, and 100%) may suffice to mitigate the PEVs impact on distribution transformer at 50%, and 100% PEV penetration, respectively.

The next chapter presents the dissertation conclusion, recommendation, and future work.

Chapter 6: Conclusion and Recommendations

6.1 Conclusion

In this dissertation, the impact of Plug-in Electric Vehicles (PEVs) charging demand on the distribution system is quantified in terms of the transformer overload, transformer hot spot temperature and transformer loss of life. The obtained results, after applying Monte Carlo simulation (MCS), confirmed that any increase in PEVs penetration may cause transformer overload. However, the overload reaches its maximum value around 7 P.M. when most people return from work.

This work investigates different means to mitigate the PEVs impact using distributed energy resources (wind DGs, solar PVs, energy storage systems) and each element of these resources is extensively investigated to measure its effectiveness.

In the first case, the synergy between wind-based DGs and PEVs charging demand is investigated, and it is found that the PEVs maximum charging demand does not coincide with the maximum generated power from wind DGs. The result shows that the PEVs peak charging and the wind DGs peak power occurs around 7:00 P.M, and 5:00 P.M, respectively. The MCS results reveal that 30% wind DG will suffice to supply 50% penetration of PEV without importing any additional power from the substation. Also, the results show that wind DGs are not able to mitigate the transformer overload (25 kVA and 50 kVA) at any penetration level.

The second case investigates the potential of rooftop solar PVs to mitigate the impact of PEVs charging which shows that any solar PVs penetration greater or equal to 10% will be able to relieve the transformer overload from 10 A.M. to 5 P.M. However, in the case

of no PVs and at PEVs penetration of 50%, the transformer hot spot temperature can reach to 121°C, this temperature can be reduced to 107°C (i.e., 13% reduction) by adding solar PVs with 50% penetration. The results show that at 50% PEV penetration the distribution transformer may require replacement after 4 years.

Finally, this work investigates the use of multi-agent system cooperative control in managing the energy storage deployed in the secondary distribution system to mitigate the PEVs impact on the distribution system. Different storage sizing penetration, location, and function are analyzed.

The novel concept of Transactive Energy (TE) is implemented in this work in order to achieve the maximum benefits for the homeowners and the electric utility and justify the cost of energy storage. The results showe that the adequate size of energy storage system is 6.4 kWh per house in order to mitigate the PEVs impact at 50% and 100% penetration. It is found that if the electric utility has no control on the energy storage system operation the distribution transformer will need replacement every 1.4 and 0.2 years in the case of 50% and 100% penetration, respectively. However, the utility can maintain the transformer lifetime to be approximately 20 years if they apply the optimal TE solution. Applying the optimal TE solution justifies the cost of energy storage either from the homeowners' or from the electric utility's perspective. The results show that the homeowners can save up to $3,220 during the energy storage lifetime which covers the cost of energy storage that is estimated to be $3,000. However, the electric utility is required to pay $6,550 and $10,400 to reach an agreement with the homeowners to apply the optimal TE solution in the case of 50% and 100% PEV penetration.

The proposed TE solution will also encourages more residential customers to install DERs in their property and can actively respond to utility requirements through the home energy management which will not add any burden on the homeowners. This active participation from the customers will definitely improve the expected outcomes from the offered incentive programs offered by the IESO for energy conservation.

6.2 Recommendations

Considering the analysis presented in this dissertation, the following recommendations are introduced; the simulation results of the work prove the importance of using a home battery energy storage system to perform a self-healing function for smart grid operation. However, most of the storage projects are related to the community storage system which is very expensive. This thesis recommends the deployment of energy storage at the home level in upcoming incentive programs.

This thesis also recommends that the utility should control the home energy storage system as opposed to allowing the customers to control their own energy storage which may have a higher negative impact on the distribution system than the Plug-in Electric Vehicles.

In order to have a flexible, robust, and reliable distribution system, three levels of energy management system should be included starting from customers (home automation), followed by the secondary distribution system management (neighborhood management) and ending with the wide area management. Lastly, applying the Transactive Energy control is the only way to organize the action and data transfer between the different management system to satisfy both electric utilities and homeowners.

6.3 Future Work

In extension of this work suggestions are presented for future work:

The Transactive Energy control platform presented in this work relies on the day ahead load forecast to setup the proper control action of all energy storage systems. However, the customers' consumption may change during the day which necessity TE control to operate in real time to ensure optimal operation of distribution system.

An additional suggestion is to extend the energy storage to perform ancillary services to both electric utilities and customers (e.g. frequency regulation, removal of power quality issues, and system backup). Investigation of coordination between these functions can maximize the benefit of storage systems and justify their cost.

Finally, The TE control decision is an optimization process which depends on different uncertainties, such as PEVs driven distance and the accuracy of the load forecast, as a result the robustness optimization is required to propose the control action that will be optimal under any circumstance.

Reference

[1] "Plug-in electric vehicles (PEVs) basic benefits [online]" Available at http://www.pge.com/myhome/ environment /whatyoucando/electricvehicles.html

[2] "Electric vehicle incentive and charging incentive programs-Ontario Ministry of Transportation [online]" Available at http://www.mto.gov.on.ca/english/dandv/vehicle/electric/ electricvehicles.html

[3] Live Smart "British Columbia's Clean Energy Vehicle Program Phase 1 Review", July 9, 2015, Available at: http://www2.gov.bc.ca/gov/content/industry/electricity-alternative-energy/transportation-energies/clean-transportation-policies-programs/clean-energy-vehicle-program

[4] "Transportation Revolution: Shifting to Electric Vehicles on Canadian Streets", WWF-Canada 2013, available: http://awsassets.wwf.ca/downloads/ev_campaign_ report.

[5] Plug'N Drive Organization "Electric Vehicles: Reducing Ontario's Greenhouse Gas Emissions", a climate change action report, May 2015.

[6] M. Yilmaz and P. T. Krein, "Review of Charging Power Levels and Infrastructure for Plug- In Electric and Hybrid Vehicles," in Proc. IEEE International Electric Vehicle Conference, Greenville, SC, USA, 2012, pp. 1-8.

[7] A. Madariaga, I. de Alegria, J. Martin, P. Eguia, and S. Ceballos, "Market forecasts, feasibility studies and regulatory framework for offshore wind energy integration," in Proc. IEEE 37th Annual Conference on Industrial Electronics, IECON, Melbourne, VIC, Nov. 2011, pp. 3170– 3175.

[8] "Ontario power authority Feed-in Tariff [online]," Available at : http://microfit.powerauthority.on.ca/

[9] T. Gonen, “Electric Power Distribution Engineering, third ed”., CRC Press, BocaRaton, FL, 2014.

[10] M. S. ElNozahy and M. M. A. Salama, “Studying the feasibility of charging plug-in hybrid electric vehicles using photovoltaic electricity in residential distribution systems,” Elect. Power Syst. Res., vol. 110, pp. 133–143, May 2014.

[11] O. Sagosen, and M. Molinas,"Large scale regional adoption of electric vehicles in Norway and the potential for using wind power as source," in Proc. 2013 International Conference on Clean Electrical Power (ICCEP), Alghero, Italy, June 2013, pp.189-196

[12] M. J. Rutherford and V. Yousefzadeh, “The impact of electric vehicle battery charging on distribution transformers,” in Proc. 26th IEEE Appl. Power Electron. Conf. Expo. (APEC), Fort Worth, TX, USA, Mar. 2011, pp. 396–400.

[13] Van Zandt, Devin, and Reigh Walling. "DSTAR’s Transformer Cost Analysis Software Enhances Utility Decision Process." Tech. General Electric (2004).

[14] "Electric Power Distribution Systems Operations.", Naval Facilities Engineering Command (NAVFAC), Virginia, USA, April 1990.

[15] Short, Thomas Allen. “Electric power distribution handbook”. CRC press, 2014.

[16] “Ontario’s Five Years Climate Change Action Plan 2016- 2020”, available at : https://www.ontario.ca/page/climate-change-action-plan

[17] Power Delivery & Utilization, “Functional Requirements for Electric Energy Storage Applications on the Power System Grid”, Electric Power Research Institute (EPRI) report, Nov, 2011

[18] J. Cobb “Top Six Plug-in Vehicle Adopting Countries – 2015”, online available at : http://www.hybridcars.com/top-six-plug-in-vehicle-adopting-countries-2015/

[19] K. Bojanczyk, “Redefining Home Energy Management Systems”, Greentech media, Sept. 2013

[20] “home energy management architecture”, online, available at : http://www.nuritelecom.com/products/in-home-device-ihd.html

[21] J. Shaver “Demand Optimization for Efficient Grid Operations”, Electric Energy Magazine, Oct. 2013.

[22] Strategy, NETL Modern Grid. "Advanced metering infrastructure." US Department of Energy Office of Electricity and Energy Reliability (2008).

[23] J. C. Fuller, K. P. Schneider and D. Chassin, "Analysis of Residential Demand Response and double-auction markets," 2011 IEEE Power and Energy Society General Meeting, San Diego, CA, 2011, pp. 1-7

[24] The GridWise Architecture Council “GridWise Transactive Energy Framework Version 1.0”, PNNL-22946 Ver1.0, Jan, 2015

[25] Toronto Hydro Corporation Annual Report, “The Measure of our Commitment”, Toronto Hydro-electric System Limited, Toronto, ON, Canada, 2012

[26] Ontario Energy Board, “Ontario Wholesale Electricity Market Price Forecast”.

[27] S. F. Abdelsamad, W. G. Morsi and T. S. Sidhu, "Impact of Wind-Based Distributed Generation on Electric Energy in Distribution Systems Embedded With Electric Vehicles," in IEEE Transactions on Sustainable Energy, vol. 6, no. 1, pp. 79-87, Jan. 2015.

[28] S. F. Abdelsamad, W. G. Morsi and T. S. Sidhu, "Probabilistic Impact of Transportation Electrification on the Loss-of-Life of Distribution Transformers in the Presence of

Rooftop Solar Photovoltaic," in IEEE Transactions on Sustainable Energy, vol. 6, no. 4, pp. 1565-1573, Oct. 2015.

[29] S. F. Abdelsamad, W. G. Morsi and T. S. Sidhu "Optimal secondary distribution system design considering plug-in electric vehicles." Electric Power Systems Research 130 (2016): 266-276.

[30] S. F. Abdelsamad, W. G. Morsi, and T. S. Sidhu, "On the impact of transportation electrification on distribution systems in the presence of rooftop solar photovoltaic," Electrical Power and Energy Conference (EPEC), 2015 IEEE, London, ON, 2015, pp. 26-31.

[31] S. Gao, K. Chau, C. Liu, D. Wu, and C. Chan, "Integrated energy management of plug-in electric vehicles in power grid with renewables," IEEE Trans. on Veh. Technol., vol. PP, no. 99, pp.1-8, Apr. 2014.

[32] A. Bouallaga, A. Merdassi, A. Davigny, B. Robyns, and V. Courtecuisse, "Minimization of energy transmission cost and CO2 emissions using coordination of electric vehicle and wind power (W2V)," in Proc. 2013 IEEE Grenoble PowerTech, Grenoble, France, June 2013, pp.1-6

[33] D. Wu, D.C. Aliprantis, and K. Gkritza, "Electric energy and power consumption by light-duty plug-in electric vehicles," IEEE Trans. Power Syst., vol.26, no.2, pp.738-746, May 2011.

[34] Y. Cao, S. Tang, C. Li, P. Zhang, Y. Tan, Z. Zhang, and J. Li. "An Optimized EV Charging Model Considering TOU Price and SOC Curve", IEEE Trans. on Smart Grid, vol. 3, no. 1, pp. 388- 393, Mar. 2012.

[35] L. Xu, M. Marshall, and L. Dow, "A Framework for Assessing the Impact of Plug-In Electric Vehicle to Distribution Systems," in Proc. Of the IEEE/PES Power Systems Conference and Exposition (PSCE), Phoenix, Arizona, USA, 2011, pp. 1-6.

[36] Q. Yan and M. Kezunovic, "Impact Analysis of Electric Vehicle Charging on Distribution System," in Proc. Of the IEEE North American Power Symposium (NAPS), Champaign, IL, USA, 2012, pp. 1-6.

[37] P. Richardson, D. Flynn, and A. Keane, "Impact Assessment of Varying Penetrations of Electric Vehicles on Low Voltage Distribution Systems," in Proc. IEEE Power and Energy Society General Meeting, 2010, pp. 1-6.

[38] J. Waddell, M. Rylander, A. Maitra, and J. A. Taylor, "Impact of Plug In Electric Vehicles on Manitoba Hydro's Distribution System," in Proc. Electrical Power and Energy Conference, Winnipeg, MB, Canada, 2011, pp. 409-414.

[39] S. Paudyal and S. Dahal, "Impact of Plug-In Hybrid Electric Vehicles and Their Optimal Deployment in Smart Grids," in Proc. 21st Australian Universities Power Engineering Conf. (AUPEC), 2011, pp. 1-6.

[40] C. Farkas, K. I. Szabo, and L. Prikler, "Impact Assessment of Electric Vehicle Charging on a LV Distribution System," in Proc. Of the 23rd International Youth Conf. on Energetics (IYCE), 2011, pp. 1-8.

[41] P. S. Moses, M. A. S. Masoum, and S. Hajforoosh, "Overloading of Distribution Transformers in Smart Grid Due to Uncoordinated Charging of Plug-In Electric Vehicles," presented at the Innovative Smart Grid Technologies, 2012.

[42] D. Wu, C. Cai, and D. C. Aliprantis, "Potential Impacts of Aggregator-Controlled Plug-in Electric Vehicles on Distribution Systems," in Proc. Of the 4th IEEE International

Workshop on Computational Advances in Multi-sensor Adaptive processing (CAMSAP), San Juan, Puerto Rico, 2011, pp. 105-108.

[43] M. k. Gray, and W. G. Morsi, "Power quality assessment in distribution systems embedded with plug-in hybrid and battery electric vehicles," IEEE Trans. Power. Syst., vol. PP, no. 99, pp. 1-9, Jul. 2014

[44] K. Clement-Nyns, E. Haesen, and J. Driesen, "The impact of charging plug-in hybrid electric vehicles on a residential distribution grid," IEEE Transactions on Power Systems, vol. 25, no.1, pp. 371–380, Feb 2010.

[45] C. Canizares, J. Nathwani, K. Bhattacharya, M. Fowler, M. Kazerani, R. Fraser, I. Rowlands, H. Gabbar, "Towards an Ontario action plan fo plug-in-electric vehicles (PEVs)," Waterloo Institute for Sustainable Energy, University of Waterloo, May 17, 2010.

[46] E. Sortomme, M. M. Hindi, S. D. MacPherson, and S. S. Venkata, "Coordinated charging of plug-in hybrid electric vehicles to minimize distribution system losses," IEEE Transactions on Smart Grid, vol. 2, no. 1, Mar 2011.

[47] A. Bosovic, M. Music, S. Sadovic, "Analysis of the impacts of plug-in electric vehicle charging on the part of a real low voltage distribution network", PowerTech, Eindhoven, 2015.

[48] Y. Assolami, and W. G. Morsi. "Impact of Second-Generation Plug-In Battery Electric Vehicles on the Aging of Distribution Transformers Considering TOU Prices." IEEE Trans. Sustainable Energy vol. 6, no. 4, Oct. 2015, pp. 1606-1614.

[49] N. G. Paterakis, O. Erdinç, I. N. Pappi, A. G. Bakirtzis, and J. P. S. Catalãao, "Coordinated Operation of a Neighborhood of Smart Households Comprising Electric

Vehicles, Energy Storage and Distributed Generation," in IEEE Trans. Smart Grid , vol.PP, no.99, pp.1-12

[50] L. Kelly, A. Rowe, and P.Wild, "Analyzing the impacts of plug-in electric vehicles on distribution networks in British Columbia," in Proc. IEEE Elect. Power Energy Conf. (EPEC), Montreal, QC, Canada, Oct. 2009, pp. 1–6.

[51] M. J. Rutherford and V. Yousefzadeh, "The impact of electric vehicle battery charging on distribution transformers," in Proc. 26th IEEE Appl. Power Electron. Conf. Expo. (APEC), Fort Worth, TX, USA, Mar. 2011, pp. 396–400.

[52] A. D. Hilshey, P. D. H. Hines, and J. R. Dowds, "Estimating the acceleration of transformer aging due to electric vehicle charging," in Proc. IEEE Power Energy Soc. Gen. Meeting, Detroit, MI, USA, Jul. 2011, pp. 1–9.

[53] S. Argade, V. Aravinthan, and W. Jewell, "Probabilistic modeling of EV charging and its impact on distribution transformer loss of life," in Proc. IEEE Int. Elect. Veh. Conf. (IEVC), Greenville, SC, USA, Mar. 2012, pp. 1–8.

[54] S. M. M. Agah and A. Abbasi, "The impact of charging plug-in hybrid electric vehicles on residential distribution transformers," in Proc. 2nd IEEE Iran. Conf. Smart Grids (ICSG), Tehran, Iran, Mar. 2012, pp. 1–5.

[55] Q. Yan and M. Kezunovic, "Impact analysis of electric vehicle charging on distribution system," in Proc. IEEE North Amer. Power Symp., Champaign, IL, USA, Sep. 2012, pp. 1–6.

[56] A. D. Hilshey, P. D. H. Hines, P. Rezaei, and J. R. Dowds, "Estimating the impact of electric vehicle smart charging on distribution transformer aging," IEEE Trans. Smart Grid, vol. 4, no. 2, pp. 905–913, Jun. 2013.

[57] Q. Gong, S. Midlam-Mohler, V. Marano, and G. Rizzoni, “Study of PEV charging on residential distribution transformer life,” IEEE Trans. Smart Grid, vol. 3, no. 1, pp. 404–412, Mar. 2012.

[58] K. Clement-Nyns, E. Haesen, and J. Driesen, “The impact of charging plug-in hybrid electric vehicles on a residential distribution Grid,” IEEE Trans. Power Syst., vol. 25, no. 1, pp. 371–380, Feb. 2010.

[59] F. M. Uriarte, A. Toliyat, A. Kwasinski, and R. E. Hebner, “Consumerdata approach to assess the effect of residential grid-tied photovoltaic systems and electric vehicles on distribution transformers,” in Proc. IEEE 5th Int. Symp. Power Electron. Distrib. Gener. Syst. (PEDG), Galway, Ireland, Jun. 2014, pp. 1–8.

[60] T. J. Geiles and S. Islam, “Impact of PEV charging and rooftop PV penetration on distribution transformer life,” in Proc. IEEE Power Energy Soc. Gen. Meeting, Vancouver, BC, Canada, Jul. 2013, pp. 1–5.

[61] Rajakaruna, Sumedha, F. Shahnia, and A. Ghosh. “Plug in electric vehicles in smart grids”, Springer Power Systems, 2015.

[62] A. Ali, M. Abdel-Akher, Z. Ziadi, T. Senjyu, "Coordinated charging of plug-in hybrid electric vehicle for voltage profile enhancement of distribution systems,"in Proc. Power Electronics and Drive Systems (PEDS), pp.399-404, Apr. 2013

[63] E. Sortomme, M. Hindi, S. MacPherson, S. Venkata,"Coordinated Charging of Plug-In Hybrid Electric Vehicles to Minimize Distribution System Losses," IEEE Trans. Smart Grid, vol.2, no.1, pp.198-205, Mar. 2011

[64] B. Geng, J.K. Mills, and D. Sun. "Coordinated charging control of plugin electric vehicles at a distribution transformer level using the vTOUDP approach." In Proc. IEEE

Vehicle Power and Propulsion Conference (VPPC), Seoul, Korea, Oct. 2012, pp.1469 – 1474.

[65] K. De Craemer, and G. Deconinck, "Balancing trade-offs in coordinated PHEV charging with continuous market-based control," in Proc. 3rd IEEE PES International Conference and Exhibition on Innovative Smart Grid Technologies (ISGT Europe), Berlin, Germany, Oct. 2012, pp.1-8.

[66] J. Linni, H. Xue, G. Xu, X. Zhu, D. Zhao and Z.Y. Shao, "Regulated charging of plug-in hybrid electric vehicles for minimizing load variance in household smart microgrid," IEEE Trans. Ind. Electron., vol.60, no.8, pp.3218-3226, Aug. 2013.

[67] Q. Yuehao, L. Haoming, D. Wang, L. Xifeng ,"Intelligent Strategy on Coordinated Charging of PHEV with TOU Price," Power and Energy Engineering Conference (APPEEC), pp.1,5, Mar. 2011

[68] T. Logenthiran and D. Srinivasan, "Multi-agent system for managing a power distribution system with Plug-in Hybrid Electrical vehicles in smart grid," in Proc. IEEE PES Innovative Smart Grid Technologies (ISGT), India, Kollam, Kerala, Dec. 2011, pp. 346-351.

[69] E. L. Karfopoulos and N. D. Hatziargyriou, "A Multi-Agent System for Controlled Charging of a Large Population of Electric Vehicles," in IEEE Trans. Pow. Sys., vol. 28, no. 2, pp. 1196-1204, May 2013.

[70] P. Papadopoulos, N. Jenkins, L. M. Cipcigan, I. Grau and E. Zabala, "Coordination of the Charging of Electric Vehicles Using a Multi-Agent System," in IEEE Trans. Smart Grid, vol. 4, no. 4, pp. 1802-1809, Dec. 2013.

[71] Y. Xu, "Optimal Distributed Charging Rate Control of Plug-In Electric Vehicles for Demand Management," in IEEE Trans. on Pow. Sys., vol. 30, no. 3, pp. 1536-1545, May 2015.

[72] L. Piao, Q. Ai and S. Fan, "Game theoretic based pricing strategy for electric vehicle charging stations," in Proc. IEEE International Conference on Renewable Power Generation (RPG), Beijing, Apr. 2015, pp. 1-6.

[73] L. A. Hurtado, A. Syed, P. H. Nguyen and W. L. Kling, "Multi-agent based electric vehicle charging method for smart grid-smart building energy management," in Proc. IEEE PowerTech, , Eindhoven, Sept. 2015, pp. 1-6.

[74] S. Weckx, R. D'Hulst, B. Claessens and J. Driesensam, "Multiagent Charging of Electric Vehicles Respecting Distribution Transformer Loading and Voltage Limits," in IEEE Trans. Smart Grid, vol. 5, no. 6, pp. 2857-2867, Nov. 2014.

[75] S. Tie, C. Tan " A review of energy sources and energy management system in electric vehicles". Renew Sustain Energy Rev 20:82–102

[76] Sheikhi A, Bahrami S, Ranjbar A, Oraee H (2013) "Strategic charging method for plugged in hybrid electric vehicles in smart grids"; a game theoretic approach. Int J Electr Power Energy Syst 53:499–506

[77] Sortomme E, Hindi M, MacPherson S, Venkata S (2011) Coordinated charging of plug-in hybrid electric vehicles to minimize distribution system losses. IEEE Trans Smart Grid 2:198–205

[78] Clement K, Haesen E, Driesen J (2009) Stochastic analysis of the impact of plug-in hybrid electric vehicles on the distribution grid. Paper presented at the 20th international

conference and exhibition on electricity distribution—Part 2, 2009 CIRED, Prague, 8–11 June 2009

[79] S. Übermasser and M. Stifter, "A multi-agent based approach for simulating G2V and V2G charging strategies for large electric vehicle fleets," Electricity Distribution (CIRED 2013), 22nd International Conference and Exhibition on, Stockholm, 2013, pp. 1-4.

[80] J. Chenrui, T. Jian, P. Ghosh,"Optimizing electric vehicle charging with energy storage in the electricity market," IEEE Trans. Smart Grid, vol.4, no.1, pp.311,320, Mar. 2013

[81] C. Gouveia, J. Moreira, C. L. Moreira, J. A. Pecas, "Coordinating storage and demand response for microgrid emergency operation," IEEE Trans. Smart Grid, vol.4, no.4, pp.1898,1908, Dec. 2013

[82] H. Melo, C. Heinrich, "Energy balance in a Renewable Energy Community," Environment and Electrical Engineering (EEEIC), pp.1,4, May 2011

[83] G. Tina, S. Gagliano, and S. Raiti, "Hybrid solar/wind power system probabilistic modelling for long-term performance assessment," Solar Energy, vol. 80, no. 5, pp. 578–588, May 2006.

[84] Y. Atwa, E. El-Saadany, and A.-C. Guise, "Supply adequacy assessment of distribution system including wind-based DG during different modes of operation," IEEE Trans. on Power Syst., vol. 25, no. 1, pp. 78–86, Feb. 2010.

[85] F. Vallee, G. Brunieau, M. Pirlot, O. Deblecker, and J. Lobry,"Optimal Wind Clustering Methodology for Adequacy Evaluation in System Generation Studies Using Nonsequential Monte Carlo Simulation," IEEE Trans. on Power Syst., vol.26, no.4, pp.2173-2184, Nov. 2011

[86] F. Duarte, J. Duarte, S. Ramos, A. Fred, and Z. Vale, "Daily wind power profiles determination using clustering algorithms," in Proc. IEEE International Conference on Power System Technology (POWERCON), Auckland, New Zealand, Oct. 2012, pp.1-6.

[87] J. H. Kim and W. B. Powell, "Optimal energy commitments with storage and intermittent supply," Operations Research, vol. 59, pp. 1347–1360, Dec 2011.

[88] Y. Riffonneau, S. Bacha, F. Barruel, S. Ploix,"Optimal power flow management for grid connected PV systems with batteries," IEEE Trans. Sustain. Energy, vol.2, no.3, pp.309,320, Jul. 2011

[89] J. Quanyuan, G. Yuzhong, W. Haijiao, "A battery energy storage system dual-layer control strategy for mitigating wind farm fluctuations," in Proc. IEEE Power & Energy Society General Meeting, National Harbor, MD, Jul. 2014, pp.1,1

[90] A. Arabali, M. Ghofrani, M. Etezadi-Amoli, M.S. Fadali, "Stochastic performance assessment and sizing for a hybrid power system of solar/wind/energy storage," IEEE Trans. Sustain. Energy, vol.5, no.2, pp.363,371, Apr. 2014

[91] Y. Kanoria, A. Montanari, D. Tse, and B. Zhang, "Distributed storage for intermittent energy sources: Control design and performance limits," in Proc. Allerton Conf. on Commun., Control, and Comput., 2011.

[92] Y. Wang, X. Lin, and M. Pedram, "Adaptive control for energy storage systems in households with photovoltaic modules," IEEE Trans. Smart Grid, vol. 5, pp. 992–1001, March 2014.

[93] Y. Zhang and M. van der Schaar, "Structure-aware stochastic storage management in smart grids," IEEE J. Sel. Topics Signal Process., vol. 8, pp. 1098–1110, Dec 2014.

[94] L. Huang, J. Walrand, and K. Ramchandran, “Optimal demand response with energy storage management,” in Proc. IEEE SmartGridComm, Nov. 2012.

[95] S. Salinas, M. Li, P. Li, and Y. Fu, “Dynamic energy management for the smart grid with distributed energy resources,” IEEE Trans. Smart Grid, vol. 4, pp. 2139–2151, Sep. 2013.

[96] C. P. Nguyen and A. J. Flueck, "Agent Based Restoration With Distributed Energy Storage Support in Smart Grids," in IEEE Transactions on Smart Grid, vol. 3, no. 2, pp. 1029-1038, June 2012.

[97] T. Wei, Q. Zhu and N. Yu, "Proactive Demand Participation of Smart Buildings in Smart Grid," in IEEE Transactions on Computers, vol. 65, no. 5, pp. 1392-1406, May 1 2016.

[98] B. Asare-Bediako, W. L. Kling and P. F. Ribeiro, "Multi-agent system architecture for smart home energy management and optimization," IEEE PES ISGT Europe 2013, Lyngby, 2013, pp. 1-5.

[99] A. Zidan and E. F. El-Saadany, "A Cooperative Multiagent Framework for Self-Healing Mechanisms in Distribution Systems," in IEEE Transactions on Smart Grid, vol. 3, no. 3, pp. 1525-1539, Sept. 2012.

[100] M. Eriksson, M. Armendariz, O. O. Vasilenko, A. Saleem and L. Nordström, "Multiagent-Based Distribution Automation Solution for Self-Healing Grids," in IEEE Transactions on Industrial Electronics, vol. 62, no. 4, pp. 2620-2628, April 2015.

[101] X. Wang, X. Chen, H. Hu, K. Yu and Z. Li, "Research on self-healing restoration strategy of urban power grid based on multi-agent technology," Advanced Power

System Automation and Protection (APAP), 2011 International Conference on, Beijing, 2011, pp. 1215-1218.

[102] P. H. Nguyen, W. L. Kling and P. F. Ribeiro, "A Game Theory Strategy to Integrate Distributed Agent-Based Functions in Smart Grids," in IEEE Transactions on Smart Grid, vol. 4, no. 1, pp. 568-576, March 2013.

[103] Kim, Jong-Yul, et al. "Cooperative control strategy of energy storage system and microsources for stabilizing the microgrid during islanded operation."IEEE Transactions on Power Electronics 25.12 (2010): 3037-3048.

[104] D. He, D. Shi and R. Sharma, "Consensus-based distributed cooperative control for microgrid voltage regulation and reactive power sharing," IEEE PES Innovative Smart Grid Technologies, Europe, Istanbul, 2014, pp. 1-6.

[105] Y. Xu, W. Zhang, G. Hug, S. Kar and Z. Li, "Cooperative Control of Distributed Energy Storage Systems in a Microgrid," inIEEE Transactions on Smart Grid, vol. 6, no. 1, pp. 238-248, Jan. 2015.

[106] F. I. Hernandez, C. A. Canesin, R. Zamora and A. K. Srivastava, "Active power management in multiple microgrids using a multi-agent system with JADE," Industry Applications (INDUSCON), 2014 11th IEEE/IAS International Conference on, Juiz de Fora, 2014, pp. 1-8.

[107] R. Fazal, J. Solanki and S. K. Solanki, "Demand response using multi-agent system," North American Power Symposium (NAPS), 2012, Champaign, IL, 2012, pp. 1-6.

[108] Ren, Fenghui, Minjie Zhang, and Danny Sutanto. "A multi-agent solution to distribution system management by considering distributed generators."IEEE Transactions on Power Systems 28.2 (2013): 1442-1451.

[109] Farag, Hany E., E. F. El-Saadany, and R. Seethapathy. "A multi-agent voltage and reactive power control for multiple feeders with distributed generation." 2013 IEEE Power & Energy Society General Meeting. IEEE, 2013.

[110] Xin, H., et al. "Cooperative control strategy for multiple photovoltaic generators in distribution networks." IET control theory & applications 5.14 (2011): 1617-1629.

[111] Chen, Yuanrui, and Jie Wu. "Agent-based energy management and control of a grid-connected wind/solar hybrid power system." Electrical Machines and Systems, 2008. ICEMS 2008. International Conference on. IEEE, 2008.

[112] Ni Zhang, Yu Yan, Shengyao Xu and Wencong Su, "Game-theory-based electricity market clearing mechanisms for an open and transactive distribution grid," 2015 IEEE Power & Energy Society General Meeting, Denver, CO, 2015, pp. 1-5.

[113] M. N. Akter and M. A. Mahmud, "Analysis of different scenarios for residential energy management under existing retail market structure," Smart Grid Technologies - Asia (ISGT ASIA), 2015 IEEE Innovative, Bangkok, 2015, pp. 1-6.

[114] S. Behboodi, D. P. Chassin, C. Crawford and N. Djilali, "Electric Vehicle Participation in Transactive Power Systems Using Real-Time Retail Prices," 2016 49th Hawaii International Conference on System Sciences (HICSS), Koloa, HI, 2016, pp. 2400-2407

[115] S. Rahman," Integration of demand response with renewable energy for efficient power system operation". In Proc. IEEE PES ISGT Middle East Conference and Exhibition (2011)

[116] I.S. Walker, A.K. Meier," Residential thermostats: Comfort controls in California homes". Project Report LBNL-938E, Lawrence Berkeley National Laboratory (March 2008)

[117] SAE International , J1772_201210 "SAE Electric Vehicle and Pug in Hybrid Electric Vehicle Conductive Charging Coupler", Feb. 2016, available at : http://standards.sae.org/j1772_201210/

[118] "Plug-in electric vehicle and infrastructure analysis". [online], Available: /https://avt.inl.gov/pdf/arra/ARRAPEVnInfrastructureFinalReportHqltySept2015.pdf

[119] C. S. K. Yeung, A. S. Y. Poon, and F. F.Wu, "Game theoretical multiagents modelling of coalition formation for multilateral trades," IEEE Trans. Power Syst., vol. 14, no. 3, pp. 929–934, 1999.

[120] W. Saad, Z. Han, and H. V. Poor, "Coalitional game theory for cooperative micro-grid distribution networks," in Proc. 2011 IEEE Int. Conf. Commun. Workshops (ICC), pp. 1–5.

[121] M. Woolridge „An Introduction to Multi-Agent-Systems", Wiley, 2001

[122] D. B. West, "Introduction to graph theory". Vol. 2. Upper Saddle River: Prentice hall, 2001.

[123] FIPA "Foundation for Intelligent Physical Agents", [Online] Available: http://www.fipa.org

[124] G. Weiss, “Multiagent Systems: A Modern Approach to Distributed Artificial Intelligence”. Cambridge, MA: The MIT Press, 2000.

[125] Gibbons, Robert. Game theory for applied economists. Princeton University Press, 1992.

[126] Hamilton, Jonathan H., and Steven M. Slutsky. "Endogenous timing in duopoly games: Stackelberg or Cournot equilibria." Games and Economic Behavior 2.1 (1990): 29-46.

[127] Anderson, Simon P., and Maxim Engers. "Stackelberg versus Cournot oligopoly equilibrium." International Journal of Industrial Organization 10.1 (1992): 127-135.

[128] Nash Jr, John F. "The bargaining problem." Econometrica: Journal of the Econometric Society (1950): 155-162.

[129] W. H. Kersting, Distribution System Modeling and Analysis. Boca Raton, FL, USA: CRC Press, 2012

[130] R. Christian, and G. Casella. “Introducing Monte Carlo Methods with R” Springer Science & Business Media, 2009.Gilks.

[131] Doucet, Arnaud, Nando De Freitas, and Neil Gordon. "An introduction to sequential Monte Carlo methods." Sequential Monte Carlo methods in practice. Springer New York, 2001. 3-14.

[132] M. Gray, “Probabilistic Assessment of the Impact of Plug-in Electric Vehicles on Power Quality in Electric Distribution Systems”. Diss. University of Ontario Institute of Technology, 2013.

[133] U.S. Department of Transportation, Federal Highway Administration. (2009). "National Household Travel Survey" [Online]. Available: http:// nhts.ornl.govD. Wu, D.C.

[134] "Electric Car Charging 101 — Types of Charging, Charging Networks, Apps, & More", available on line at : http://evobsession.com/electric-car-charging-101-types-of-charging-apps-more/

[135] A. Madariaga, I. M. Alegria, J. L. Martin, P. Eguia, and S. Ceballos, "Market forecasts, feasibility studies and regulatory framework for offshore wind energy integration," in Proc. IEEE 37th Annu. Conf. Ind. Electron. (IECON), Melbourne, Australia, Nov. 2011, pp. 3170–3175.

[136] P.-N. Tan, Introduction to Data Mining. Boston, MA, USA: Pearson Education, 2007.

[137] National Oceanic and Atmospheric Administration. (2010). National Climatic Data Center (NCDC) Stations Database [Online]. Available: http:// www.ncdc.noaa.gov/cdo-web/datasets/normal_hly/stations/GHCND:US W00014732/detail

[138] R. H. Abdel-Hamid, M. A. A. Adma, A. A. Fahmy, and S. F. A. Samed, "Optimization of wind farm power generation using new unit matching technique," in Proc. 7th IEEE Int. Conf. Ind. Informat. (INDIN), Cardiff, U.K., Jun. 2009, pp. 378–383.

[139] G. Tina, S. Gagliano, and S. Raiti, "Hybrid solar/wind power system probabilistic modeling for long-term performance assessment," Sol. Energy, vol. 80, no. 5, pp. 578–588, May 2006.

[140] Canadian Solar (2015). Residential Solar Power System [Online]. Available: http://www.canadiansolar.com/

[141] Environment Canada, Canadian Weather Energy Engineering Datasets (CWEEDS) [Online]. Available: http://climate.weather.gc.ca/prods_servs/engineering_e.html

[142] Q. Zhao, V. Hautamaki, and P. Fränti, “Knee point detection in BIC for detecting the number of clusters,” in ACIV, New York, NY, USA: Springer, 2008.

[143] Y. Riffonneau, "Optimal power flow management for grid connected PV systems with batteries." IEEE Transactions on Sustainable Energy 2.3 (2011): 309-320.

[144] T. Guena, and P. Leblanc. "How depth of discharge affects the cycle life of lithium-metal-polymer batteries." INTELEC 06-Twenty-Eighth International Telecommunications Energy Conference. IEEE, 2006.

[145] Ng, Kong Soon, et al. "Enhanced coulomb counting method for estimating state-of-charge and state-of-health of lithium-ion batteries." Applied energy 86.9 (2009): 1506-1511.

[146] T. Mosher, “Economic valuation of energy storage coupled with photovoltaics: current technologies and future projections,” M.S. thesis, Aeroastro Dept., MIT.,Cambridge, Mass. State, 2010.

[147] American National Standard for Electric Power Systems and Equipment-voltage Ratings (60 Hz), American National Standards Institute, Inc. (ANSI),Rosslyn, VA, US, 2011, C84.1-2011.

[148] IEEE Guide for Loading Mineral-Oil-Immersed Transformers and Step- Voltage Regulators, IEEE Standard C57.91-2011, Mar. 2012.

[149] R. Vicini, O. Micheloud, H. Kumar, and A. Kwasinski, “Transformer and home energy management systems to lessen electrical vehicle impact on the grid,” IET Gener. Transm. Distrib., vol. 6, no. 12, pp. 1202–1208, Dec. 2012.

[150] D. C. Park, M. A. El-Sharkawi, R. J. Marks, L. E. Atlas and M. J. Damborg, "Electric load forecasting using an artificial neural network," in IEEE Transactions on Power Systems, vol. 6, no. 2, pp. 442-449, May 1991

[151] Baltimore Gas and Electric Company, Load Profiles, [Online]. Available: https://supplier.bge.com/electric/load/profiles.asp, accessed Sept. 2014.

[152] J. Bishop, Profiles on Residential Power Consumption. MA, USA: Fire Protection Research Foundation, Mar. 2010

[153] Sheikh, Samsher Kadir, and M. G. Unde. "Short Term Load Forecasting using ANN Technique." International Journal of Engineering Sciences & Emerging Technologies 1.2 (2012): 97-107.

[154] L. C. P. Velasco, C. R. Villezas, P. N. C. Palahang and J. A. A. Dagaang, "Next day electric load forecasting using Artificial Neural Networks," Humanoid, Nanotechnology, Information Technology,Communication and Control, Environment and Management (HNICEM), 2015 International Conference on, Cebu City, 2015, pp. 1-6.

[155] Lera, Gabriel, and Miguel Pinzolas. "Neighborhood based Levenberg-Marquardt algorithm for neural network training." IEEE Transactions on Neural Networks 13.5 (2002): 1200-1203.

[156] L. M. Saini and M. K. Soni, "Artificial neural network based peak load forecasting using Levenberg-Marquardt and quasi-Newton methods," in IEE Proceedings - Generation, Transmission and Distribution, vol. 149, no. 5, pp. 578-584, Sep 2002

[157] Mathworks team,"Mixed-Integer Linear Programming Algorithms" available at: https://www.mathworks.com/help/optim/ug/mixed-integer-linear-programming-algorithms.html

[158] Distribution Test Feeders. (2001). IEEE 123-Bus Standard Test Distribution System [Online]. Available: http://ewh.ieee.org/soc/pes/ dsacom/testfeeders/index.html.

[159] Electric Power Research Institute (EPRI), Distribution System Simulator (OpenDSS), simulating environment software, California, US, 2008 [Online].Available: http://smartgrid.epri.com/SimulationTool.aspx.

[160] Z. Liu, F. Wen, G. Ledwich, and X. Ji, "Optimal sitting and sizing of distributed generators based on a modified primal-dual interior point algorithm," in Proc. IEEE 4th Int. Conf. Elect. Utility Deregul. Restruct. Power Technol. (DRPT), Weihai, China, Jul. 2011, pp. 1360–1365.

[161] Reliability Test System Task Force, "The IEEE reliability test system," IEEE Trans. Power Syst., vol. 14, no. 3, pp. 1010–1020, Aug. 1999

[162] Distribution test system commercial load profiles [Online]. Available: http://www2.iee.or.jp/ver2/pes/23–st–model/english/index.html

[163] T. K. Au, "Assessment of plug-in electric vehicles charging on distribution networks," Ph.D. dissertation, Univ. Washington, Seattle, WA, USA, 2012.

[164] Distribution test feeders, IEEE 34 bus Distribution System Analysis Subcommittee, Power, and Energy Society (PES), New Jersey, US, 1991 [Online]. Available:http://ewh.ieee.org/soc/pes/dsacom/testfeeders/.

[165] “Technology Advisory – Tesla Energy PowerWall”, available: https://www.nreca.coop/wpcontent/uploads/2015/05/BTS_Review_of_Tesla_Offering.pdf

Appendix A Solar Photovoltaic and Energy Storage Data

Table A.1 Electrical Specification of PV System [140]

Item	Specs	2 kW PV	10 kW PV
Input DC Data	Max PV generation power (W)	2300	10200
	Max DC voltage (V)	500	1000
	Max DC current (A)	15	22
	Number of inputs/MPPT tracker	2/1	4/2
	DC connector	MC IV Connector	
	Standby power consumption (W)	5	5
Output AC data	Nominal AC power (W)	2000	10000
	Max AC power (W)	2000	10000
	Nominal output voltage (V)	120	120
	AC grid frequency (Hz)	60	60
	Power factor	~ 1	~ 0.9
	AC connector	Single phase	
PV efficiency	Max. Efficiency	97%	98%
	MPPT Adaptation Efficiency	>99.5%	>99.5%

Table A.2 Tesla Energy POWERWALL [165]

Energy	10 kWh (50 cycles/year), 7 kWh (daily cycling)
Power	2.0 kW continuous, 3.3 kW peak
Voltage	350 – 450VDC (current system designs use 48 volts)
Inverter	Not included
Dimension Weight	51.2" x 33.9" x 7.1" (1300 mm x 860 mm x 180 mm)
Temperature	100 kg / 220 lbs., wall mounted
DC Round Trip Efficiency	-4°F to 110°F / -20°C to 43°C
Battery Type	92%
Life Time	10 to 15 years
Other	“Liquid thermal cooling”
Pricing	
7 kWh “Daily Cycling” Model	$3,000-- $429/kWh-DC
10 kWh “Backup” Model	$3,500 -- $350/kWh-DC
System Included	Tesla website says quoted price includes the battery, enclosure, cooling system and the battery management system

Appendix B IEEE 123 Bus Standard Test Distribution System Data [158]

Table B.1 Line Segment Data

Node A	Node B	Length (ft.)	Config.
1	2	175	10
1	3	250	11
1	7	300	1
3	4	200	11
3	5	325	11
5	6	250	11
7	8	200	1
8	12	225	10
8	9	225	9
8	13	300	1
9	14	425	9
13	34	150	11
13	18	825	2
14	11	250	9
14	10	250	9
15	16	375	11
15	17	350	11
18	19	250	9
18	21	300	2
19	20	325	9
21	22	525	10
21	23	250	2
23	24	550	11
23	25	275	2
25	26	350	7
25	28	200	2
26	27	275	7
26	31	225	11
27	33	500	9
28	29	300	2
29	30	350	2
30	250	200	2
31	32	300	11
34	15	100	11
35	36	650	8
35	40	250	1
36	37	300	9

Table B.1 Line Segment Data (Continued)

Node A	Node B	Length (ft.)	Config.
36	38	250	10
38	39	325	10
40	41	325	11
40	42	250	1
42	43	500	10
42	44	200	1
44	45	200	9
44	47	250	1
45	46	300	9
47	48	150	4
47	49	250	4
49	50	250	4
50	51	250	4
51	151	500	4
52	53	200	1
53	54	125	1
54	55	275	1
54	57	350	3
55	56	275	1
57	58	250	10
57	60	750	3
58	59	250	10
60	61	550	5
60	62	250	12
62	63	175	12
63	64	350	12
64	65	425	12
65	66	325	12
67	68	200	9
67	72	275	3
67	97	250	3
68	69	275	9
69	70	325	9
70	71	275	9
72	73	275	11
72	76	200	3
73	74	350	11
74	75	400	11
76	77	400	6
76	86	700	3

Table B.1 Line Segment Data (Continued)

Node A	Node B	Length (ft.)	Config.
77	78	100	6
78	79	225	6
78	80	475	6
80	81	475	6
81	82	250	6
81	84	675	11
82	83	250	6
84	85	475	11
86	87	450	6
87	88	175	9
87	89	275	6
89	90	225	10
89	91	225	6
91	92	300	11
91	93	225	6
93	94	275	9
93	95	300	6
95	96	200	10
97	98	275	3
98	99	550	3
99	100	300	3
100	450	800	3
101	102	225	11
101	105	275	3
102	103	325	11
103	104	700	11
105	106	225	10
105	108	325	3
106	107	575	10
108	109	450	9
108	300	1000	3
109	110	300	9
110	111	575	9
110	112	125	9
112	113	525	9
113	114	325	9
135	35	375	4
149	1	400	1
152	52	400	1
160	67	350	6
197	101	250	3

Table B.2 Overhead Line Configurations

Config.	Phasing	Phase Cond.	Neutral Cond.	Spacing
		ACSR	ACSR	ID
1	A B C N	336,400 26/7	4/0 6/1	500
2	C A B N	336,400 26/7	4/0 6/1	500
3	B C A N	336,400 26/7	4/0 6/1	500
4	C B A N	336,400 26/7	4/0 6/1	500
5	B A C N	336,400 26/7	4/0 6/1	500
6	A C B N	336,400 26/7	4/0 6/1	500
7	A C N	336,400 26/7	4/0 6/1	505
8	A B N	336,400 26/7	4/0 6/1	505
9	A N	1/0	1/0	510
10	B N	1/0	1/0	510
11	C N	1/0	1/0	510

Table B.3 Underground Line Configuration

Config.	Phasing	Cable	Spacing ID
12	A B C	1/0 AA, CN	515

Table B.4 Transformer Data

	kVA	kV-high	kV-low	R - %	X - %
Substation	5,000	115 - D	4.16 Gr-W	1	8
XFM – 1	150	4.16 - D	.480 - D	1.27	2.72

Table B.5 Three Phase Switches

Node A	Node B	Normal
13	152	closed
18	135	closed
60	160	closed
61	610	closed
97	197	closed
150	149	closed
250	251	open
450	451	open
54	94	open
151	300	open
300	350	open

Table B.6 Shunt Capacitors

Node	Ph-A	Ph-B	Ph-C
	kVAr	kVAr	kVAr
83	200	200	200
88	50	-	-
90	-	50	-
92	-	-	50
Total	250	250	250

Table B.7 Regulator Data

ID	Line Segment	Location	Phase	Bandwidth	PT Ratio	Primary CT Rating	R	X	Voltage Level
1	150-149	150	A	2.0V	20	700	3	7.5	120
2	9-14	9	A	2.0V	20	50	0.4	0.4	120
3-A	25-26	25	A	1V	20	50	0.4	0.4	120
3-C	25-26	25	C	1V	20	50	0.4	0.4	120
4-A	160-67	160	A	2V	20	300	0.6	1.3	124
4-B	160-67	160	B	2V	20	300	1.4	2.6	124
4-C	160-67	160	C	2V	20	300	0.2	1.4	124

Table B.8 Spot Load Data

Node	Load	Ph-1	Ph-1	Ph-2	Ph-2	Ph-3	Ph-3
	Model	kW	kVAr	kW	kVAr	kW	kVAr
1	Y-PQ	40	20	0	0	0	0
2	Y-PQ	0	0	20	10	0	0
4	Y-PR	0	0	0	0	40	20
5	Y-I	0	0	0	0	20	10
6	Y-Z	0	0	0	0	40	20
7	Y-PQ	20	10	0	0	0	0
9	Y-PQ	40	20	0	0	0	0
10	Y-I	20	10	0	0	0	0
11	Y-Z	40	20	0	0	0	0
12	Y-PQ	0	0	20	10	0	0
16	Y-PQ	0	0	0	0	40	20
17	Y-PQ	0	0	0	0	20	10
19	Y-PQ	40	20	0	0	0	0
20	Y-I	40	20	0	0	0	0
22	Y-Z	0	0	40	20	0	0
24	Y-PQ	0	0	0	0	40	20
28	Y-I	40	20	0	0	0	0
29	Y-Z	40	20	0	0	0	0

Table B.8 Spot Load Data (Continued)

Node	Load	Ph-1	Ph-1	Ph-2	Ph-2	Ph-3	Ph-3
	Model	kW	kVAr	kW	kVAr	Kw	kVAr
30	Y-PQ	0	0	0	0	40	20
31	Y-PQ	0	0	0	0	20	10
32	Y-PQ	0	0	0	0	20	10
33	Y-I	40	20	0	0	0	0
34	Y-Z	0	0	0	0	40	20
35	D-PQ	40	20	0	0	0	0
37	Y-Z	40	20	0	0	0	0
38	Y-I	0	0	20	10	0	0
39	Y-PQ	0	0	20	10	0	0
41	Y-PQ	0	0	0	0	20	10
42	Y-PQ	20	10	0	0	0	0
43	Y-Z	0	0	40	20	0	0
45	Y-I	20	10	0	0	0	0
46	Y-PQ	20	10	0	0	0	0
47	Y-I	35	25	35	25	35	25
48	Y-Z	70	50	70	50	70	50
49	Y-PQ	35	25	70	50	35	20
50	Y-PQ	0	0	0	0	40	20
51	Y-PQ	20	10	0	0	0	0
52	Y-PQ	40	20	0	0	0	0
53	Y-PQ	40	20	0	0	0	0
55	Y-Z	20	10	0	0	0	0
56	Y-PQ	0	0	20	10	0	0
58	Y-I	0	0	20	10	0	0
59	Y-PQ	0	0	20	10	0	0
60	Y-PQ	20	10	0	0	0	0
62	Y-Z	0	0	0	0	40	20
63	Y-PQ	40	20	0	0	0	0
64	Y-I	0	0	75	35	0	0
65	D-Z	35	25	35	25	70	50
66	Y-PQ	0	0	0	0	75	35
68	Y-PQ	20	10	0	0	0	0
69	Y-PQ	40	20	0	0	0	0
70	Y-PQ	20	10	0	0	0	0
71	Y-PQ	40	20	0	0	0	0
73	Y-PQ	0	0	0	0	40	20
74	Y-Z	0	0	0	0	40	20
75	Y-PQ	0	0	0	0	40	20
76	D-I	105	80	70	50	70	50
77	Y-PQ	0	0	40	20	0	0
79	Y-Z	40	20	0	0	0	0
80	Y-PQ	0	0	40	20	0	0

Table B.8 Spot Load Data (Continued)

Node	Load	Ph-1	Ph-1	Ph-2	Ph-2	Ph-3	Ph-3
	Model	kW	kVAr	kW	kVAr	kW	kVAr
82	Y-PQ	40	20	0	0	0	0
83	Y-PQ	0	0	0	0	20	10
84	Y-PQ	0	0	0	0	20	10
85	Y-PQ	0	0	0	0	40	20
86	Y-PQ	0	0	20	10	0	0
87	Y-PQ	0	0	40	20	0	0
88	Y-PQ	40	20	0	0	0	0
90	Y-I	0	0	40	20	0	0
92	Y-PQ	0	0	0	0	40	20
94	Y-PQ	40	20	0	0	0	0
95	Y-PQ	0	0	20	10	0	0
96	Y-PQ	0	0	20	10	0	0
98	Y-PQ	40	20	0	0	0	0
99	Y-PQ	0	0	40	20	0	0
100	Y-Z	0	0	0	0	40	20
102	Y-PQ	0	0	0	0	20	10
103	Y-PQ	0	0	0	0	40	20
104	Y-PQ	0	0	0	0	40	20
106	Y-PQ	0	0	40	20	0	0
107	Y-PQ	0	0	40	20	0	0
109	Y-PQ	40	20	0	0	0	0
111	Y-PQ	20	10	0	0	0	0
112	Y-I	20	10	0	0	0	0
113	Y-Z	40	20	0	0	0	0
114	Y-PQ	20	10	0	0	0	0
Total		1420	775	915	515	1155	630

Line Impedances

Configuration 1:

$$z = \begin{bmatrix} 0.4576 + j1.0780 & 0.1560 + j0.5017 & 0.1535 + j0.3849 \\ & 0.4666 + j1.0482 & 0.1580 + j0.4236 \\ & & 0.4615 + j1.0651 \end{bmatrix} \Omega / mile$$

$$b = \begin{bmatrix} 5.6765 & -1.8319 & -0.6982 \\ & 5.9809 & -1.1645 \\ & & 5.3971 \end{bmatrix} \mu S / mile$$

Configuration 2:

$$z = \begin{bmatrix} 0.4666 + j1.0482 & 0.1580 + j0.4236 & 0.1560 + j0.5017 \\ & 0.4615 + j1.0651 & 0.1535 + j0.3849 \\ & & 0.4576 + j1.0780 \end{bmatrix} \Omega / mile$$

$$b = \begin{bmatrix} 5.9809 & -1.1645 & -1.8319 \\ & 5.3971 & -0.6982 \\ & & 5.6765 \end{bmatrix} \mu S / mile$$

Configuration 3:

$$z = \begin{bmatrix} 0.4615 + j1.0651 & 0.1535 + j0.3849 & 0.1580 + j0.4236 \\ & 0.4576 + j1.0780 & 0.1560 + j0.5017 \\ & & 0.4666 + j1.0482 \end{bmatrix} \Omega / mile$$

$$b = \begin{bmatrix} 5.3971 & -0.6982 & -1.1645 \\ & 5.6765 & -1.8319 \\ & & 5.9809 \end{bmatrix} \mu S / mile$$

Configuration 4:

$$z = \begin{bmatrix} 0.4615 + j1.0651 & 0.1580 + j0.4236 & 0.1535 + j0.3849 \\ & 0.4666 + j1.0482 & 0.1560 + j0.5017 \\ & & 0.4576 + j1.0780 \end{bmatrix} \Omega / mile$$

$$b = \begin{bmatrix} 5.3971 & -1.1645 & -0.6982 \\ & 5.9809 & -1.8319 \\ & & 5.6765 \end{bmatrix} \mu S / mile$$

Configuration 5:

$$z = \begin{bmatrix} 0.4666 + j1.0482 & 0.1560 + j0.5017 & 0.1580 + j0.4236 \\ & 0.4576 + j1.0780 & 0.1535 + j0.3849 \\ & & 0.4615 + j1.0651 \end{bmatrix} \Omega / mile$$

$$b = \begin{bmatrix} 5.9809 & -1.8319 & -1.1645 \\ & 5.6765 & -0.6982 \\ & & 5.3971 \end{bmatrix} \mu S / mile$$

Configuration 6:

$$z = \begin{bmatrix} 0.4576 + j1.0780 & 0.1535 + j0.3849 & 0.1560 + j0.5017 \\ & 0.4615 + j1.0651 & 0.1580 + j0.4236 \\ & & 0.4666 + j1.0482 \end{bmatrix} \Omega / mile$$

$$b = \begin{bmatrix} 5.6765 & -0.6982 & -1.8319 \\ & 5.3971 & -1.1645 \\ & & 5.9809 \end{bmatrix} \mu S / mile$$

Configuration 7:

$$z = \begin{bmatrix} 0.4576 + j1.0780 & 0.0000 + j0.0000 & 0.1535 + j0.3849 \\ & 0.0000 + j0.0000 & 0.0000 + j0.0000 \\ & & 0.4615 + j1.0651 \end{bmatrix} \Omega / mile$$

$$b = \begin{bmatrix} 5.1154 & 0.0000 & -1.0549 \\ & 0.0000 & 0.0000 \\ & & 5.1704 \end{bmatrix} \mu S / mile$$

Configuration 8:

$$z = \begin{bmatrix} 0.4576 + j1.0780 & 0.1535 + j0.3849 & 0.0000 + j0.0000 \\ & 0.4615 + j1.0651 & 0.0000 + j0.0000 \\ & & 0.0000 + j0.0000 \end{bmatrix} \Omega / mile$$

$$b = \begin{bmatrix} 5.1154 & -1.0549 & 0.0000 \\ & 5.1704 & 0.0000 \\ & & 0.0000 \end{bmatrix} \mu S / mile$$

Configuration 9:

$$z = \begin{bmatrix} 1.3292 + j1.3475 & 0.0000 + j0.0000 & 0.0000 + j0.0000 \\ & 0.0000 + j0.0000 & 0.0000 + j0.0000 \\ & & 0.0000 + j0.0000 \end{bmatrix} \Omega / mile$$

$$b = \begin{bmatrix} 4.5193 & 0.0000 & 0.0000 \\ & 0.0000 & 0.0000 \\ & & 0.0000 \end{bmatrix} \mu S / mile$$

Configuration 10:

$$z = \begin{bmatrix} 0.0000 + j0.0000 & 0.0000 + j0.0000 & 0.0000 + j0.0000 \\ & 1.3292 + j1.3475 & 0.0000 + j0.0000 \\ & & 0.0000 + j0.0000 \end{bmatrix} \Omega / mile$$

$$b = \begin{bmatrix} 0.0000 & 0.0000 & 0.0000 \\ & 4.5193 & 0.0000 \\ & & 0.0000 \end{bmatrix} \mu S / mile$$

Configuration 11:

$$z = \begin{bmatrix} 0.0000 + j0.0000 & 0.0000 + j0.0000 & 0.0000 + j0.0000 \\ & 0.0000 + j0.0000 & 0.0000 + j0.0000 \\ & & 1.3292 + j1.3475 \end{bmatrix} \Omega / mile$$

$$b = \begin{bmatrix} 0.0000 & 0.0000 & 0.0000 \\ & 0.0000 & 0.0000 \\ & & 4.5193 \end{bmatrix} \mu S / mile$$

Configuration 12:

$$z = \begin{bmatrix} 1.5209 + j0.7521 & 0.5198 + j0.2775 & 0.4924 + j0.2157 \\ & 1.5329 + j0.7162 & 0.5198 + j0.2775 \\ & & 1.5209 + j0.7521 \end{bmatrix} \Omega / mile$$

$$b = \begin{bmatrix} 67.2242 & 0.0000 & 0.0000 \\ & 67.2242 & 0.0000 \\ & & 67.2242 \end{bmatrix} \mu S / mile$$

Appendix C IEEE 34 bus Standard Test Distribution System Data [164]

Table C.1 Line Segment Data

Node A	Node B	Length (ft.)	Config.
800	802	2580	300
802	806	1730	300
806	808	32230	300
808	810	5804	303
808	812	37500	300
812	814	29730	300
814	850	10	301
816	818	1710	302
816	824	10210	301
818	820	48150	302
820	822	13740	302
824	826	3030	303
824	828	840	301
828	830	20440	301
830	854	520	301
832	858	4900	301
832	888	0	XFM-1
834	860	2020	301
834	842	280	301
836	840	860	301
836	862	280	301
842	844	1350	301
844	846	3640	301
846	848	530	301
850	816	310	301
852	832	10	301
854	856	23330	303
854	852	36830	301
858	864	1620	303
858	834	5830	301
860	836	2680	301
862	838	4860	304
888	890	10560	300

Table C.2 Overhead Line Configurations

Config.	Phasing	Phase ACSR	Neutral ACSR	Spacing ID
300	BAC-N	1/0	1/0	500
301	BAC-N	#2 6/1	#2 6/1	500
302	A-N	#4 6/1	#4 6/1	510
303	B-N	#4 6/1	#4 6/1	510
304	B-N	#2 6/1	#2 6/1	510

Table C.3 Transformer Data

	kVA	kV-high	kV-low	R - %	X - %
Substation	2500	69 - D	24.9 -Gr. W	1	8
XFM – 1	500	24.9 - Gr.W	4.16 - Gr. W	1.9	4.08

Table C.4 Spot Load Data

Node	Node	Load	Ph-1	Ph-1	Ph-2	Ph-2	Ph-3
		Model	kW	kVAr	kW	kVAr	kW
860	Y-PQ	20	16	20	16	20	16
840	Y-I	9	7	9	7	9	7
844	Y-Z	135	105	135	105	135	105
848	D-PQ	20	16	20	16	20	16
890	D-I	150	75	150	75	150	75
830	D-Z	10	5	10	5	25	10
Total		344	224	344	224	359	229

Table C.5 Distributed Load Data

Node	Node	Load	Ph-1	Ph-1	Ph-2	Ph-2	Ph-3	Ph-3
		Model	kW	kVAr	kW	kVAr	kW	kVAr
802	806	Y-PQ	0	0	30	15	25	14
808	810	Y-I	0	0	16	8	0	0
818	820	Y-Z	34	17	0	0	0	0
820	822	Y-PQ	135	70	0	0	0	0
816	824	D-I	0	0	5	2	0	0
824	826	Y-I	0	0	40	20	0	0
824	828	Y-PQ	0	0	0	0	4	2
828	830	Y-PQ	7	3	0	0	0	0
854	856	Y-PQ	0	0	4	2	0	0
832	858	D-Z	7	3	2	1	6	3
858	864	Y-PQ	2	1	0	0	0	0
858	834	D-PQ	4	2	15	8	13	7
834	860	D-Z	16	8	20	10	110	55
860	836	D-PQ	30	15	10	6	42	22
836	840	D-I	18	9	22	11	0	0
862	838	Y-PQ	0	0	28	14	0	0
842	844	Y-PQ	9	5	0	0	0	0
844	846	Y-PQ	0	0	25	12	20	11
846	848	Y-PQ	0	0	23	11	0	0
	Total		262	133	240	120	220	114

Table C.6 Shunt Capacitors

Node	Ph-A (kVAr)	Ph-B (kVAr)	Ph-C (kVAr)
844	100	100	100
848	150	150	150
Total	250	250	250

Table C.7 Regulator Data

ID	Line Segment	Location	Phase	Bandwidth	PT Ratio	Primary CT Rating	R	X	Voltage Level
1	814-850	814	ABC	2.0V	120	100	3	7.5	120
2	9-14	9	A	2.0V	20	50	0.4	0.4	120

Table C.8 Regulator-1 Data

Item	Specification		
ID	1		
Line Segment	814 - 850		
Location	814		
Bandwidth	2.0 volts		
PT Ratio	120		
Primary CT Rating	100		
Phase	Ph-A	Ph-B	Ph-C
R	2.7	2.7	2.7
X	1.6	1.6	1.6
Voltage Level	122	122	122

Table C.9 Regulator-2 Data

Item	Specification		
ID	2		
Line Segment	852 – 832		
Location	852		
Bandwidth	2.0 volts		
PT Ratio	120		
Primary CT Rating	100		
Phase	Ph-A	Ph-B	Ph-C
R	2.5	2.5	2.5
X	1.5	1.5	1.5
Voltage Level	124	124	124

Line Impedances
Configuration 300:

$$z = \begin{bmatrix} 1.3368 + j1.3343 & 0.2101 + j0.5779 & 0.2130 + j0.5015 \\ & 1.3238 + j1.3569 & 0.2066 + j0.4591 \\ & & 1.3294 + j1.34711 \end{bmatrix} \Omega / mile$$

$$b = \begin{bmatrix} 5.3350 & -1.5313 & -9943 \\ & 5.0979 & -0.6212 \\ & & 4.8880 \end{bmatrix} \mu S / mile$$

Configuration 301:

$$z = \begin{bmatrix} 1.9300 + j1.4115 & 0.2327 + j0.6442 & 0.2359 + j0.5691 \\ & 1.91571 + j\,1.428 & 0.2288 + j0.5238 \\ & & 1.9219 + j1.4209 \end{bmatrix} \Omega / mile$$

$$b = \begin{bmatrix} 5.1207 & -1.4364 & -0.9402 \\ & 4.9055 & -0.5951 \\ & & 4.7154 \end{bmatrix} \mu S / mile$$

Configuration 302:

$$z = \begin{bmatrix} 2.7995 + j1.4855 & 0.0 + j0.0 & 0.0 + j0.0 \\ & 0.0 + j0.0 & 0.0 + j0.0 \\ & & 0.0 + j0.0 \end{bmatrix} \Omega / mile$$

$$b = \begin{bmatrix} 4.2251 & 0.0 & 0.0 \\ & 0.0 & 0.0 \\ & & 0.0 \end{bmatrix} \mu S / mile$$

Configuration 303:

$$z = \begin{bmatrix} 0.0 + j0.0 & 0.0 + j0.0 & 0.0 + j0.0 \\ & 2.7995 + j1.4855 & 0.0 + j0.0 \\ & & 0.0 + j0.0 \end{bmatrix} \Omega / mile$$

$$b = \begin{bmatrix} 0.0 & 0.0 & 0.0 \\ & 4.2251 & 0.0 \\ & & 0.0 \end{bmatrix} \mu S / mile$$

Configuration 304:

$$z = \begin{bmatrix} 0.0 + j0.0 & 0.0 + j0.0 & 0.0 + j0.0 \\ & 1.9217 + j1.4212 & 0.0 + j0.0 \\ & & 0.0 + j0.0 \end{bmatrix} \Omega / mile$$

$$b = \begin{bmatrix} 0.0 & 0.0 & 0.0 \\ & 4.3637 & 0.0 \\ & & 0.0 \end{bmatrix} \mu S / mile$$